UNIVERSITÀ
DEGLI STUDI
DI PADOVA

Università degli Studi di Padova

Dipartimento di Ingegneria Industriale - DII

Dipartimento di Tecnica e Gestione dei Sistemi Industriali - DTG

Corso di Laurea Magistrale in Ingegneria dei Materiali

Experimental and numerical investigation of the effect of temperature and curing history on the viscoelastic behaviour of epoxy resin

Relatore: Prof. Marino Quaresimin

Correlatore: Prof. Janis Varna

Laureando: Pietro Cuccarollo

matricola n. 1179194

Anno Accademico 2018 / 2019

Università degli Studi di Padova

Dipartimento di Ingegneria Industriale - DII
Dipartimento di Tecnica e Gestione dei Sistemi Industriali - DTG
Corso di Laurea Magistrale in Ingegneria dei Materiali

Experimental and numerical investigation of the effect of temperature and curing history on the viscoelastic behaviour of epoxy resin

Relatore: Prof. Marino Quaresimin

Correlatore: Prof. Janis Varna

Laureando: Pietro Cuccarollo
matricola n. 1179194

Anno Accademico 2018 / 2019

Preface

The presented Thesis summarizes the project work I have done in collaboration with the Division of Materials Science at Luleå University of Technology (LTU) in Sweden. Experiments were performed during my Erasmus period in Luleå, from February to June 2019. Raw materials for the production of specimens were supplied by RISE SICOMP AB in Piteå, where I was taught the manufacturing procedure in greater detail by Research Engineer Dr. Sibin Saseendran.

I would like to express my gratitude also to all the members of the group of Polymeric Composite Materials at LTU for their valuable support in answering my questions and clearing my doubts. Special thanks are dedicated to my supervisor Prof. Janis Varna, PhD students Luca Di Stasio and Zainab Al-Maqdasi and Assistant Prof. Liva Pupure. Last but definitely not least, I would like to acknowledge my Italian supervisor, Prof. Marino Quaresimin.

Padova, 5th December 2019

Abstract

Research presented in this Thesis deals with the characterization of the mechanical behaviour of the commercial epoxy resin system LY5052 / 5052CH at elevated temperatures and at different curing conditions. This is one of the most common thermoset matrices for reinforced polymeric composite materials and its cure during manufacturing is a process that requires special attention. Specimens are produced in a mold by means of pouring technique and subjecting them to different cure cycles. The Instron 3366 tensile testing machine is then used to perform different kinds of mechanical test, namely loading-unloading, creep and strain recovery, stress relaxation.

Viscoelastic modelling is needed to describe the properties of the resin, considering in particular the effect of testing temperature and cure state parameters. Several studies have previously established experimental methodologies to evaluate both temperature and cure shift factors. Indeed, by applying the time-temperature-cure superposition (TTCS) principle, it is possible to generate a unique master curve that represents in a condensed form the viscoelastic behaviour of the resin. The main aims of this work are: the development of an efficient testing and data reduction methodology, to understand the response of epoxy; the validation of a thermodynamically consistent viscoelastic model developed at LTU using Schapery's approach, named VisCoR and herein considered in its incremental form. Although the focus is on viscoelasticity, some viscoplastic analysis is also performed. It is found that the degree of cure seems not sufficient to solely identify the cure state of the resin from a mechanical point of view. Its behaviour, in fact, appears to be significantly affected by the previous curing history, given by the applied thermal cycle.

These considerations will lead to an improved understanding of the complex chemical and thermo-mechanical phenomena occurring at high temperature and during the curing process, in particular the evolution of residual stresses within the part and the consequent shape distortions. The development of industrially available prediction tools will enable to easily and quickly set up efficient manufacturing processes, thus achieving a compromise between high quality of the final component and cost savings.

Sommario

L'attività di ricerca presentata in questa Tesi riguarda la caratterizzazione del comportamento meccanico del sistema epossidico LY5052 / 5052CH, ad elevata temperatura ed in differenti condizioni di cura. Si tratta di una delle matrici termoindurenti più comunemente utilizzate nei materiali compositi a livello commerciale, e la sua cura durante la produzione è un processo che richiede particolare attenzione. I campioni sono prodotti versando la resina in uno stampo e sottoponendola a diversi cicli di cura. Varie tipologie di test meccanico – più precisamente loading-unloading, creep e strain recovery, stress relaxation – sono poi svolte utilizzando la macchina di prova a trazione Instron 3366.

Per descrivere le proprietà della resina è richiesto un modello viscoelastico, che consideri in particolare gli effetti della temperatura e dello stato di cura. Vari studi hanno proposto delle metodologie sperimentali per valutare i fattori di shift relativi alla temperatura e alla cura. Tramite il principio di sovrapposizione tempo-temperatura-cura (TTC), si può infatti generare una curva maestra in grado di rappresentare in forma condensata il comportamento viscoelastico della resina. Gli scopi principali di questo lavoro sono: lo sviluppo di una metodologia efficiente di test e di analisi dei dati, in maniera tale da comprendere la risposta meccanica della matrice; la validazione di un modello viscoelastico sviluppato presso la LTU utilizzando l'approccio termodinamico di Schapery, chiamato VisCoR e qui considerato nella sua formulazione incrementale. Pur focalizzandosi sulla viscoelasticità, anche la viscoplasticità è in parte analizzata. Si scopre che il grado di cura non è un parametro sufficiente per caratterizzare la risposta meccanica della resina, che sembra infatti essere significativamente influenzata dalla precedente storia di cura, data dal ciclo termico applicato.

Tali considerazioni permetteranno di comprendere più a fondo i complessi fenomeni chimici e termo-meccanici che avvengono ad alte temperature e durante la cura, in particolare l'evoluzione di stress residui nel componente e le sue conseguenti variazioni di forma. Lo sviluppo di strumenti predittivi da utilizzare a livello industriale consentirà di instaurare processi manifatturieri efficienti, in maniera tale da raggiungere un compromesso tra qualità del prodotto e risparmio economico.

Table of contents

Nomenclature

T_g	glass transition temperature
α	degree of cure (DoC)
T_c	cure temperature
t_c	cure time
α_{max}	maximum degree of cure attainable at a certain cure temperature
ΔH	heat of cross-linking reaction
a_T	temperature shift factor
a_c	cure shift factor
a	total shift factor
w	specimen width
t	specimen thickness
A	specimen cross section
F	load
Δl	elongation
σ	stress
ε	strain
CTE	coefficient of thermal expansion
CCS	coefficient of chemical shrinkage
E_a	apparent modulus
E_{rel}	relaxation modulus
τ	relaxation time
ΔC	term of the Prony series
H	Helmholtz free energy function
ξ	internal state variable
ψ	reduced time
E_r	rubbery modulus

1. Introduction to polymeric composite materials

Polymeric composite materials are made of a reinforcement, mostly in the form of fibers, embedded in a polymer matrix. Generally speaking, their high performances are related to ease of molding complex shapes, high environmental resistance and especially high specific strength, stiffness and toughness [21]. This makes them attractive for a multitude of industrial applications, where lightness provides benefits such as cost saving, lower environmental impact and improved handiness. The most outstanding are the transportation sector, including aerospace, automotive and naval, and sports equipment. Another important advantage of composites over traditional heavier metallic structures is the reduced need for finishing operations, since the molding techniques allow enhanced dimensional accuracy, in addition to a fairly good flexibility in the design of parts.

The study of the behaviour of composites as a whole requires knowledge of the properties of the individual constituents, namely the reinforcement and the matrix, as well as of the interface between them [21]. The high ratio of mechanical properties with respect to density derives from an appropriate coupling of the two phases. The most common materials for fibers are glass, carbon and aramid whereas matrices are usually thermosets, in particular epoxy and polyester resins. Thermoplastics are less used because of their inferior structural performance. Thanks to their ecological sustainability, natural fibers, such as flax, hemp, kenaf and ramie, are showing increasing potential as possible substitutes of conventional synthetic fibers and some bio-based resins are also being investigated [15]. However, the sensitivity to moisture and temperature typical of natural materials, as well as their very high scattering of properties, still limit the use of these composites to less demanding applications [39].

The reinforcement system is very often produced and handled as bundles of fibers. The purpose of its incorporation is mainly to enhance the stiffness and strength of the matrix, which in turn spreads the loads applied to the part between the individual fibers and protects them from damage, caused for example by chemical attack, abrasion and impact. Both the type of fibers and the way in which they are distributed within the matrix may vary according to the design requirements [21]. Depending on their aspect ratio, fibers can be short or continuous, the latter featuring larger increase in mechanical properties but more complicated processing. While short randomly oriented fiber composites are more versatile, those containing long aligned fibers allow to exploit higher stiffness and strength in direction parallel to the reinforcement. Such materials exhibit marked anisotropy, meaning that their properties vary significantly when measured in different orientations. This might seem a drawback, but actually allows to more efficiently suit the mechanical performance of the structure to the service conditions and design purposes. Considering a perfect bonding at the interface between fibers and matrix, the iso-strain assumption states that the longitudinal strains acting on the fiber and the matrix are equal to each other. Of course, being the tensile modulus of fibers much larger than that of the matrix, the majority of the applied stress is supported by the fibers. The mechanical response in the transverse direction is instead mostly controlled by the matrix.

Proper adhesion between fibers and matrix is fundamental, in order to have a material exhibiting strength and resistance closer to the theoretical values. However, the detailed nature of the interfacial region always includes some imperfections and this affects the fatigue and damage behaviour [21]. The maximum fiber volume fraction V_f that can be impregnated into the resin is given by geometrical considerations and it is further limited by production issues. It shall also be taken into account that real manufacturing processes always lead to some fiber misalignment and wrinkling, which have to be avoided as much as possible. High performance composite products are usually made of various plies, each containing long aligned fibers, oriented at different angles ϑ and stacked to form a laminate [21]. If the numbers of layers at $+\vartheta$ and $-\vartheta$ are equal, the laminate is said to be balanced; if plies are arranged symmetrically with respect to the mid-plane, it is symmetric. In a unidirectional ply, the reinforcement effect of fibers acts in a unique direction. Stiffness is therefore significantly lower transversely, whereas thermal expansion is larger, being less constrained by fibers. If the layers are differently oriented, the degree of anisotropy of the laminate at the macroscopic scale is reduced. It is in this way possible to obtain orthotropic materials, having different and reciprocally independent thermo-mechanical properties along three perpendicular directions. Besides debonding, i.e. the detachment of fibers from the resin, in the case of a laminated component there may also be separation between lamina, called delamination and caused by processing defects or too severe service condition.

The most common methods to produce thermoset composites are resin transfer molding (RTM) and prepreg lay-up [21]. RTM consists in the injection of resin into a preheated mold where the reinforcement has been placed in appropriate configuration. Injection may be assisted either by pressure or vacuum. In the laying-up technique, pre-impregnated sheets of matrix and fibers are draped over a mold, until the total plate thickness is achieved, and thermal treated. Sometimes vacuum bagging is used in order to reduce porosity but usually no additional polymer injection is necessary. In both techniques, breather fabrics are often used to absorb excess resin, as well as releasing agents that make the demolding stage easier. The modus operandi differs according to the specific technology employed, but all these methods include a stage called cure, during which the resin becomes solid [4]. Cure is performed at elevated temperatures, usually in the presence of hardening agents or accelerators, and consists in the polymerization of monomers into a three-dimensional interconnected network of long chains. After its solidification, the part is removed from the mold and is very often post-cured, i.e. kept at high temperature to increase its mechanical performance.

The molecular mechanisms involved in the curing process are quite complex and not totally understood. Most of the thermoset polymerization reactions are exothermic, meaning that they are accompanied by generation of heat [56]. As the cross-link density of the resin increases, the initial liquid gels into a rubbery state and finally vitrifies into solid glassy material. During the whole process, polymer chains are tightly pulled together and their movement is restricted, thus determining a reduction in the free volume of the matrix [2]. The properties of the resin during the overall process change by varying order of magnitude. Being their mechanical performance not very high, in structural applications resins have limited use on their own. Nevertheless, it is very important to characterize their behaviour, in order to avoid problems during manufacturing and to achieve good quality of the finished product. Indeed, the properties of composites are severely undermined by shape distortions and build-up of residual stresses [5, 6]. These phenomena have a direct effect on the strength and dimensional accuracy of the part. The need to understand thoroughly the evolution of material properties during cure has led to the development of several models to simulate and predict the outcomes of manufacturing processes. Since the mechanical

behaviour of polymeric materials is dominated by their viscoelasticity, the most accurate models take into account the time-dependence of strains and stresses.

Several concurrent factors cause the development of residual stresses in composites. The most relevant ones are the chemical shrinkage of the matrix and the mismatch between the coefficients of thermal expansion (CTE) of matrix and fibers [65]. The cross-linking reactions determine a reduction of the volume of the matrix, thus resulting in chemically induced internal stresses. On the other hand, since the coefficient of thermal expansion is higher for the resin than for the reinforcement, thermal stresses generated in the cooled part at the end of manufacturing are tensile in the matrix and compressive in the fibers. Other factors contributing to the evolution of the internal stress distribution, although to a smaller extent, are tool-part interaction, moisture absorption and aging of the matrix. It is the constraint exerted by the fibers and the mold that determines the development of the internal stresses, whose magnitude obviously depends on the viscoelastic and viscoplastic properties of the resin, and particularly on its relaxation behaviour.

The evolution of residual stresses in the matrix is more rapid as the resin passes from the rubbery to the glassy state [13]. Indeed, in the glass transition region, in addition to volumetric shrinkage there is also a simultaneous rapid increase in stiffness and slow-down of stress relaxation. Both phenomena contribute to increase the residual stresses, especially if the resin is constrained by the mold and tools or by the fibers themselves. Moreover, between the glassy and the rubbery domains there is a significant difference in the thermal expansion coefficient. These are the reasons why detailed study focused on the glass transition region is important in order to better understand the evolution of residual stresses. At the demolding stage the part is removed from the mold and, no longer being constrained, the internal stress field relax somewhat, sometimes leading to dimensional changes in the part [5]. One of the most typical examples of shape distortion is the so-called spring-in angle phenomenon [6, 24]. The inequality between the cured and the nominal geometry has to be minimized, or at least must fall within the specified tolerance. Factors affecting shape distortions are more related to design than mechanical performance; on the other hand, residual stresses combine with the externally applied loads, and therefore tend to weaken the structure leading to premature failure.

It is clear that the quality of composite products depends on factors that are initiated in the manufacturing stage. In addition to shape distortions and the build-up of internal stresses, other common defects that may be induced by poor processing are the formation of voids and porosity within the matrix, fiber misalignment, non-homogeneous local fiber volume fraction, debonding, delamination, etc. [6]. As already mentioned, an in-depth understanding of the evolution of material properties during manufacturing is required to eliminate these problems and to achieve a good-quality finished product. Effective models, being at the same time simple and accurate, are desirable to account for the dependence of viscoelastic and viscoplastic properties on cure and temperature and to better understand and improve the curing process itself, as well as the mold filling and layering techniques. If shape distortions can be predicted, the mold design can be modified in order to compensate for them. Thus, accurate models and simulations come in handy because, by avoiding or limiting the trial-and-error procedure, the cost of mold manufacturing can be minimized.

In literature there are numerous studies aimed at developing constitutive viscoelastic models to characterize composite material behaviour, usually combining features and parameters of the constituent phases [21]. The assumption that the longitudinal properties of a unidirectional ply are the volume-weighted average of those of fibers and matrix is at the basis of the so-called rule of mixtures. This approach is of course an approximate estimation of the properties of the whole material but has proven its

accuracy if equations sophisticated enough are used. Several properties are estimated thereby, such as density, the coefficient of thermal expansion, tensile and shear moduli, the Poisson's ratio, etc. It follows that the viscoelastic and viscoplastic behaviour of thermoset matrices, strongly depending on the operating temperature and the degree of cure, remarkably affects the performance of the composite in its entirety [28, 30, 34]. Nevertheless, the time-dependent response is still much better understood for fully cured resin because literature on varying cure state is rather limited and still characterized by insufficient experimental support to theory [7, 17]. Considering in particular the evolution of internal stresses during cure, linear and non-linear viscoelastic models have been introduced, including temperature and cure state parameters [26]. It should be stressed that, in order to develop reliable simulation tools, showing good agreement with experimental reality, the above-listed defects and uncertainties resulting from manufacturing should also be taken into account.

2. The effect of temperature and cure on viscoelasticity

In the course of manufacturing, a thermoset resin undergoes phase change from an uncured liquid to a solid state material. Since the resin gradually becomes denser, the curing process is accompanied by volumetric shrinkage [33]. The rate of transformation depends on the specific cure cycle applied, in terms of temperature profile over time, and results in a slightly different internal structure of the solidified resin [56]. Both the mechanical properties and the thermal expansion coefficient are continuously changing during the overall process. This is the main reason for the difficulties in developing a simplified methodology to characterize and simulate the evolution of viscoelastic material properties.

From a molecular point of view, mechanisms occurring during cure start with an unreacted liquid resin consisting of very short monomer chains and result in a fully cross-linked network [13]. At elevated temperatures, and in the presence of proper agents, sufficient energy is provided to adjacent monomers that begin to bond with each other. This process is called protonation, since it mainly involves the formation of hydrogen bonds, and is promoted by protonating agents called hardeners. The molecules keep increasing in length but still maintain a certain degree of free body motion, allowing them to slide reciprocally. As the polymeric chains get longer and longer, the rate of protonation starts slowing down until it is taken over by the mechanism of nucleophilic attack. At this stage, adjacent molecules begin to bond together, through weak Van der Waals forces or the formation of complexes, until the final interconnected three-dimensional network is formed. The viscosity of the resin increases with the chain length, with a very sharp increment when protonation reactions slow down and the network begins to form. This is usually called the gelation point of the resin [35]. Then, with the progressive formation of multi-chain complexes, the material slowly vitrifies from the rubbery to the glassy state, until the final solid form is reached. With the progression of cure, the reaction rate slows down and, when there is insufficient energy and free body motion, the material is assumed to be fully cross-linked, although theoretically the reactions never stop entirely [13]. The mechanism of curing epoxy with commonly used amine hardeners is illustrated in Figure 2.1 and leads to the network structure displayed in Figure 2.2 [43].

The degree of cure (DoC) is the parameter that describes the advancement of the cross-linking reactions, that is to say the conversion progress from uncured to fully cured resin. It may be expressed in percentage or equivalently by a figure in the range $0 \div 1$. Different phenomenological models have been proposed to describe the temporal evolution of the degree of cure, which is a monotonously and irreversibly increasing parameter [25]. Kamal's equation is one of the most successfully used and is presented below, in Section 4.1 [23]. Almost all the physical properties of the polymer are affected by its cure state. As the cross-linking reactions proceed, all the viscoelastic and viscoplastic characteristics of the resin, and of the composite as well, continuously change. In particular, at low degree of cure, the stiffness is low and the viscosity is high. Irreversible strains can be rather large if cross-linking is incomplete, i.e. for partially cured resin, and may be responsible for shape distortions in the part [8]. One of the most important properties

of polymers is their glass transition temperature T_g. As known, it is the temperature at which there is the passage from the glassy to the rubbery state and vice versa. Above this temperature, the weakened Van der Waals forces allow a certain degree of freedom of the chains in the network and their micro-Brownian motion. It follows that, besides the chemical formulation of the resin, T_g is determined by several factors including the cross-link density and intermolecular interactions. The well-established DiBenedetto equation formulates a biunivocal relationship between T_g and the degree of cure α [9]

$$\frac{T_g - T_{g,0}}{T_{g,\infty} - T_{g,0}} = \frac{\lambda\alpha}{1-(1-\lambda)\alpha} \tag{2.1}$$

where $T_{g,0}$ and $T_{g,\infty}$ are respectively the glass transition temperatures of the uncured and fully cured resin, whereas λ is a fitting parameter.

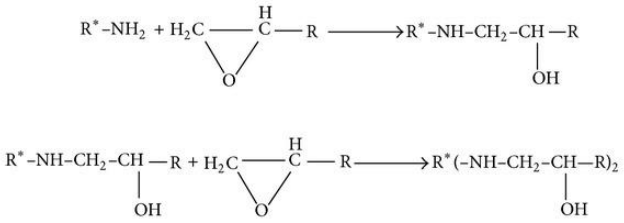

Figure 2.1 Mechanism of curing epoxy resin with amine hardeners

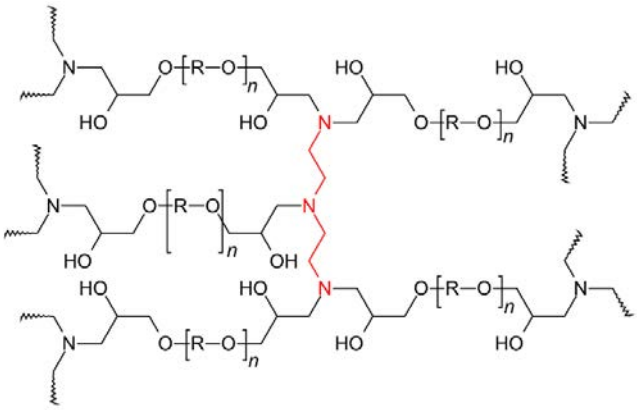

Figure 2.2 Structure of cured epoxy, showing in red a tri-amine cross-link

In simple terms, a viscoelastic material exhibits both viscous and elastic effects when it undergoes deformation. This means that strains and stresses are time-dependent, and in particular that there is a non-negligible response time when the material is subjected to forces or deformations. As a generalization, it can be said that, while elasticity is usually the result of bond stretching along crystallographic planes in an ordered solid, viscosity derives from the diffusion of atoms or molecules inside an amorphous material [44]. Being polymers amorphous or semi-crystalline, viscoelastic effects are relevant and simple elasticity usually not applicable. In order to describe the viscoelastic properties of polymers, use is made of the time-temperature superposition (TTS) principle, which states a sort of equivalence between the

effects of time and temperature. This means that analogous results can be obtained in experiments at long measurement time and low temperature or at high temperature and short time. The apparent modulus of the polymer is in fact observed to decrease by increasing either temperature or time. The main usefulness of the TTS principle is that it allows to report data obtained at various temperatures to a unique curve called master curve, that is then used to predict the behaviour at any temperature.

TTS is applied to relaxation curves, meaning that the specimen is subjected to a constant deformation and the stress required to maintain it is measured at constant temperature in function of time or after the same time at different temperatures [12, 35]. A method to more quickly look at the rheological response of polymers is the Dynamic Mechanical and Thermal Analysis (DMTA), which allows to study the relaxation behaviour at high frequencies [48]. The obtained data can be plotted in the graph storage modulus versus frequency in logarithmic scale. Both conventional relaxation and DMTA curves show well-defined glassy and rubbery plateaus, and therefore in the glass transition region the modulus is observed to drastically change, of about a couple of orders of magnitude [44]. If the polymer is semi-crystalline the modulus drop becomes smaller with increasing degree of crystallinity. This is because the amorphous domains are mostly responsible for the rubbery behaviour. It should be stressed that in the DMTA instrument, the applied strain level is infinitesimally small and hence the development of non-linearity is restrained. This characterization is therefore more representative for the glassy material in comparison to the rubbery state.

Constitutive mechanical models for thermosets may be based on elasticity or viscoelasticity. As a general indication, simple elasticity can handle the glassy-rubbery transition quite effectively but is quite insufficient for the opposite transformation, i.e. from rubbery to glassy state [46]. On the other hand, models based on the more elaborated incremental linear elasticity, such as the path-dependent model mentioned in Section 3.1, accurately describe the rubbery-glassy transition and not vice versa [10]. Consequently, more advanced and reliable constitutive models should consider viscoelastic effects. Nevertheless, currently full viscoelastic models are either not well defined or computationally tasking. Depending on their molecular weight and chemical constituents, viscoelastic materials can be classified into thermo-rheologically simple and complex [13, 64]. In general, polymers composed of large and heavy monomer sub-units tend to exhibit thermo-rheologically complex behaviour. Thermo-rheologically simple materials are those that obey the TTS principle with the same dependence for all viscoelastic properties. Using the temperature shift function, master curves can be generated extending the time-scale beyond the range that could normally be covered in a single experiment [56]. TTS cannot generally be applied correctly to thermo-rheologically complex materials like block and graft copolymers, polymer blends and some semi-crystalline polymers.

TTS has been widely used to study polymer viscoelasticity and states that all viscoelastic functions have the same temperature dependence. Hence, the observed relaxation curve could be rendered independent of the influence of temperature by an appropriate redefinition in time, that is to say by means of horizontal shifting of data in logarithmic time axis. Various models have been proposed over the years to generalize the temperature-dependence of the response times. Among these, for most polymers it is very often used the Williams-Landel-Ferry (WLF) equation, which establishes a linear relationship between the temperature shift factor and the testing temperature T [63]

$$\log a_T = -\frac{c_1\left(T - T_{ref}\right)}{c_2 + \left(T - T_{ref}\right)} \tag{2.2}$$

The reference temperature T_{ref} is usually selected as about room temperature. In the case of DMTA testing, constants c_1 and c_2 are determined by performing the frequency scans at various temperatures on fully cured specimens, i.e. having degree of cure 1. Using the WLF equation, the effect of temperature is mathematically described with better accuracy if the material is above its glass transition temperature [35]. On the contrary, below T_g the backbone motion of chains ceases and the rate-dependent Arrhenius equation is found to be more reliable [44]. According to this, at the absolute zero the relaxation time becomes infinite, implying that there is no relaxation. However for simplicity, in the presented work, the temperature-dependence of response times will be defined using the WLF equation, even though most of the selected test temperatures are well below T_g.

Therefore, the temperature shift function defines how the retardation or relaxation time of fully cured resin is affected by temperature. If the temperature shift is applied to differently cured specimens, a set of master curves is obtained, each corresponding to a different cure state. The effect of cure is thereby evaluated by introducing a cure shift function, along with the already defined temperature shift. Changes in the degree of cross-linking of the polymer network and in its structure are in this way dealt with. Both the cure temperature T_c and the cure duration t_c should be included as parameters in the shift function, since they together define the applied cure cycle. Given a certain cure temperature, the cure shift function has been found to be fairly linear in cure time [48]

$$\log a_c = C \cdot \left(t_c - t_{c,ref}\right) \tag{2.3}$$

where C is a quadratic function of the cure temperature, whereas $t_{c,ref}$ is the time required to reach an arbitrary percentage of cure. The same linear dependence is not exhibited if the cure shift factors are plotted against the degree of cure, and therefore cure time is more often used to shift the curves. Using the already mentioned Kamal's model, it is quite straightforward to calculate the degree of cure from the cure temperatures and times. Assuming thermo-rheologically simple behaviour, master curves are generated from tests performed at the same temperature on different cure states. This is analogous and complementary to temperature shifting and enables to predict the response of any degree of cure, by knowing the behaviour of an arbitrary reference cure state, usually that of fully cured material, and the cure shift function.

The total shift function a can be defined as the product of the temperature and cure shift factors, whose influences are therefore considered separately [12, 44]

$$a(T, \alpha) = a_T(T) \cdot a_c(\alpha) \tag{2.4}$$

By means of a dual-shifting methodology, this allows to generate unique super-master curves, assumed continuous and having a defined shape and collocation. A reference curve has to be chosen for the construction of the master curve, for example corresponding to room temperature and unit degree of cure. Horizontal shifts account for the change of modulus with temperature and cure state. The shifting procedure with respect to temperature is exemplified in Figure 2.3 for both conventional relaxation and DMTA curves. Assumed that the two shift factors are non-interactive, the sequence of shifting, with respect to temperature and degree of cure, can be inverted so that two different approaches are possible. It has been proven by Saseendran et al. that the resulting super-master curves superimpose fairly well using both routines, thus demonstrating the complementary nature of the two shift functions [48]. The product

formulation of the total shift factor a results in a linear summation when logarithmic axis is used for time or frequency

$$\log a = \log a_T + \log a_c \tag{2.5}$$

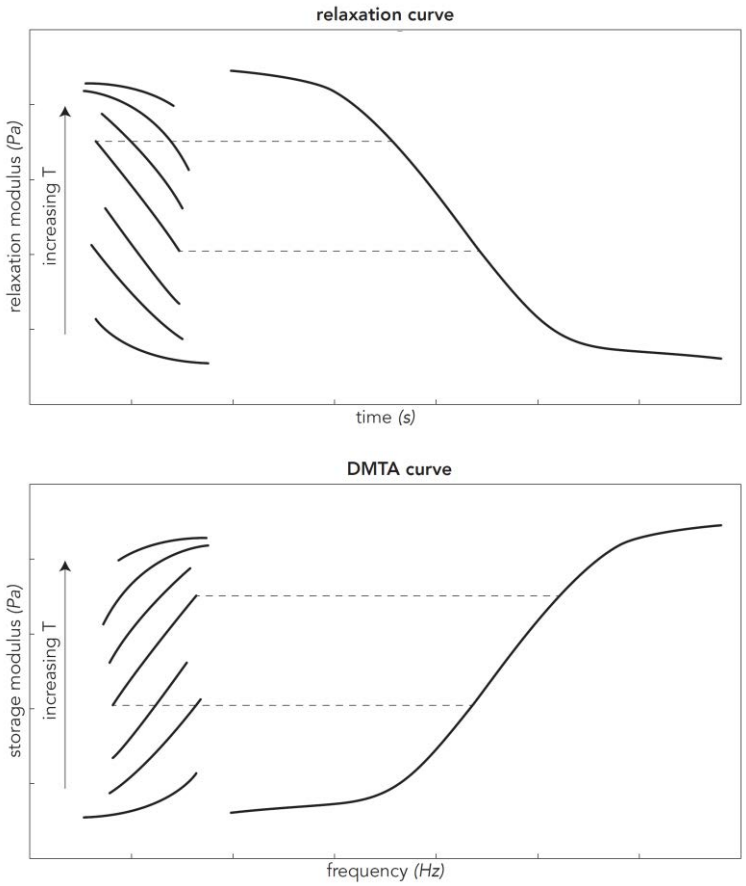

Figure 2.3 Temperature-shifting of relaxation and DMTA curves

Several studies on the combined effect of temperature and cure are available in literature. Hossain et al. have described the stiffness increase during the cross-linking process as an increasing number of spring elements [19, 20]. The proposed viscoelastic model can be represented as a cure-dependent elastic element connected in parallel with a Maxwell element, in turn composed of a time-independent elastic spring and a cure-dependent viscous dashpot. Using a rheometer, Eom et al. have found a linear dependence of the time-temperature shift factor on cure temperature [12]. In the work of O'Brien et al., the degree of cure of epoxy cured at the same temperature is shown not to affect the elastic response [34] whereas according to Sadegninia et al., the shear storage modulus of the glassy state is independent of the degree of cure [42]. Once realized that the key state variables are the degree of cure and temperature, Brockman et al. have introduced the concept of reduced temperature [8]. This is an internal state variable responsible by itself for both temperature and degree of cure, the latter expressed in function of the glass transition temperature. One of the first in-depth descriptions of the dual-shift methodology is attributable to Adolf and Martin, who worked on DMTA data obtained in the shear modulus domain [1]. Experimentally

determined shift factors for epoxy have been presented by Kim and White, studying the relaxation behaviour in the frequency domain [27].

All these findings confirm that TTS is insufficient to characterize the viscoelastic behaviour of thermosets. It has already been explained that, in addition to temperature shifting, another shifting in the horizontal direction allows to account for the dependence of the apparent modulus on the degree of cure. Glassy and rubbery moduli are instead constant for rheologically simple materials. Most of the methods incorporating time-temperature and time-cure superpositions imply using these two shifts, for example of DMTA data, to arrive at master curves. In doing so, the combined influence of test temperature and degree of cure is taken into account by the comprehensive time-temperature-cure superposition (TTCS) principle. Given that appropriate shift functions are used, the viscoelastic behaviour of the material may be obtained from the super-master curve, providing in particular a tool to estimate the relaxation modulus at any temperature and cure state. However, once the super-master curves have been generated, different rubbery plateaus are observed depending on the cure state [49]. This divergence of the rubbery moduli E_r has to be considered in order to define a truly unique master curve. A way to remove this dependence, assuming that the Poisson's ratio is constant in the rubbery region, is to further reduce the super-master curves into a normalized one. Thanks to normalization, the variation of E_r during cure is implicitly taken into consideration but formally excluded from the model, making it robust. Normalization scaling results in a vertical shifting of data, which is more evident in the rubbery region than in the glassy domain. In this way, the rubbery modulus is collapsed into a single super-master curve and scatter of data in the glassy region is also slightly decreased.

The trends of both temperature and cure shift functions are displayed below in Figure 5.32. They are complementary in the sense that the response times of polymers depend on them both in a similar fashion. Viscoelastic effects are enhanced as the relaxation time becomes shorter, which is expected if temperature increases and the degree of cure decreases. These state variables have in fact analogous effects on the molecular structure [64, 67]. Dual-shifting enables the development of simplified experimental methodologies and models to characterize viscoelasticity. Notably, the evaluation of viscoelastic properties during cure is of particular interest, as explained in the previous Section. The onset of residual stresses can in fact result in undesired shape distortions, so that the geometry of the final product does not fit the design specifications, or in the weakening of the structure. The glass transition region is where residual stress start to build-up, because below T_g the polymer is not in equilibrium and a certain amount of entropy is "frozen" in the material.

It has been shown by Saseendran et al. that, for thermo-rheologically simple materials, the cure and temperature shift factors are likely to be the same for all viscoelastic properties, namely relaxation modulus, creep compliance, Poisson's ratio, storage and loss modulus [47]. A necessary condition for this is that cure and temperature only affect the reduced time. The fact that all viscoelastic compliance matrix elements have the same shift factor is in agreement with the experimental observation that also the Poisson's ratio exhibits a small dependence on time, despite it is often assumed constant for simplicity. This is mainly for the sake of simulation convenience and due to difficulties in obtaining reliable experimental data. The importance of studying the dependency of Poisson's ratio on state variables is related to the fact that the interaction between fibers and matrix in the transverse direction is critical for the evolution of residual stresses. In particular, the Poisson's ratio of epoxy, that according to manufacturer's specifications is in the range $0.33 \div 0.35$ for fully cured resin, is found to slightly decrease with increasing degree of cure. In the rubbery region, however, there is experimental evidence that it remains constant, and it can be assumed equal to 0.5 with good approximation [14]. It is exactly the weak

time-dependence of the Poisson's ratio that seems to justify the assumption of rheological simplicity [47]. By means of creep testing, O'Brien et al. have shown that it obeys the TTS principle with the same horizontal shifting as other viscoelastic properties [34].
Conversely, thermo-rheologically complex materials display two or more distinct distributions of response functions, each with its own time-temperature dependence. Most of the resins used within composite industry have low-to-medium molecular weight and therefore may be considered thermo-rheologically simple. Accordingly, the viscoelastic model this Thesis is focused on, called VisCoR, will be presented in Section 3.2 also in its simple formulation, which will be then used to perform some simulations in Section 5.6. Adolf and Martin argue that high molecular weight systems tend not to provide unique master curves, because they show a non-linear dependence of shift factors on response time [1]. While the universality of the temperature shift function has been supported by quite abundant experimental evidence, it should be stressed the importance to further investigate if also the cure shifting applies equally well to all the aforementioned properties. If the shift factors are indeed universal, data from dynamic testing and "macroscopic" long term relaxation can be easily compared, using an interconversion between frequency and time [47].
Even though power law fitting is sometimes also employed, the relaxation modulus E_{rel} is usually approximately described using the Prony series [18, 44]. Considering the tensile stress-strain relationship of a linear viscoelastic material in one-dimension

$$\sigma(t) = \int_{-\infty}^{t} E_{rel}\,(\,t - t'\,)\,\frac{d\varepsilon}{dt'}\,dt' \tag{2.6}$$

the relaxation modulus is

$$E_{rel} = E_{\infty} + \sum_{m=2}^{M} E_m \cdot e^{-\frac{t}{\tau_m}} \tag{2.7}$$

where the relaxation time τ_m, the infinite modulus E_{∞} and the constant E_m are found experimentally [44]. If the temperature varies, a new variable is introduced, called reduced time

$$\psi = \int_{-\infty}^{t} \frac{dt'}{a_T(T)} \tag{2.8}$$

and Equation (2.6) has to be modified in

$$\sigma(t) = \int_{-\infty}^{\psi} E_{rel}\,(\,\psi - \psi'\,)\,\frac{d\varepsilon}{d\psi'}\,d\psi' \tag{2.9}$$

TTS is in this case interpreted as the shifting in reduced time of several isothermal plot segments, obtained within a reasonable experimental window. If it is to consider also the effect of varying cure state, the definition of reduced time given by Equation (2.8) has to be re-written by substituting the temperature shift factor a_T with the total shift factor a

$$\psi = \int_{-\infty}^{t} \frac{dt'}{a(T,\alpha)} \tag{2.10}$$

Over the last decades numerous studies have been dedicated to predicting the non-linear viscoelastic behaviour of polymers. One of the most successful models, offering an excellent compromise between accuracy and ease of implementation, has been presented by Schapery using a set of internal state variables [51, 52]. As exposed in Section 3.2, the starting point for its development is the Helmholtz free energy expression, thus ensuring the thermodynamic consistency of the resulting constitutive relationship.
Besides viscoelasticity, also irreversible viscoplastic strains ε_{VP} may develop in polymers and their composites [8, 16, 18]. Their evolution may be effectively characterized by means of Zapas's and Crissman's power law of stress [66]

$$\varepsilon_{VP}(\sigma) = C_{VP}\left\{\int_0^{\frac{t}{t^*}}\left[\frac{\sigma(\tau)}{\sigma^*}\right]^M d\tau\right\}^m \tag{2.11}$$

where C_{VP}, $M$and m are material constants, whereas t^* and σ^* are values of time and stress arbitrarily chosen to obtain dimensionless variables. While the parameter M quantitatively describes the sensitivity to the applied stress level, m is related to the time-dependence itself of the evolution of ε_{VP}. All these parameters may be determined by means of creep and strain recovery tests. Viscoelastic and viscoplastic mechanisms can be separated, so that the total strain can be decomposed in the sum of two terms [45]. Their combined effect controls the equilibrium shape of the part at the end of manufacturing, i.e. after demolding and eventual post-cure, and may cause its premature failure in service. But it is also important to point out that among the phenomena affecting the mechanical performance of composites there is also evolving microdamage, including cracking, debonding, delamination, etc. [21]. Fatigue resistance is herein not considered but may result in elastic properties degradation and the development of irreversible strains, effects that are drastically magnified when the material is exposed to elevated temperatures or if it is only partially cured.

3. Viscoelastic modelling of the thermo-rheological behaviour of thermosets

The manufacturing techniques of polymeric composites are rapidly evolving, allowing to produce parts that meet both the dimensional specifications and the design criteria for strength. Traditionally, components have been developed through trial-and-error methods, resulting in a long and expensive design procedure. In order to minimize the number of experimental loops, thus facilitating the set-up of efficient manufacturing processes, in the last decades the trend in composites design has moved towards virtual methods [4]. However, the development of the so-called computer-aided engineering (CAE) requires an increased understanding of the physics of phenomena that are intended to model. Simulating these processes using numerical methods is very important in order to optimize the production: according to the specific application, the aim is to find out processes that give the optimum between high quality of the final component and cost saving. Nevertheless, these models are nowadays still not very mature. The main reasons of this are the inherently heterogeneous nature of composites and the difficulties in characterizing the resin behaviour in uncured and high temperature conditions.
The prediction of manufacturing-induced residual stresses and deformations is one of the aspects of major interest [62]. As explained in Section 1 and now considering the neat resin, internal stress evolution may be due to various factors: volumetric shrinkage of the resin during curing and the continuous change of its mechanical properties and thermal expansion coefficient; external constraints like the action of the tool on the part; environmental conditions such as thermal gradients and the non-uniform thermal expansion of the tool and the component. The simultaneity of all these phenomena, even in the absence of fibers, significantly complicates the prediction of the onset and development of the residual stress field [65]. Nevertheless, its simulation is of paramount importance in order to minimize shape distortions, by employing compensation methods and procedures for the release of deformations [24, 57].

3.1. Overview of elastic and viscoelastic models

Several numerical models have been developed over the years to predict the processes occurring during the manufacturing of composites. Depending on the desired product quality and the available computational resources, some of them may be more suitable than others in specific applications. Indeed, if the number of input parameters and variables is small, and the discretization level is not too fine, requirements for memory and calculation time are modest. An easier implementation of the model means a lower computational cost, but may however jeopardize the prediction accuracy [45]. Assuming an elastic behaviour of the resin, and of the composite as well, is a too rough approximation of reality. An accurate

description of the material must in fact take into account that time-dependent phenomena are significant even at relatively low temperatures. Viscoelasticity should therefore be included in the model to be representative. The drawback is that viscoelastic testing is time-consuming and numerical implementation of these models is computationally expensive. As a result, the overall characterization cost is higher than merely considering elasticity. The challenge is therefore to develop a viscoelastic model as simple as possible, requiring minimum costs without sacrificing accuracy. This is very important in order to create commercial tools for process simulation that are relevant from an industrial point of view.

Currently, among the most widely used models for the prediction of residual stresses in composites there are the so called CHILE and path-dependent models [5, 32]. CHILE is the Cure Hardening Instantaneously Linear Elastic model and is a very common approach, assuming linear elastic properties within both phases, i.e. the matrix and the reinforcement [22]. Spring-in angles and warpage are usually predicted with sufficient accuracy but frozen-in deformations occurring during cure cannot be taken into account. This is because history-dependent state variables are not considered. The linear elastic path-dependent model has been proposed by Svanberg and Holmberg [58]. It can be said to be an "hybrid" model since elasticity is assumed both in the glassy and rubbery states, but with different elastic constants in the two regions. In this sense it is pseudo-viscoelastic and is therefore an improvement of CHILE model. It considers that stress relaxation and strain recovery are instantaneous in the rubbery state whereas they do not occur at all in the glassy domain. From a mathematical point of view, only two extreme values of the shift factor in reduced time are used: zero and infinity respectively for rubbery and glassy state. Consequently, after the transition to the glassy region, the material retains the strains and stresses which are "frozen" in it, but that are suddenly and completely released when it goes to the rubbery state. This is however a rough approximation of reality. Indeed, stress relaxation and strain recovery also occur quite fast in the glassy region at relatively high temperatures, whereas they still are gradual in the rubbery state. Accordingly, built-in residual stresses and shape distortions predicted using this model are significantly overestimated, as shown by Saseendran et al [45].

Despite being quite easy to implement, the assumptions of the CHILE and path-dependent models do not allow an accurate quantification of residual stresses. Moving on to the more realistic viscoelastic models, it is worth mentioning the ABAQUS implementation made by Benavente et al. to study the relaxation during cure of epoxy reinforced with 3D woven fabric [5]. In this and several other viscoelastic models, the degree of cure and temperature only affect the shift factor. As explained in Section 2, according to the time-temperature-cure superposition (TTCS) principle, both high temperature and low degree of cure shorten the viscoelastic relaxation time. Shift factors change in a quite wide range and they can be determined experimentally, for example in a Dynamic Mechanical Analysis (DMA). Using the DiBenedetto equation, Simon et al. considered the glass transition temperature T_g as the reference point for the expression of the temperature shift factor, thus including in their description the effect of both temperature and cure [54]. The cure-dependency of viscoelastic parameters has been analysed by O'Brien et al. through parallel plate rheometry and three-point bending creep [34]. An attempt to model the cure-dependency of the storage modulus of epoxy has been published by Zarrelli et al. by means of a modified form of Kohlrausch-Williams-Watts (KWW) stretched exponential function [67]. Experimental studies of the viscoelastic behaviour have usually been performed at temperatures below T_g but some recent studies have tried to investigate the dependence on temperature and degree of cure of both glassy and rubbery stiffness [49, 68].

Most of the just mentioned constitutive models are based on the idea of replacing some physical quantities, which are constants in elastic relationships, with functions of temperature and degree of cure. While the

descriptions of the thermo-rheological complex behaviour are usually empirical, the VisCoR model on which the presented Thesis is focused on is thermodynamically consistent. Its complete derivation is a generalization of Schapery's approach, based on the expansion of Helmholtz energy, and has been illustrated by Varna et al., including also the effect of temperature and cure [52, 60]. Once the relationships are written incrementally, simple thermo-rheological behaviour is treated as a particular case of the general complex formulation [45].
As already said, significantly large errors are introduced by the assumption of linear elastic behaviour, because all polymers and polymeric composites behave in a viscoelastic manner. It is still to be clarified whether material properties during cure are linearly or non-linearly viscoelastic with respect to the applied stress or strain level. However, stresses and strains that are encountered in the manufacturing stage are small and therefore it is reasonable to assume linear viscoelasticity [19]. In the light of the theoretical background explained in Section 2, both the operating temperature and parameters of the cure state affect the rate of viscoelastic processes, particularly the rubbery and glassy moduli, and hence need to be included in the model.

3.2. The VisCoR model

Since shape distortions and residual stresses are a disadvantage when high-precision and highly-resistant parts are to be manufactured, several models to predict their development have been implemented in a variety of industrial simulation softwares. The viscoelastic model which is dealt with in this Thesis is called VisCoR and has been developed for thermo-rheologically complex materials. It can be successfully used to analyse the material behaviour under various conditions, including loading and unloading at high temperatures, stress relaxation, stress build-up during cure and following cool-down, etc. [45]. Hence, it is a very general model and straightforwardly adaptable to computational methods. The complete derivation based on Schapery's approach is herein more briefly discussed, focusing on its main steps. Some assumptions are introduced: the material is linear viscoelastic and viscoplasticity is not included; the changes in temperature and degree of cure may have the same time scale as the process; time-derivatives of material functions cannot be neglected. Moreover, for simplicity, the model is presented in one-dimension, thus analysing only uni-axial strains.
Strains due to free thermal expansion and curing are subtracted from the measured strain ε_{total}

$$\varepsilon = \varepsilon_{total} - \left(\varepsilon_{thermal} + \varepsilon_{curing}\right) \tag{3.1}$$

The first terms of the expansion of the Helmholtz free energy function H are written in terms of strain ε and viscoelastic internal state variables (ISVs) ξ_i

$$H = \phi_0(\alpha, T)\frac{\varepsilon^2}{2} - \sum_i \left(A_i^0 \cdot h_1(\alpha, T) \cdot \varepsilon(t) \cdot \xi_i \right) + \frac{1}{2}\sum_{in} \left(B_{in}^0 \cdot a_2(\alpha, T) \cdot \xi_i \cdot \xi_n \right) \tag{3.2}$$

where parameters with upper index 0 are constants. Since strain is defined as the negative first stress-derivative of the energy function, the resulting stress-strain relationship is

$$\sigma = \Omega_0(\alpha, T) \cdot \varepsilon - h_1(\alpha, T) \sum_i \left(A_i^0 \cdot \xi_i \right) \tag{3.3}$$

It is assumed that the ISVs have a linear evolution rate with respect to the conjugated thermodynamic forces

$$f_n = -\frac{\partial H}{\partial \xi_n} \tag{3.4}$$

and that all the coefficients in this linear combination have the same dependence on degree of cure α and temperature T. These two assumptions allow to introduce the reduced time

$$\psi(t) = \int_0^t \frac{1}{a(\alpha, T)} d\zeta \tag{3.5}$$

where a is the total shift factor. It follows that the dependence of ISVs on reduced time is described by a system of linear differential equations with constant coefficients. The solution of this system includes linear combination of exponents with constant relaxation times. The as-expressed ISVs are substituted into the stress-strain relationship, after re-defining some arbitrary constants

$$\sigma = E_r(\alpha, T) \cdot \varepsilon + h_1(\alpha, T) \int_0^{\psi} \Delta C\ (\psi - \psi') \frac{d(h_2(\alpha, T) \cdot \varepsilon)}{d\psi'} d\psi' \tag{3.6}$$

where E_r is the rubbery modulus, relative to the fully relaxed material, h_1 is a weight factor in front of the convolution integral, directly affecting the value of stress at a particular instant, and h_2 is a multiplier factor of strain at the current instant, which depends on how strain has previously changed during the overall loading history. The term ΔC inside the integral is the Prony series

$$\Delta C(t) = \sum_i \left(C^i \cdot e^{-\frac{t}{\tau_i}} \right) \tag{3.7}$$

where C^i are constants and τ_i are constant relaxation times. These two terms are not dependent on degree of cure and temperature as a consequence of the introduction of the reduced time ψ. This is one of the main differences between VisCoR model and other models proposed by Msallem et al. [32], Simon et al. [54], Ding et al. [11]. It is noted that α- and T- dependent functions in Equation (3.6) can be in front of the integral or inside the integral under the sign of derivative or in both places.

As already said, one of the main assets of the as-developed model is its thermodynamical consistency. In order to be made suitable for numerical computation, the model is written in incremental form [45]. Considering the time interval $\Delta t_{k+1} = t_{k+1} - t_k$, the increment of any function f is denoted as $\Delta f^{k+1} = f(t_{k+1}) - f(t_k)$. The upper index is used except for the reduced time. Considering an infinitesimal time-increment, derivatives of these functions are indicated as df^{k+1} and represent their slope at the considered instant. If the time interval Δt_{k+1} is small enough, the viscoelastic parameters can be approximated with linear functions of time. The incremental form of the constitutive equation is

$$\Delta\sigma^{k+1} = \left(\Delta C^{k+1} \cdot \Delta\varepsilon^{k+1} \right) + \Delta {\sigma_R}^k \tag{3.8}$$

containing the Prony series

$$\Delta C^{k+1} = {E_r}^{k+1} + \left\{ {h_1}^{k+1} \sum\nolimits_i \left[C^i \cdot \left({h_2}^k \cdot \Delta \hat{I}_i^{\,k+1} + 2 \cdot \Delta {h_2}^{k+1} \cdot \Delta \widehat{N}_i^{\,k+1} \right) \right] \right\} \tag{3.9}$$

and the stress increment

$$\begin{aligned} \Delta {\sigma_R}^k = & \left(\Delta {E_r}^{k+1} \cdot \varepsilon^k \right) + \left[{h_1}^{k+1} \cdot \Delta {h_2}^{k+1} \cdot \varepsilon^k \cdot \sum\nolimits_i \left(C^i \cdot \Delta \hat{I}_i^{\,k+1} \right) \right] \\ & + \left\{ \Delta {h_1}^{k+1} \cdot \sum\nolimits_i \left(C^i \cdot {S_i}^k \right) - {h_1}^{k+1} \cdot \sum\nolimits_i \left[C^i \cdot {S_i}^k \cdot \left(1 - e^{-\frac{\Delta \psi_{k+1}}{\tau_i}} \right) \right] \right\} \end{aligned} \tag{3.10}$$

The reduced time $\Delta\psi_{k+1}$ and the terms $\Delta \hat{I}_i^{\,k+1}$, $\Delta \widehat{N}_i^{\,k+1}$ and ${S_i}^k$ are calculated as

$$\Delta \psi_{k+1} = \frac{\Delta t_{k+1}}{\Delta a^{k+1}} \cdot \ln\left(1 + \frac{\Delta a^{k+1}}{a^k} \right) = \frac{1}{da^{k+1}} \cdot \ln\left(1 + \frac{da^{k+1}}{a^k} \cdot \Delta t_{k+1} \right) \tag{3.11}$$

$$\Delta \hat{I}_i^{\,k+1} = \frac{1}{da^{k+1} + \frac{1}{\tau_i}} \cdot \left(da^{k+1} + \frac{1 - e^{-\frac{\Delta \psi_{k+1}}{\tau_i}}}{\frac{\Delta t_{k+1}}{a^k}} \right) \tag{3.12}$$

$$\Delta \widehat{N}_i^{\,k+1} = \frac{1}{2da^{k+1} + \frac{1}{\tau_i}} \cdot \left[\frac{a^{k+1}}{\Delta t_{k+1}} - \left(\frac{a^k}{\Delta t_{k+1} \cdot \left(da^{k+1} + \frac{1}{\tau_i} \right)} \cdot \frac{a^{k+1} - \left(a^k \cdot e^{-\frac{\Delta \psi_{k+1}}{\tau_i}} \right)}{\Delta t_{k+1}} \right) \right] \tag{3.13}$$

$${S_i}^k = \left({S_i}^{k-1} \cdot e^{-\frac{\Delta \psi_k}{\tau_i}} \right) + \left[\left({h_2}^{k-1} \cdot \Delta \hat{I}_i^{\,k} + 2 \cdot \Delta {h_2}^k \cdot \Delta \widehat{N}_i^{\,k} \right) \cdot \Delta \varepsilon^k \right] + \left(\Delta {h_2}^k \cdot \Delta \hat{I}_i^{\,k} \cdot \varepsilon^{k-1} \right) \tag{3.14}$$

Qualitatively S may be considered a sort of history internal state variable, telling about previous events the resin was subjected to, and the deriving structural changes. If the shift factor a is constant or changes extremely slowly, in order to avoid numerical inaccuracies, instead of Equation (3.11) it is used the expression

$$\Delta \psi_{k+1} = \frac{\Delta t_{k+1}}{a^k} \tag{3.15}$$

For very small values of the ratio $\Delta\psi_k/\tau_i$, indicatively below 10^{-6}, there are usually problems of numerical instability and it is therefore mandatory to use the first expansion terms in the calculation of

$$1 - e^{-\frac{\Delta \psi_{k+1}}{\tau_i}} = \frac{\Delta \psi_{k+1}}{\tau_i} - \frac{1}{2}\left(\frac{\Delta \psi_{k+1}}{\tau_i} \right)^2 \tag{3.16}$$

Using this approximation in Equations (3.12) and (3.13) it is obtained

$$\Delta\hat{I}_i^{\,k+1} = \frac{1}{da^{k+1} + \frac{1}{\tau_i}} \cdot \left(da^{k+1} + \frac{\Delta\psi_{k+1} \cdot a^k}{\tau_i \cdot \Delta t_{k+1}} \left[1 - \frac{\Delta\psi_{k+1}}{2\tau_i} \right] \right) \tag{3.17}$$

$$\begin{aligned} \Delta\hat{N}_i^{\,k+1} = & \frac{1}{\left(2da^{k+1} + \frac{1}{\tau_i}\right)\left(da^{k+1} + \frac{1}{\tau_i}\right)} \\ & \cdot \left\{ (da^{k+1})^2 + \frac{a^{k+1}}{\Delta t_{k+1} \cdot \tau_i} - \left[\left(\frac{a^k}{\Delta t_{k+1}} \right)^2 \cdot \frac{\Delta\psi_{k+1}}{\tau_i} \cdot \left(1 - \frac{\Delta\psi_{k+1}}{2\tau_i} \right) \right] \right. \\ & \left. + \left[\left(\frac{\Delta\psi_{k+1} \cdot a^k}{\tau_i \cdot \Delta t_{k+1}} \right)^2 \cdot \left(1 - \frac{\Delta\psi_{k+1}}{2\tau_i} \right)^2 \right] \right\} \end{aligned} \tag{3.18}$$

For a thermo-rheologically simple material, some of the above functional dependencies do not exist, namely E_r is assumed as independent on α and T and both h_1 and h_2 are taken equal to 1. This means that the same "importance" is given in Equation (3.6) to the time-dependent viscoelastic contribution and to the previous strain-history. Hence, Equation (3.9), (3.10) and (3.14) simplify in

$$\Delta C^{k+1} = E_r^{\,k+1} + \sum\nolimits_i C^i \cdot \Delta\hat{I}_i^{\,k+1} \tag{3.19}$$

$$\Delta\sigma_R^{\,k} = -\sum\nolimits_i \left[C^i \cdot S_i^{\,k} \cdot \left(1 - e^{-\frac{\Delta\psi_{k+1}}{\tau_i}} \right) \right] \tag{3.20}$$

$$S_i^{\,k} = S_i^{\,k-1} \cdot e^{-\frac{\Delta\psi_k}{\tau_i}} + \Delta\hat{I}_i^{\,k} \cdot \Delta\varepsilon^k \tag{3.21}$$

In Section 5.6 some test cases will be analysed using this simple formulation of the VisCoR model. According to Equation (2.4) the shift factor $a(\alpha, T)$ is calculated as the product of α- and T-dependent functions, so that the effects of cure and temperature are decoupled. Named $t_{c,\infty}$ the time that approximates maximal cure at a given temperature, and by inserting in the parabolic function C in Equation (2.3) the coefficients experimentally determined for epoxy, the cure shift factor a_c is expressed as proposed by Saseendran et al. [45]

$$\log a_c = \left(0.0026 \cdot T_c^{\,2} - 0.0903 \cdot T_c + 1.39\right) \cdot \frac{\left(t_c - t_{\,c,ref}\right)}{60} \tag{3.22}$$

if $t_c < t_{c,\infty}$ and

$$\log a_c = 0 \tag{3.23}$$

if $t_c \geq t_{c,\infty}$. In other words, Equations (3.22) and (3.23) are respectively used for partially and fully cured specimens. In the latter case, in fact, a_c is unit. Times in Equation (3.22) are measured in min and $t_{c,ref}$ is usually arbitrary chosen to attain an 80% reference cure state. Although the cure time and the degree of cure are mutually dependent, the former is more frequently used to define the cure shift function because the relationship is in this case linear.

On the other hand, the temperature shift factor is defined using the Williams-Landel-Ferry (WLF) equation [63]

$$\log a_T = -\frac{c_1 \cdot (T - T_{ref})}{c_2 + (T - T_{ref})} \tag{3.24}$$

where the constants c_1 and c_2 for the given epoxy system are 131.4 and 614.9 K respectively [45]. Of course, if the testing and reference temperatures are equal, a_T is unit. It should be highlighted that logarithms in Equations (3.22), (3.23) and (3.24) have base 10.

The as-developed material model includes the mechanical testing temperature T, and the parameters defining the cure cycle, that is to say the cure temperature T_c and time t_c. Hence, the model takes into account the curing history of the resin, including multi-stage cure profiles comprising several thermal cycles. The mechanical model by Schapery was initially developed in its stress formulation, with parameters identified in creep tests [53]. However, most of the numerical codes used for structural analysis in composites, as well as analytical micromechanics models and the classical laminate theory require constitutive equations that express stresses as a function of applied strain. In order to simulate the more common strain-controlled tests, the VisCoR model has been herein presented in its strain formulation [60]. Strain has therefore been used as an input variable and the appearing parameters are strain-dependent, meaning that they are obtained from relaxation tests, in which deformation is kept constant. The eventual development of viscoplasticity may however complicate their identification. If the material is non-linearly viscoelastic with respect to stress and strain level, stress and strain formulations are theoretically speaking incompatible [39]. The simple reversal of the stress-based model does not lead to the correct strain formulation. For reasons that are still not totally understood, such inversion is possible only if the stress form is first re-written incrementally.

As mentioned in Section 3.1, it has been shown by Saseendran et al. that the path-dependent model is a particular case of VisCoR model in its simple form, assuming extreme values of the shift factor a: infinite and zero respectively below and above the glass transition temperature T_g. From a computational point of view, they have been assumed equal to 10^8 and 10^{-8} respectively [45]. Even though the identification of phenomenological variables and parameters may be more difficult, VisCoR model can also be applied to study the complex material behaviour during cure. The development of time-dependent internal stresses and the related potential distortion of structures are the most interesting aspects [7]. However a multitude of factors has to be considered, including temperature changes and thermal gradients, progressing cross-linking resulting in chemical shrinkage, non-uniform thermal expansion, constraints applied from fibers or from larger scale elements, such as the mold or tools, etc.

4. Materials and methods

The experimental part of the project is to manufacture differently cured epoxy specimens and to characterize their viscoelasticity in function of testing temperature and cure state. Several mechanical tests are designed in order to reveal the most significant viscoelastic phenomena: tensile loading-unloading, creep and strain recovery, stress relaxation. Test results are then used to verify the accuracy of the proposed VisCoR model.

4.1. Manufacturing

The studied material is an epoxy system made of two chemicals, both produced by ABIC Kemi AB: the low viscosity epoxy resin *Araldite LY 5052* and the hardener *Aradur 5052 CH*. Araldite is a blend of 1,4-butanediol diglycidyl ether and epoxy phenol novolac. Aradur is a mixture of polyamines: 2,2'-dymethil-4,4'-methylenebis (cyclohexylamine), 3-aminomethyl-3,5,5-trimethylcyclohexylamino and 2,4,6-tris(dimethylaminomethyl)phenol. Some data relative to the two components are shown in Table 4.1 according to a global manufacturer [70].

Table 4.1 Some properties of the employed resin and hardener

Araldite LY 5052		
aspect (visual)	clear liquid	
UN classification	3082	
viscosity at 25°C (ISO 12058-1)	1000 ÷ 1500	[$mPa\ s$]
density at 25°C (ISO 1675)	1.17	[g/cm^3]
epoxide index (ISO 3001)	6.65 ÷ 6.85	[eq/kg]
Aradur 5052 CH		
aspect (visual)	clear liquid	
UN classification	2922	
viscosity at 25°C (ISO 12058-1)	40 ÷ 60	[$mPa\ s$]
density at 25°C (ISO 1675)	0.94	[g/cm^3]
amine value (ISO 9702)	9.55 ÷ 9.75	[eq/kg]

This matrix system is very common for many industrial composites and suitable for different kinds of processing, including wet lay-up, resin transfer molding, pressure molding and filament winding. Its low viscosity allows easy impregnation of the reinforcement and its long pot-life is appropriate for the ample

processing time required to produce big objects. Relatively high temperature resistance and good mechanical and dynamic properties are obtained after ambient cure, and especially after post-cure at elevated temperatures.

The resin and the hardener are mixed in the ratio $100 \div 38$ by weight, or equivalently $100 \div 47$ parts by volume. In order to obtain optimal properties of the specimens and repeatability in the results, the components must be weighted accurately and stirred properly. In industrial applications it is important to consider that large mix quantities will show considerable exotherm, leading to short pot-lives. This problem is not encountered in laboratory practice, being the batch usually small and used just after its preparation. According to UN classification, the resin is environmentally hazardous whereas the hardener is corrosive and toxic; therefore safety precautions must be taken in handling and disposal. Mixing must be done thoroughly but taking care to limit air bubbles as much as possible, even though they are subsequently removed by degassing in a vacuum system.

The mold is made of silicon rubber and it is sandwiched between two aluminium plates, covered with Teflon sheets. This setup supports the mold and assists the heat transfer in the oven, at the same time avoiding the sticking of the resin. The assembly is clamped securely to prevent leakage once the mixed resin is poured into it. Pouring is performed slowly and preventing air entrapment. Although the optimum cure cycle has to be determined case by case, depending on the processing and economic requirements, typical heat treatments have been drawn up in order to obtain specimens with the desired degree of cure, as shown in Table 4.2.

Table 4.2 Curing temperatures and times and the attained degrees of cure

	DoC	temperature	time
fully cured	1	RT + 105 °C	24 h + 4 h
partially cured	0.74	70 °C	30 min
	0.83		40 min
	0.89		55 min
	0.91		70 min

Therefore, for fully cured specimens pouring is performed at room temperature and curing is completed after one day, by putting the filled mold in a convection oven at $105\ °C$ for $4\ h$. Instead, for partially cured specimens the mix is poured into the mold preheated at $70\ °C$ and kept at this temperature for a time increasing with the degree of cure to get. In order to stop curing at the wanted percentage, partially cured specimens must be cooled down by means of compressed air immediately after they are taken out of the oven and they are then stored in the freezer until their testing.

The obtained specimens are parallelepipeds with nominal dimensions in mm $200 \times 15 \times 4$. Their preparation is done just before the tensile test through mechanical grinding of their sides with sandpaper P240 at about $350\ rpm$. This is done to prevent premature damage due to edge effects. Particularly for partially cured specimens, water is used abundantly in order to limit frictional heating and the consequent local increase in the degree of cure. Exact width w and thickness t of each specimen are measured with a caliper and two small pieces of sandpaper are glued at the ends of the gauge length, equal to $50\ mm$, so that the slipping of the extensometer is hindered. The choice of using the pouring technique is due to the need to manufacture also partially cured specimens; indeed cutting specimens from a previously produced

plate would determine a local increase in temperature and therefore would not allow a quick and easy way to cease the curing process at the desired degree.
The cure cycles reported in Table 4.2 for partially cured specimens have been determined by means of the well-established Kamal's cure kinetic model, which describes the curing rate as an analytical function of temperature T, in K, and the instant degree of cure α [23]

$$\dot{\alpha} = \frac{d\alpha}{dt} = A \cdot e^{-\frac{B}{RT}} \cdot \alpha^m \cdot (\alpha_{max} - \alpha)^n \tag{4.1}$$

where $A = 274906\ s^{-1}$ is the pre-exponential term, representing the rate constant, $B = 54888\ J/mol$ is the reaction energy, R is the ideal gas constant, $m = 0.25$ and $n = 1.01$ are constants independent of cure temperature that are obtained from least-squares fitting of Differential Scanning Calorimetry (DSC) data. Named T_c the curing temperature in $°C$, α_{max} is the maximum degree of cure attainable at that temperature, calculated using the following equation, that likewise results from the linear fitting of experimental DSC data [58]

$$\alpha_{max} = (0.002 \cdot T_c) + 0.782 \tag{4.2}$$

The plot of this relationship is the straight line in Figure 4.1, having slope 0.002 and intercept 0.782. The three temperatures that are selected for the manufacturing of partially cured specimens, that is to say 50, 70 and 90 $°C$ are marked with circles. Values of α_{max} calculated at these temperatures are 0.882, 0.922 and 0.962 respectively. Only if the degree of cure of the produced specimens is higher than 0.828, which is α_{max} at RT, storing them in the freezer is just a precaution, since in principle the degree of cure should not increase.

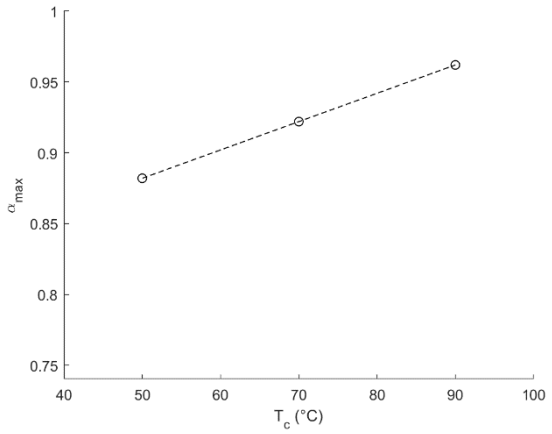

Figure 4.1 Plot α_{max} VS T_c marking the three temperatures used in the manufacturing, namely 50, 70 and 90 $°C$

By replacing the derivative in Equation (4.1) with right-sided finite differences

$$\dot{\alpha} = \frac{\alpha_{k+1} - \alpha_k}{\Delta t_{k+1}} = A \cdot e^{-\frac{B}{RT}} \cdot {\alpha_k}^m \cdot (\alpha_{max} - \alpha_k)^n \tag{4.3}$$

it is possible to plot the trend of the degree of cure for any curing history, as will be illustrated with some examples in Section 5.1. This is done by step-wise calculating the current degree of cure α_{k+1} at each temperature of the thermal cycle, as long as $\alpha_k < \alpha_{max}$. When α_k equals α_{max} there is no more curing and the degree of cure remains constant. It appears that considering the time interval $\Delta t_k = 1\ s$, in order to discretize the temperature ramp, results in a more than enough accurate numerical evaluation of the cure profile. The equation can be reversed in order to calculate the heating time required to obtain a specific degree of cure in a certain thermal cycle. Although the real trend is asymptotic, it is in this way possible to determine the "infinite" cure time, that is to say the time after which α_{max} is approximately reached at the relative temperature. For 50, 70 and $90\ °C$, this time is assumed equal to 30179, 9110 and $3135\ s$ respectively.

As will be shown clearly by the experimental results in Section 5, the viscoelastic behaviour of epoxy seems not only affected by the degree of cure, but also by the thermal cycle used to achieve that degree of cure. Indeed, this affects the rate of phase change, thus resulting in slightly different arrangement of polymeric chains in the network structure. In order to observe this effect, the same procedure is used to calculate the time, in min, needed to cure the epoxy at 50 and $90\ °C$ to the same degrees shown in Table 4.2. For the sake of completeness, Table 4.3 also reports times at $70\ °C$, which are of course the same given above. Being 0.882 the maximum degree of cure achievable at $50\ °C$, higher percentages are not possible.

Table 4.3 Times, in min, to attain various degrees of cure at different temperatures

$T_c\ (°C)$	degree of cure			
	0.74	0.83	0.89	0.91
50	110	155	–	–
70	30	40	55	70
90	9	12	14	16

Again in order to investigate the effect of curing history, 88.2% cured specimens are manufactured also at 70 and $90\ °C$, requiring 51 and $14\ min$ respectively. It should be pointed out that of course control over the attained degree of cure cannot be extremely accurate in practice. There are in fact several aspects that may introduce small uncertainties in the manufacturing process, such as the exact temperature in the oven and the times taken to pour the resin and to remove the specimens from the mold and to cool them down. Moreover, stopping cure at the desired percentage can be tricky due to the very fast reaction kinetics. Table 4.3 shows that, by increasing the curing temperature, time in the oven is significantly reduced because the cure profile is initially steep, as visualized below in Figure 5.1. Some DSC analyses performed herein and others presented by Saseendran et al. [44] seem to prove quite good agreement between the degree of cure predicted from Kamal's equation and the measured value. However, further study should be done on the reliability of the characterization by means of DSC. As explained in Section 2, the glass transition temperature T_g can be empirically quantified as a function of the degree of cure α using the DiBenedetto relationship [9]. By substituting into Equation (2.1) the parameters typical of epoxy, i.e. $T_{g,0} = -40\ °C$, $T_{g,\infty} = 136\ °C$ and $\lambda = 0.44$, T_g is calculated for all the manufactured degrees of cure. Its values vary in a very wide range and are reported in Table 4.4 and plotted in Figure 4.2. It is seen that the lower is α the lower is T_g. Its maximum value is $136\ °C$ for fully cured specimens, that is to say after post-cure.

Table 4.4 T_g calculated for various degrees of cure using the DiBenedetto equation

α	0.74	0.83	0.882	0.89	0.91	0.922	0.962	1
$T_g(°C)$	57.41	79.78	94.73	97.18	103.52	107.46	121.42	136.00

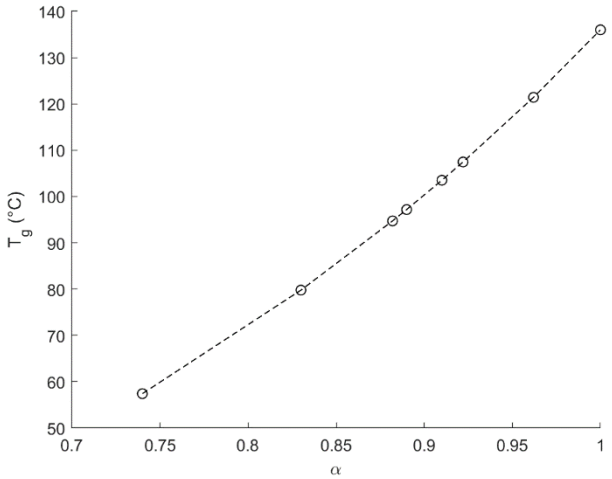

Figure 4.2 Trend of T_g versus degree of cure according to the DiBenedetto equation

Specimens with the lower degrees of cure are very soft when removed from the mold because they are close or even above their glass transition. In addition to the necessity of avoiding additional cure, this is another reason for the impossibility of testing these specimens at high temperatures. It has been found by Saseendran et al. that the gelation point for the considered resin system is at 64% cure state, below which the resin is effectively liquid [49].

4.2. Mechanical testing

The mechanical characterization of epoxy specimens is done using an Instron 3366 tensile testing machine, equipped with 10 kN load cell and manual grips. The distance between grips is 100 mm. In the clamping zones the specimen is wrapped by dense metallic nets or pieces of sandpaper, in order to improve its fixing and especially to protect it from superficial cracking. Axial strain is measured using a standard Instron 2620-601 dynamic extensometer which is attached to the gauge length, equal to 50 mm, by means of numerous rubber bands. Its slipping is prevented by the sandpaper previously glued on the specimen. A temperature chamber is used to perform tests above room temperature. After being mounted in the testing machine, specimens are visually assessed to see if they are deformed, especially those with low degree of cure.

Three principal methods are set up to highlight the dependence of viscoelasticity on testing temperature and cure state: tensile loading-unloading, creep and strain recovery, stress relaxation. Differently from composite materials, neat epoxy specimens can be considered perfectly isotropic [36]. Of course, uni-axial tests also determine a mechanical response in the transverse direction, which is controlled by the Poisson's ratio. Only if it is 0.5%, the principle of volume conservation is valid.

In order to avoid post-cure during the test, partially cured specimens should never tested at a temperature to which corresponds an α_{max} higher than their current degree of cure. Indeed, if the increase in the degree of cure was not negligible, corrections would have to be applied to the dataset to counteract the temporal change in mechanical properties. Specimens having degree of cure 0.74 are however tested with the loading-unloading mode at RT because additional curing is extremely slow compared to the duration of the test itself.

4.2.1. Tensile loading – unloading

This testing method consists of axially loading the specimen at $2\ mm/min$ until longitudinal strain equals 0.5% and then unloading it at the same speed until load is $1\ N$. This final value of load is chosen to avoid compression on the specimen and, with good approximation, corresponds to zero applied stress. As already stated, the chamber is used for tests above room temperature. In this case the profile imposed by the machine is modified to enable the specimen to heat up to the testing temperature and to allow its almost free thermal expansion: a constant load of $2\ N$ is kept for $20\ min$ just before the loading ramp. The test and the heating process are started simultaneously. In this way, the central part of the specimen has plenty of time to reach the same temperature as the chamber and its longitudinal expansion is not hindered by clamping. Again, the stress associated with this small load can be considered approximately zero. In its absence however, there would be buckling of the specimen because its elongation during heating at high temperature is not permitted by stationary grips. A permanent deformation would be observed, with the specimen bulging towards the side on which the extensometer is attached. This is due to the bending moment applied by the extensometer, whose weight is small but still considerable in unstable equilibrium.
The occurrence of strain recovery at high temperatures can be observed by holding a constant load of $2\ N$ after the unloading ramp. In order to avoid the risk of compressive stresses in the specimen, the unloading rate is lowered to $-0.25\ mm/min$ in the final part of the ramp, more precisely between $5\ N$ and $2\ N$. Strain relaxation, if present, could provide a way to recover deformations induced by industrial manufacturing [64]. This is of course true if deformations are within the viscoelastic limits: eventual viscoplasticity cannot be nullified by heating at high temperature.

4.2.2. Creep and strain recovery

Creep and strain recovery is performed at high temperature, namely $110\ °C$ and $70\ °C$. Being the test quite long, it is essential not to additionally cure the specimen. Therefore, it is done only on fully cured specimens and on those having degree of cure greater than or equal to the α_{max} corresponding to the testing temperature. As for the loading-unloading method, almost-free thermal expansion of the resin is allowed by applying a constant load of $2\ N$ for $20\ min$ just before the actual test. The constant axial creep stress is set as equal to the approximate average maximum stress resulting from the previous

loading-unloading tests on fully cured specimens at $110\,°C$, whose calculated value is $6\,MPa$. For each specimen, the value in N of the creep load F is given by the product of the creep stress and the cross-sectional rectangular area, in mm^2

$$F = 6\,MPa \cdot (w \cdot t) \tag{4.4}$$

The load is maintained for 10 and $30\,min$ respectively for the test at 110 and $70\,°C$. This is because, as known, the effect of creep is enhanced by temperature [56]. The specimen is then unloaded to $2\,N$ and maintained at this almost-zero condition for $12h$, in order to allow strain recovery. According to literature, recovery requires a time 8-fold longer than the constant loading [50]. Nevertheless, some preliminary tests have shown that strain recovery needs more time to occur to any significant extent.
With respect to the much longer creep and strain recovery, the loading and unloading ramps can be assumed as applied instantly. Both of them are subdivided in order to enable the machine to properly control the load. More specifically, loading is done at $5\ mm/min$ until $90\%\,F$ and then at $2\ mm/min$ until F is reached. After the creep itself, the specimen is unloaded sequentially to $20\,N$ at $-5\ mm/min$, to $7\,N$ at $-2\ mm/min$ and to $2\,N$ at $-0.1\ mm/min$.

4.2.3. Stress relaxation

Stress relaxation is carried out at the same temperatures used for creep, that is to say $110\,°C$ and $70\,°C$. In order to avoid additional cure, the test is limited to specimens with degree of cure at least equal to the α_{max} calculated for the testing temperature. Again, a constant load of $2\,N$ is applied for $20\,min$ in order to allow the specimen to heat up uniformly without hindering its expansion. The loading ramp is controlled in strain with a rate of $2\%/min$ until 0.45% and thereafter of $0.1\%/min$ until 0.5%. The reached axial strain level is maintained constant for $12\,h$, the same time used in strain recovery. The residual stress is then unloaded to $5\,N$ at $-2\ mm/min$ so that the demounting of the specimen from the machine is easier.

5. Results and discussion

Table 5.1 shows the combinations of testing temperature, degree of cure and curing temperature selected to run the experimental methods described in Section 4.2.

Table 5.1 Cure cycle, resulting degree of cure and temperature used for each mechanical test

test method	cure cycle	degree of cure	testing temperature
tensile loading-unloading	24 h at RT + 4 h at 105 °C	1	RT 50 °C 70 °C 90 °C 110 °C
	30 min at 70 °C	0.74	RT
	40 min at 70 °C	0.83	
	55 min at 70 °C	0.89	
	70 min at 70 °C	0.91	
	110 min at 50 °C 9 min at 90 °C	0.74	RT
	155 min at 50 °C 12 min at 90 °C	0.83	
	maximally cured at 50 °C	0.882	RT 50 °C
	maximally cured at 70 °C	0.922	RT 50 °C 70 °C
	maximally cured at 90 °C	0.962	RT 50 °C 70 °C
	51 min at 70 °C	0.882	RT 50 °C
	14 min at 90 °C	0.882	RT 50 °C
creep and strain recovery	24 h at RT + 4 h at 105 °C	1	70 °C 110 °C
	maximally cured at 70 °C	0.922	70 °C
	maximally cured at 90 °C	0.962	
stress relaxation	24 h at RT + 4 h at 105 °C	1	70 °C 110 °C
	maximally cured at 70 °C	0.922	70 °C
	maximally cured at 90 °C	0.962	

Room temperature RT is assumed to be equal to $23\ °C$. All the tests at higher temperature are performed in the convection chamber of which the Instron 3366 tensile testing machine is provided with. Raw data are processed in MATLAB to find out the most significant results and correlations. Strain ε is given in percentage and stress σ, in MPa, is calculated by dividing the load, in N, by the specimen cross-sectional area A, which is equal to the product of its initial width w and thickness t, both in mm

$$\sigma = \frac{F}{A} = \frac{F}{w \cdot t} \tag{5.1}$$

The "shifted" values of load $F_{shifted}$ and strain $\varepsilon_{shifted}$ are considered, given by subtracting the initial values assumed by such variables, that is to say at the very beginning of the actual test and corresponding to an almost-zero stress condition

$$F_{shifted} = F_{real} - F_{initial} = F \tag{5.2}$$

$$\varepsilon_{shifted} = \varepsilon_{real} - \varepsilon_{initial} = \varepsilon \tag{5.3}$$

$F_{shifted}$ is very close to the real load, measured by the machine, whereas $\varepsilon_{shifted}$ excludes the strains due to thermal expansion and, if there is additional curing, due to chemical shrinkage, as expressed by Equation (3.1). Multiple tests, performed consecutively on the same specimen, are in this way readily analysed [40]. For simplicity the shifted load and strain will be hereinafter denoted without subscript. Trends of the average quantities calculated for each test are visualized along with error bars, in order to have an indication of the variability of data in the reported measurement. For increased statistical significance, four specimens are tested under the same set of experimental conditions. Usually for the most time-consuming experiments, only two specimens are considered. All the error bars below represent one standard deviation of uncertainty. Because of the relatively reduced number of data points, mean values are simply interconnected with segments.

5.1. Numerical evaluation of cure kinetics

As stated in Section 2, cure kinetics can be modelled with great accuracy by means of Kamal's equation and its differential form [23]. Several thermal cycles are designed, resulting from combinations of three "building blocks": constant temperature, increase of temperature with constant rate, transient conduction inside the specimen. It is in this way possible to simulate different curing histories, thus assessing whether they determine significant differences in the profile DoC VS time. By substituting the temperature changes along time into Equation (4.3) the degree of cure α is calculated at each instant. A time interval Δt_{k+1} equal to $1\ s$ is considered in order to trace some remarkable plots.

Curing at constant temperature starting from the completely uncured state is illustrated in Figure 5.1 at the three temperatures used in the manufacturing of specimens: 50, 70 and $90\ °C$. The thermal chamber and the specimen are considered to be under isothermal conditions. At each temperature the maximum degree of cure α_{max} is calculated through Equation (4.2), resulting equal to 0.882, 0.922 and 0.962 respectively. The "infinite" times required to achieve these asymptotes are approximately computed by

inverting Kamal's equation and are respectively 30179, 9110 and 3135 s. It is seen that the cure profile becomes much steeper increasing the temperature, meaning that a specified degree of cure is reached in a shorter time. The final plateau starts earlier for higher curing temperatures. The same procedure is used to determine the other curing cycles described in Section 4.1 and reported in Table 5.1.

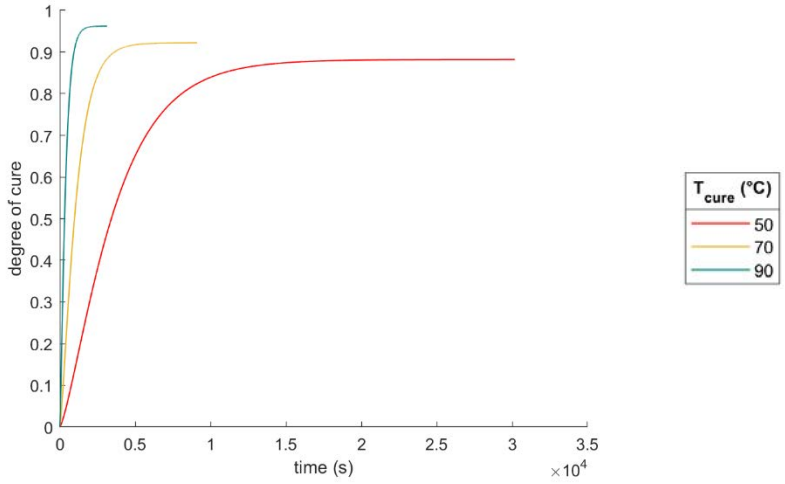

Figure 5.1 Increase of the degree of cure with time at various curing temperatures

As a preliminary study for the following mechanical tests, the increase of degree of cure during the applied 20 min heating stage is simulated. By estimating the heating rate of the thermal chamber as about 0.2 $°C/s$, temperature is considered to increase with constant rate from room temperature to the testing temperature and is then kept constant for the remaining time interval. Temperature in the specimen at each instant is assumed equal to that of the chamber. Profiles resulting from Kamal's equation are plotted in Figure 5.2 starting from the lowest degree of cure manufactured, i.e. 0.74. It is obviously observed that the final degree of cure increases with the final testing temperature. More evidently for the higher testing temperatures, it is noted that as temperature increases over time, the instantaneous increment of the degree of cure becomes larger before tending to a plateau.

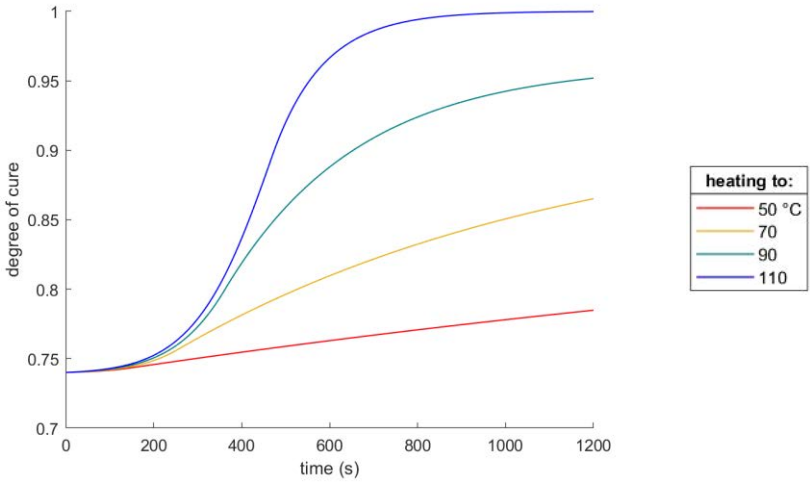

Figure 5.2 Increase of the degree of cure with time from 74% during heating at constant rate from RT to various testing temperatures

A more realistic and detailed temperature ramp inside the specimen occurs according to transient conduction mechanism, for simplicity considered one-dimensional [29]. Again using a time unit of $1\ s$ and a total time of $20\ min$, the temperature profile $T(t)$ is found from the relationship

$$\frac{T - T_\infty}{T_i - T_\infty} = A_1\, e^{\left(-{\lambda_1}^2 \frac{\alpha\, t}{L^2}\right)} \tag{5.4}$$

where T_i is room temperature, assumed equal to $23\ °C$, T_∞ is the testing temperature and L is half thickness of the specimen, i.e. $2\ mm$. Indeed, it is mainly the smaller dimension that controls heating in its centre. The introduced parameters are the coefficient A_1, the dimensionless eigenvalue λ_1 and the thermal diffusivity α. Typical values for epoxy are 1.0577, 0.5642 and $4.2193 \cdot 10^{-7}\ m^2/s$ respectively. In this way the heating dynamics of the resin is considered, when exposed to an air flow at the constant temperature T_∞. By substitution of the as-determined temperature exponential into Kamal's equation, the cure profiles are plotted in Figure 5.3. The color legend is the same as for Figure 5.2. Curves are similar to the previous case, but there is faster increase in the degree of cure to parity of time. The values of degree of cure attained after $20\ min$ are almost the same for the two thermal ramps.

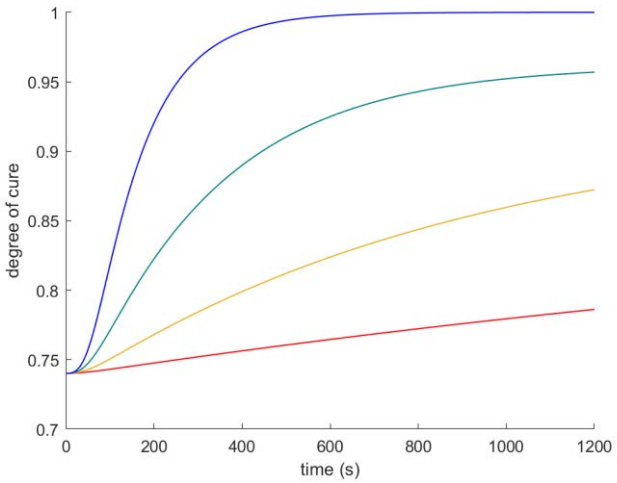

Figure 5.3 Increase of the degree of cure with time from 74% during heating from RT to various testing temperatures, according to the transient solution

It should be pointed out that the cure profiles that have been traced are theoretical, in the sense that they are predicted using Kamal's relationship. Despite being a well-established model, more research may be needed to verify its accuracy, by comparison with the experimentally measured degree of cure. As mentioned in Section 4.1, a common technique is Differential Scanning Calorimetry (DSC) [46]. What is more interesting for the purposes of this work is to verify that additional cure during the heating stage can be ruled out. In principle, it is avoided by the selected cure states and testing temperatures, listed in Table 5.1. A small piece of material is therefore cut from the same specimen before and after its tensile testing. Great amount of water is used in the cutting machine in order to limit local frictional heating as much as possible. As usual for partially cured resin, these small fragments are stored in the freezer in order to exclude with absolute certainty their additional curing in the meanwhile. They are then characterized by means of isothermal DSC measurement at 105 and $200\ °C$.

The degree of cure α is defined as [47]

$$\alpha = 1 - \frac{\Delta H}{\Delta H_R} \tag{5.5}$$

where ΔH is the residual heat of reaction and ΔH_R is the total heat of reaction, which has been determined equal to $482\ J/g$ for the given resin system [48]. By measuring from the DSC pattern the area of the exothermic peak, equivalent to the residual enthalpy ΔH, the degree of cure is calculated for the two pieces of material. If the two values are the same or very similar, it means that there has been negligible cure during the test. This seems to be confirmed by few measurements runned herein. However, more tests should be carried out on specimens with different degrees of cure, taking into account that DSC is a quite expensive technique because of the supply of liquid nitrogen. As already stated in Section 4.1, the reliability of DSC measurement is another aspect to be verified. In all the experiments presented below, post-curing is neglected, meaning that the degree of cure remains constant throughout the test.

5.2. Experimental investigation of thermal expansion

The definition of $\varepsilon_{shifted}$ according to Equation (5.3) allows to disregard the effect of thermal expansion of epoxy when heated to a certain temperature. As explained in Section 4.2 buckling of the specimen is avoided thanks to the maintenance of $2\ N$ during the heating stage, in all experiments lasting $20\ min$. Since this can be considered an almost-zero stress condition, the measured strain is attributable to thermal expansion. This is of course true if there is no additional cure, that is to say if epoxy is fully cured or if it is not exposed to a temperature at which α_{max} is higher than the current degree of cure. Instead, if the degree of cure of the specimen was lower than the maximum attainable at the temperature used in the test, calculated using Equation (4.2), there would be chemical shrinkage due to further cross-linking. Hence, taking care not to increase the degree of cure, it is possible to investigate the effect of thermal expansion on differently cured specimens as they are heated to the temperatures used in the tests.
Figure 5.4 is the plot normalized strain VS normalized elapsed time, relative to fully cured specimens heated from room temperature to various testing temperatures. The same typical shape is observed for all of them. Normalized quantities are obtained by dividing the measured values by those at the end of the heating stage. This allows to have the curves of the four specimens overlapping after a certain time, approximately equal to $700\ s$. The coefficient of linear thermal expansion CTE is herein assumed constant in the considered temperature interval ΔT. Called $l_0 = 50\ mm$ the initial gauge length of the specimen, its elongation due to thermal expansion is

$$\Delta l = l - l_0 = CTE \cdot l_0 \cdot \Delta T \tag{5.6}$$

By reversing this formula, CTE is defined as the ratio of strain at the end of heating and the temperature difference

$$CTE = \frac{\Delta l}{l_0 \cdot \Delta T} = \frac{\varepsilon}{\Delta T} \tag{5.7}$$

The as-calculated values, averaged between the four specimens tested at each temperature, are listed in Table 5.2, together with the time required to reach 90%, 95% and 99% of the final strain. This provides an indication of the rate with which thermal expansion occurs. Even though these values of the coefficient of thermal expansion are a rougher estimation than performing linear regression, it seems that they tend to increase with the temperature difference. It is therefore likely that CTE is not constant but changes with temperature. Given a certain percentage of the maximum thermal strain, the time needed to reach it increases with the final temperature. This is more obvious and in agreement with the assumption of constant heating rate of the chamber, evaluated as about 0.2 $°C/s$.

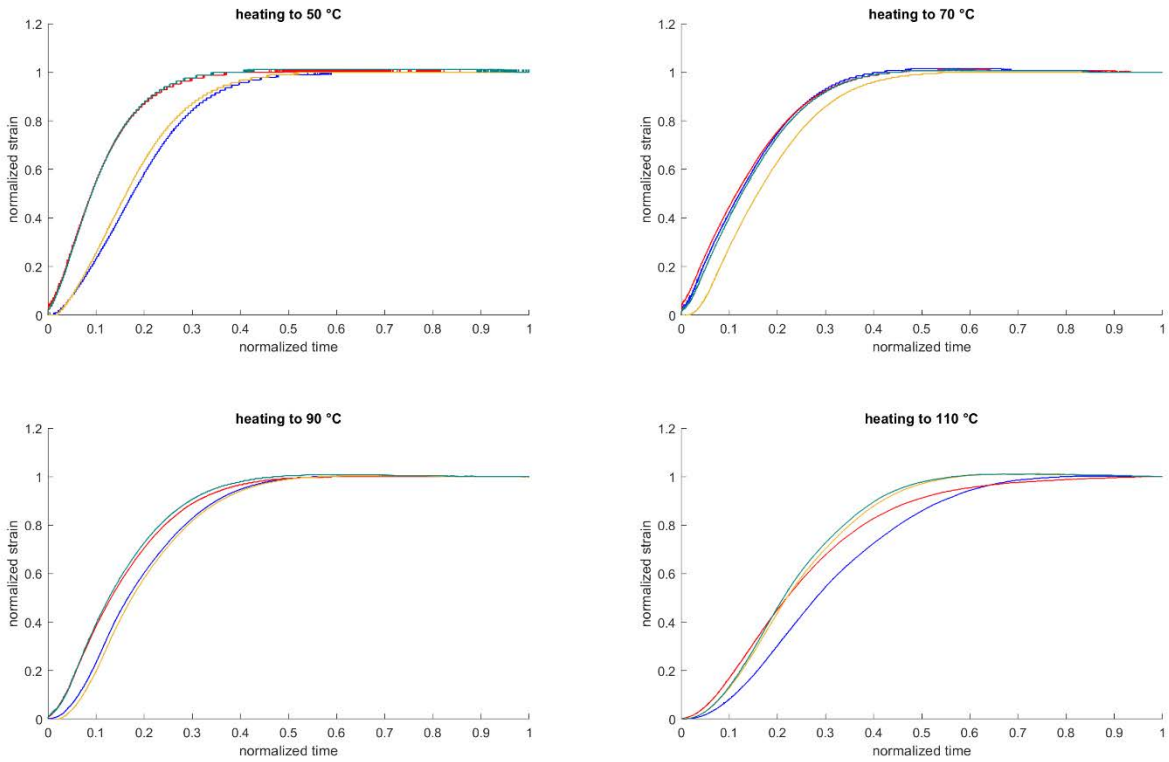

Figure 5.4 Normalized strain VS normalized time plots for fully cured specimens heated from RT to various testing temperatures

Table 5.2 CTE of fully cured specimens, subjected to various heating ramps starting from RT, and times required to reach increasing percentages of maximum strain

heating to	CTE $(10^{-5}\ °C^{-1})$	time (s) to reach % of final strain		
		90%	95%	99%
50 $°C$	3.3148	317.5	377.4	467.7
70 $°C$	3.5213	343.6	402.3	484.3
90 $°C$	4.2761	383.5	450.8	548.6
110 $°C$	5.0316	501.1	579.4	703.3

Thermal expansion during the 20 min heating stage is also investigated for specimens maximally cured at various temperatures. Their degrees of cure are 0.882, 0.922, and 0.962, resulting from treatment at 50, 70, and 90 °C respectively. The considered specimens are exposed to two heating ramps, from RT to 50 °C and subsequently from 50 to 70 °C. Normalized strain VS normalized time curves are traced in Figure 5.5, showing also fully cured specimens for comparison.

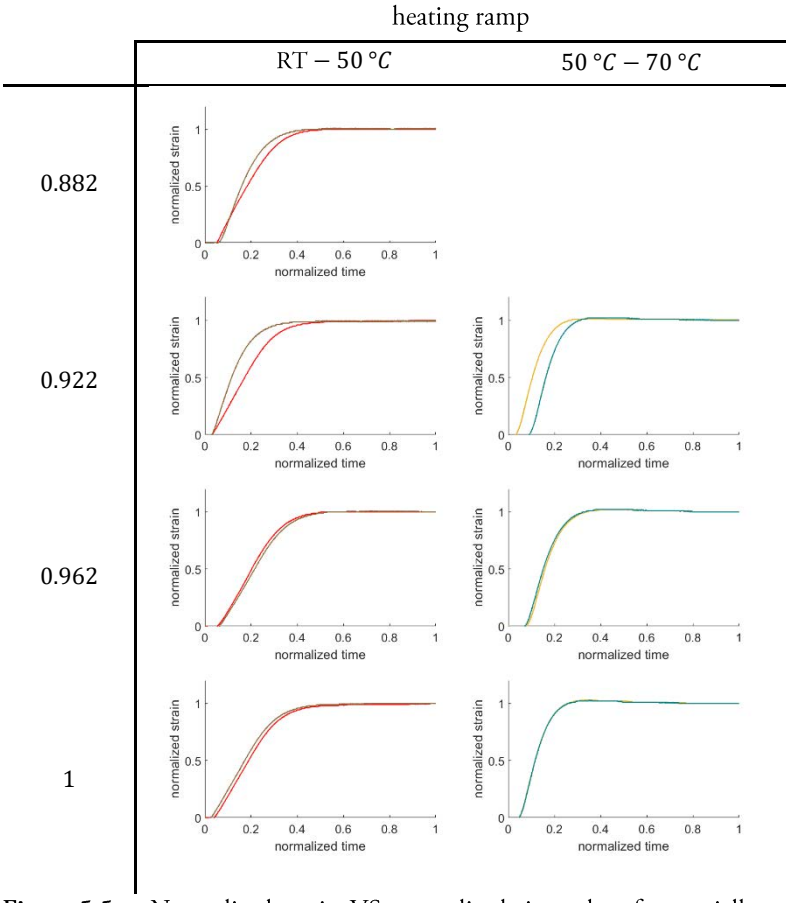

Figure 5.5 Normalized strain VS normalized time plots for partially cured specimens heated from RT to 50 °C and from 50 to 70 °C

Table 5.3 CTE for various partially cured specimens in specified heating ramps, and times required to reach increasing percentages of maximum strain

degree of cure	heating ramp	CTE $(10^{-5}\ °C^{-1})$	time (s) to reach % of final strain		
			90%	95%	99%
0.882	RT − 50 °C	3.8148	366.0	416.7	500.1
0.922	RT − 50 °C	3.4630	332.0	399.8	521.2
	50 °C − 70 °C	4.7750	256.2	284.2	320.5
0.962	RT − 50 °C	3.6852	426.1	484.4	566.7
	50 °C − 70 °C	4.7000	272.3	328.3	371.5
1	RT − 50 °C	3.7963	405.3	476.7	638.5
	50 °C − 70 °C	4.7000	230.9	258.0	291.0

Specimens cured at $50\,°C$ are not taken to $70\,°C$ because otherwise there would be additional cure. Table 5.3 reports the calculated CTEs and the times at which 90%, 95% and 99% of the final strain is achieved. CTEs calculated in the range RT $-$ $50\,°C$ are quite similar to each other and even more those in the interval $50-70\,°C$. As regards the rate of thermal expansion, generalizations cannot be made from the available data. It appears that specimens cured at 50 and $70\,°C$ elongate faster between RT and $50\,°C$. Instead fully cured specimens are those whose expansion occurs at shorter times between 50 and $70\,°C$.
It is worth mentioning that, if there is a concurrent increase in the degree of cure, the profiles of strain versus time during the heating stage are much more complicated and consequently deeper study should be done to interpret them. By analogy with Equation (5.7), strain due to cure may be expressed as

$$\varepsilon_{curing} = CCS \cdot \Delta\alpha \tag{5.8}$$

where $\Delta\alpha$ is the variation in the degree of cure, of course greater than or equal to zero, and CCS is the defined coefficient of chemical shrinkage [45]. As already said, additional cure is avoided by the selected experimental conditions. After briefly examining thermal expansion, the following chapter focus on the mechanical tests themselves.

5.3. Tensile loading – unloading

Loading-unloading is initially performed on fully cured specimens in order to evaluate the effect of temperature. Indeed, there is certainly no additional curing during the test. The same method is then conducted on partially cured specimens at constant room temperature to find out the dependence on the cure state. Viscoelasticity is in this way assessed at various extents of the cross-linking reaction. As explained above in Section 2, temperature shift factors a_T and cure shift factors a_c are the parameters that are used to report data obtained in specific experimental conditions to a general master curve, capable of describing in itself the thermo-rheological behaviour of the epoxy system. Once isolated the dependencies on temperature and degree of cure, some tests are performed on partially cured specimens at higher temperatures, taking care not to exceed the curing temperature T_c. As illustrated in Section 5.1 this theoretically avoids a significant increase in the degree of cure and seems to be confirmed by some DSC analyses done before and after the test. Finally, the effect of the loading rate is examined on fully cured specimens and on specimens cured for infinite time at 50, 70 and $90\,°C$, again preventing further curing in the meantime. Therefore, stress-strain curves are plotted with the purpose of visualizing the effect of individual parameters: testing temperature, degree of cure and curing history, loading rate. In order to have the curves starting from the axes origin, the "shifted" values of load and strain are considered. Raw data are used to get quantities useful to characterize viscoelasticity and to compare the stress-strain curves relating to different experimental conditions: maximum stress, "apparent" and "interpolation" modulus, residual strain, the area of the hysteresis cycle. The apparent modulus E_a is simply calculated as the ratio of the maximum stress and the corresponding strain, which is set by the method as equal to 0.5%

$$E_a = \frac{\sigma_{max}}{\varepsilon_{max}} = \frac{\sigma_{max}}{0.5\%} \tag{5.9}$$

At the applied strain level, damage and other irreversible phenomena are not expected to develop in the loading-unloading cycle. As shown below, the value of the apparent modulus results quite close to the interpolation modulus as it is commonly defined, that is to say as the linear regression of $\sigma - \varepsilon$ data in the loading ramp between 0.05% and 0.2% strain [41]. Even the deviation of the curve from linearity at high temperatures and low degrees of cure does not make the two definitions of the modulus to diverge significantly. Generally speaking, it is noted that in almost all tests the interpolation modulus is slightly lower than the apparent modulus, usually with a difference in the order of $0.01\ GPa$. Nevertheless, the apparent modulus is more meaningful from the point of view of viscoelasticity and will therefore be used as the preferred measure of stiffness. It is in fact possible to assess the dependency of E_a on testing temperature, cure-state and loading rate. It should be emphasized that, strictly speaking, the apparent modulus is not a material property, but the result of viscoelastic processes, and it is always lower than the instant elastic response that would correspond to ideally infinite loading rate. The residual strain is the value of ε at the end of the unloading ramp, which is quite small but non-zero due to a certain amount of hysteresis. This can be quantified by the area of the loading-unloading cycle, equivalent to the difference between the definite integers of the loading and unloading ramps, here calculated using the trapezoidal rule. Its value is a measure of the energy per unit volume dissipated in the material during the cycle, and its measurement unit is therefore J/m^3.

5.3.1. Fully cured specimens

Fully cured specimens have a degree of cure equal to 100% and are produced through a whole day room temperature cure and $4\ h$ post-cure at $105\ °C$. They are tested with the loading-unloading method at five different temperatures: RT, 50, 70, 90 and $110\ °C$. Room temperature is assumed as about $23\ °C$ whereas tests at higher temperatures are done within the thermal chamber. Figure 5.6 shows at each temperature the stress-strain graphs of four specimens, identified by different colors. Already from the curves, it is clearly observed that at higher temperatures there are lower maximum stress and modulus, whereas the residual strain and the area of hysteresis are larger. One "central" curve is assumed as representative for each temperature and displayed in Figure 5.7. The quantities calculated for each tested specimen are listed in Table 5.4 and plotted in Figure 5.8, in order to visualize their trend with the temperature used in the test. Standard deviation at $110\ °C$ results quite large both for residual strain and hysteresis area.
For some of the tests above RT, recovery of the residual strain is allowed for $20\ min$ just after the unloading ramp, at the same temperature used in the test itself. It is seen that, even at $50\ °C$, the remaining strain is almost completely recovered and therefore the loading-unloading cycle can be considered to be characterized by negligible irreversible strains. This is also confirmed by the fact that the curves resulting from the repetition of the loading-unloading cycle on the same specimen are superimposed on each other with good approximation. This is true even without allowing strain recovery in between consecutive tests, but simply demounting the specimen from the grips and re-mounting it. It means that the selected strain level is lower than the critical value that would cause modulus degradation, i.e. the reduction of the material stiffness [37]. Hence, it may be concluded that the observed hysteresis is not due to irreversible plastic effects.

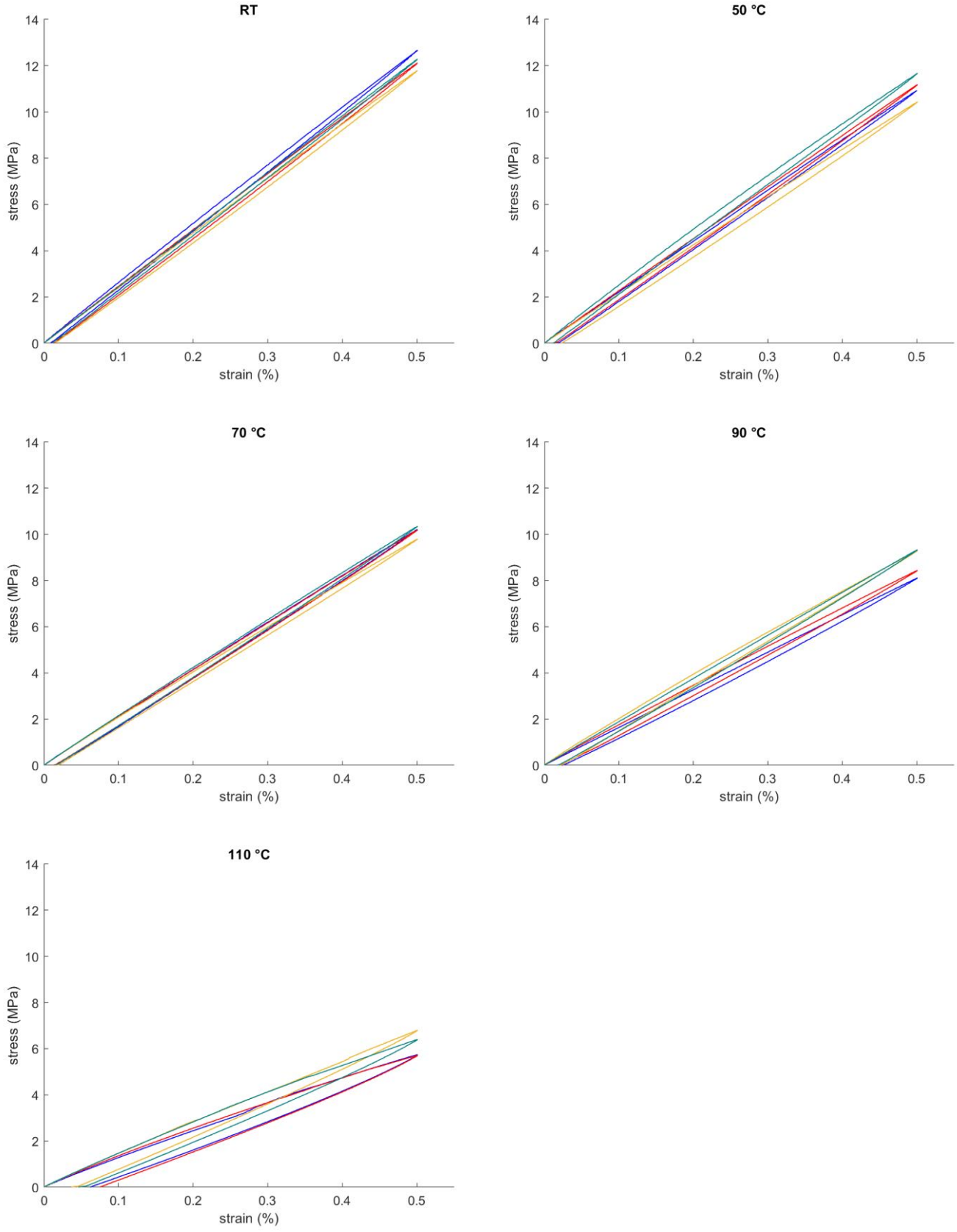

Figure 5.6 Stress-strain curves of fully cured specimens at each testing temperature

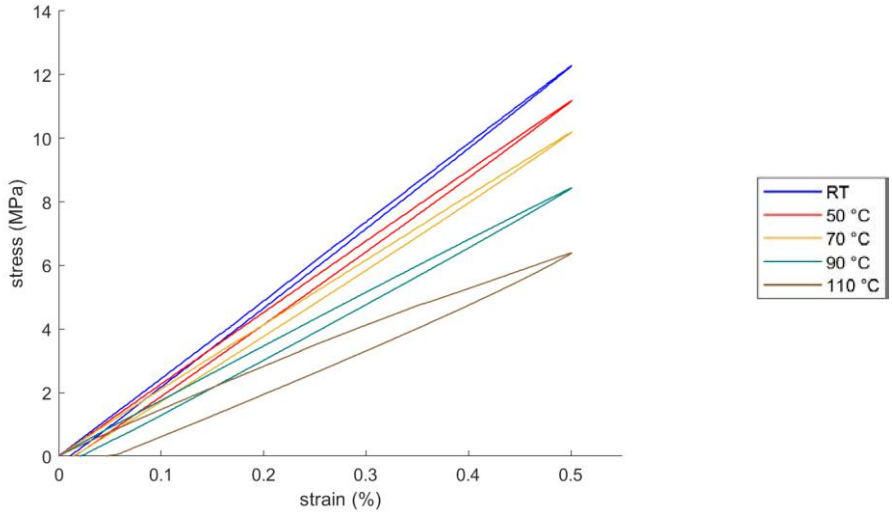

Figure 5.7 Stress-strain curves of fully cured specimens at various testing temperatures

Table 5.4 Quantities calculated from the loading-unloading of fully cured specimens at various testing temperatures

testing temperature (°C)	maximum stress (MPa)	apparent modulus (GPa)	interpolation modulus (GPa)	residual strain (%)	area of hysteresis $(10^4\ J/m^3)$
RT	12.6701	2.5340	2.5232	0.0090	0.1351
	12.1166	2.4233	2.4216	0.0130	0.1549
	11.7934	2.3587	2.3540	0.0150	0.1689
	12.2857	2.4571	2.4618	0.0110	0.1027
50 °C	10.9346	2.1869	2.1891	0.0180	0.1524
	11.1864	2.2373	2.2363	0.0130	0.1526
	10.4388	2.0878	2.0830	0.0220	0.2046
	11.6762	2.3352	2.3247	0.0110	0.1653
70 °C	10.2133	2.0427	2.0395	0.0170	0.1568
	10.1977	2.0395	2.0306	0.0130	0.1503
	9.8006	1.9601	1.9498	0.0170	0.1692
	10.3526	2.0705	2.0644	0.0150	0.1691
90 °C	8.1158	1.6232	1.6231	0.0230	0.1808
	8.4419	1.6884	1.6834	0.0200	0.1773
	9.2935	1.8587	1.8412	0.0210	0.1914
	9.3373	1.8675	1.8652	0.0170	0.1576
110 °C	5.7399	1.1480	1.1519	0.0620	0.3318
	5.7056	1.1411	1.1274	0.0750	0.3799
	6.8021	1.3604	1.3401	0.0370	0.2482
	6.3982	1.2796	1.2707	0.0460	0.3353

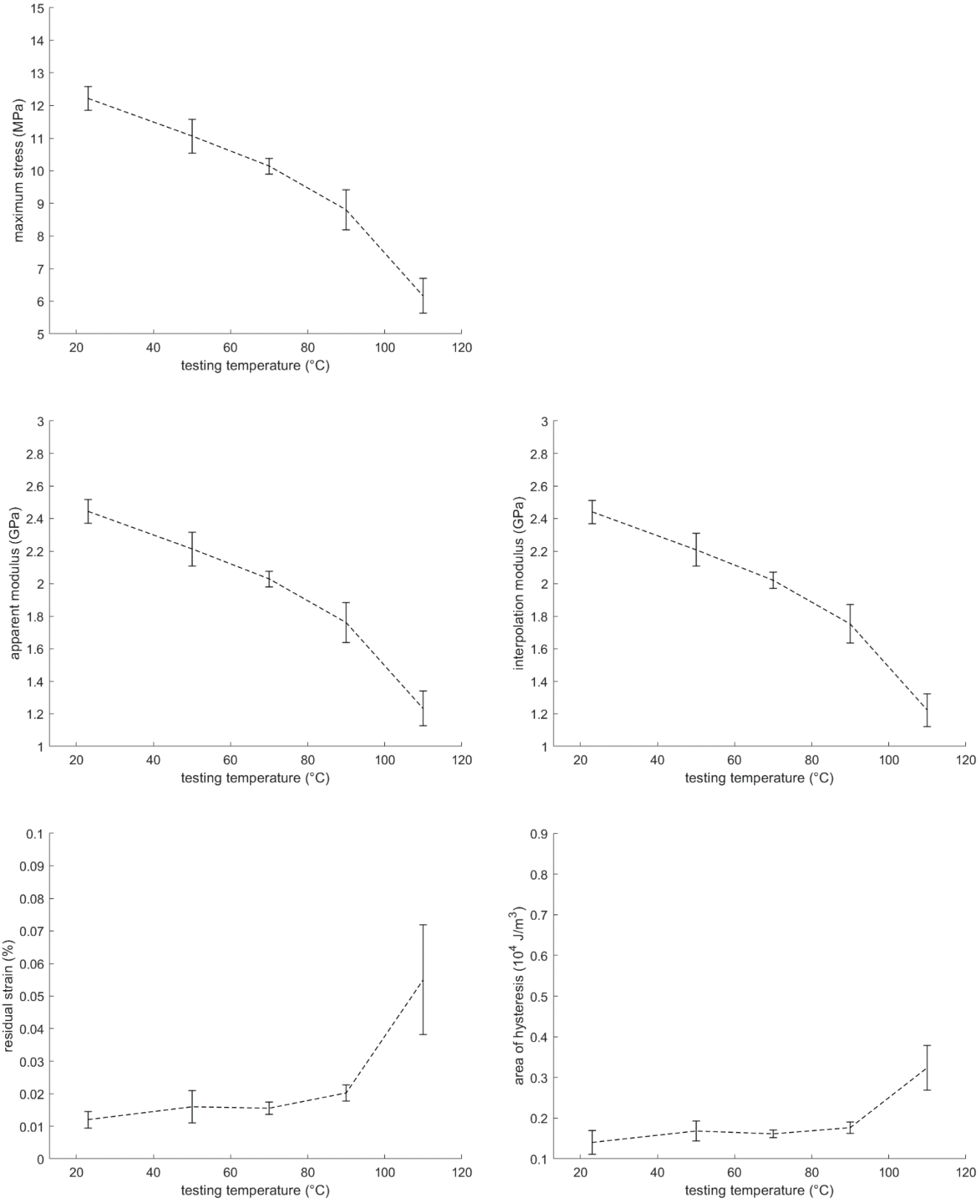

Figure 5.8 Error bars and trends for the loading-unloading of fully cured specimens at various testing temperatures

5.3.2. Partially cured specimens

Partially cured specimens with degree of cure 74%, 83%, 89% and 91% are manufactured through thermal treatment at 70 °C for 30, 40, 55 and 70 min respectively. These cure cycles are in agreement with the corresponding yellow profile in Figure 5.1. The stress-strain curves are shown in Figure 5.9 for four equally cured specimens, distinguished by different colors. As expected, it is clearly noted that the strain remaining after unloading and the hysteresis area are quite large for the lowest degree of cure and progressively decrease with increasing percentage of cure. Differences in the maximum stress and in the apparent and interpolation moduli are less evident than those due to varying test temperature. The quantities determined for each test are shown in Table 5.5 and graphed in Figure 5.10 against the degree of cure, where fully cured specimens of Figure 5.6 at RT are also reported for comparison. A "central" curve for each kind of specimen is displayed in Figure 5.11.

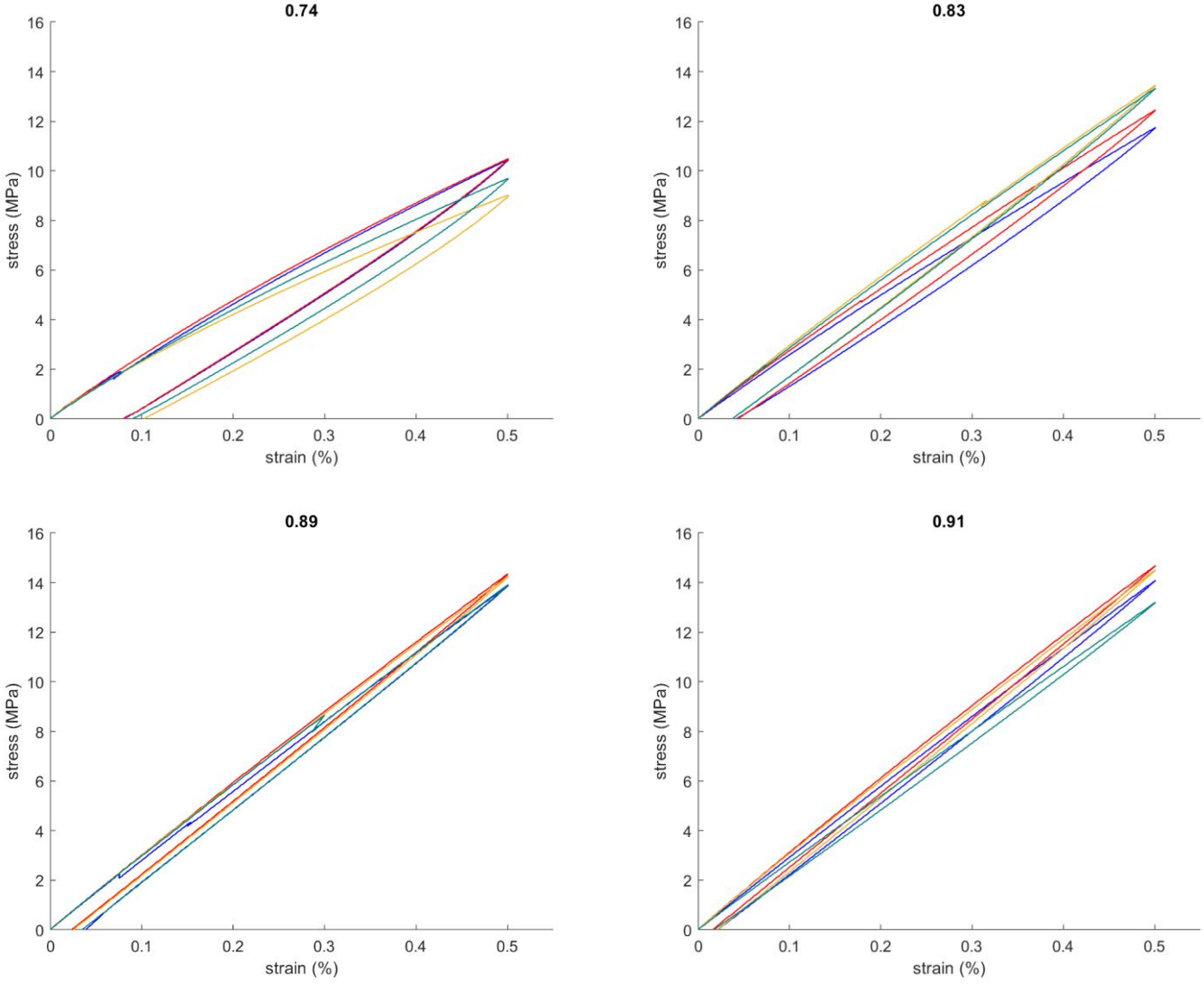

Figure 5.9 Stress-strain curves of specimens with various degrees of cure tested at RT

Table 5.5 Quantities calculated from the loading-unloading of various partially cured specimens tested at RT

degree of cure	maximum stress (MPa)	apparent modulus (GPa)	interpolation modulus (GPa)	residual strain (%)	area of hysteresis $(10^4\ J/m^3)$
0.74	10.4513	2.0903	2.0691	0.0810	0.7078
	10.4932	2.0986	2.0643	0.0800	0.7462
	9.0212	1.8042	1.7587	0.1030	0.8085
	9.6950	1.9390	1.9061	0.0900	0.7692
0.83	11.7508	2.3502	2.3269	0.0420	0.4816
	12.4563	2.4913	2.4622	0.0440	0.4856
	13.4563	2.6913	2.6605	0.0380	0.4620
	13.3334	2.6667	2.6471	0.0370	0.4345
0.89	13.8907	2.7781	2.7700	0.0390	0.3158
	14.3541	2.8708	2.8590	0.0230	0.2914
	14.2505	2.8501	2.8351	0.0250	0.2957
	13.9174	2.7835	2.7434	0.0350	0.3670
0.91	14.0903	2.8181	2.8081	0.0210	0.2672
	14.6868	2.9374	2.9220	0.0160	0.2398
	14.5074	2.9015	2.8820	0.0210	0.2706
	13.2025	2.6405	2.6288	0.0180	0.2177

While residual strain and hysteresis area show the expected monotonously decreasing trend with increasing degree of cure, the measured maximum stress and moduli are more surprising: it results that the values of 83% cured epoxy are comparable, or even slightly higher, than those of fully cured resin. Specimens with degree of cure 89% and 91% have the highest modulus, with a very small difference between them. This observation points out that the degree of cure is not a sufficient parameter to characterize the cure-related mechanical state of epoxy. Curing history, that is to say the combination of temperatures and times used in the manufacturing, has a considerable effect on the resulting mechanical properties.

The cure cycle utilized for fully cured specimens, consisting in $24\ h$ at RT and $4\ h$ post-cure at $105\ °C$, seems to be detrimental from the point of view of stiffness, even though the attained degree of cure is higher. This result is promising since cure at lower temperatures and for shorter times allows cost saving in the production of parts. It must however be considered that the presence of unreacted monomers is responsible for the toxicity of partially cured epoxy. Moreover, the lower residual strain and hysteresis area of fully cured resin are beneficial and therefore more research should be done to determine the best cure cycle for structural applications. It should be added that full cure determines the best mechanical performance of epoxy when exposed to high temperature conditions. This is because additional cure does not occur at any temperature and because the resulting glass transition point is the highest attainable, equal to $136\ °C$ according to the DiBenedetto Equation (2.1).

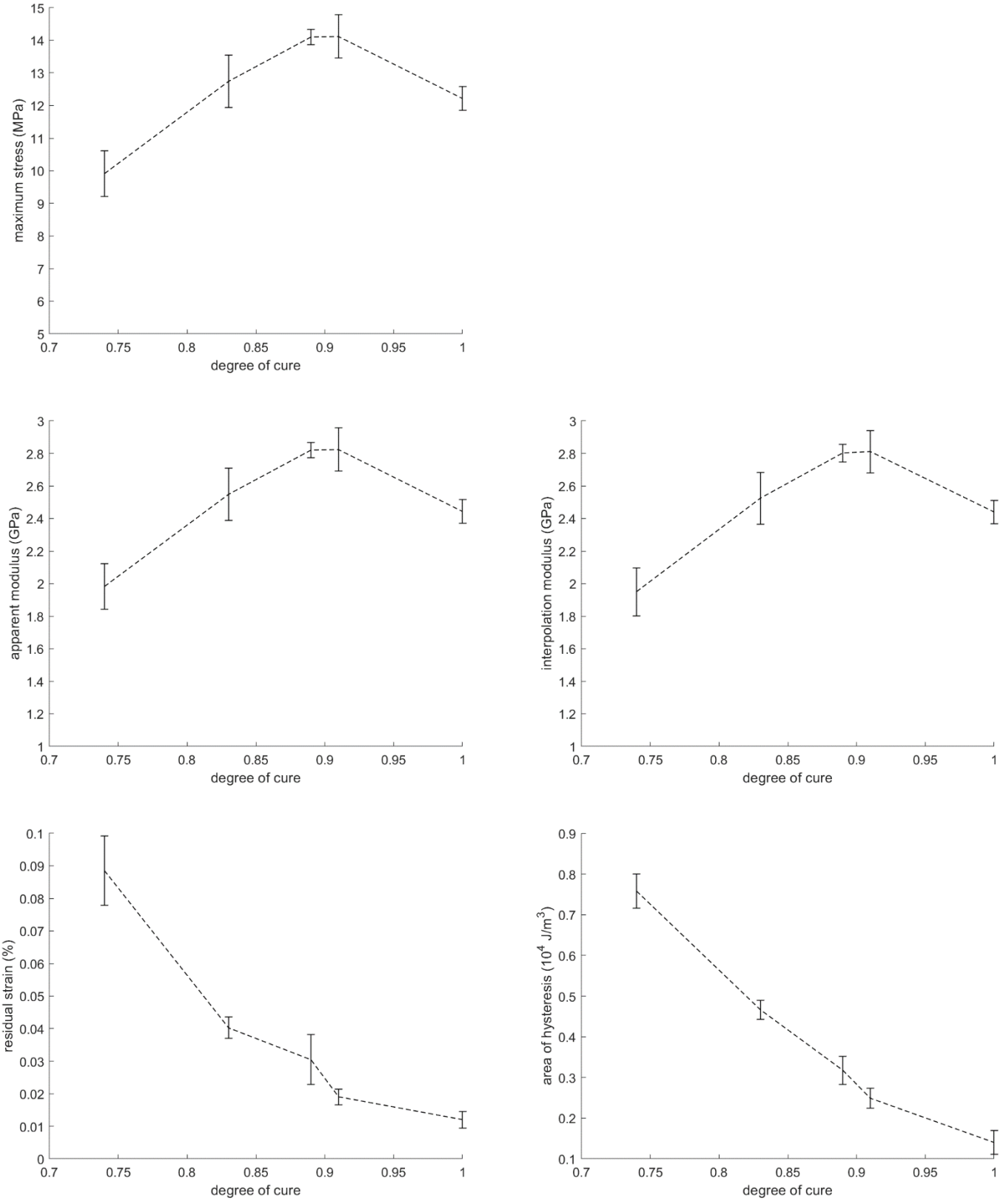

Figure 5.10 Error bars and trends for the loading-unloading of specimens with different degree of cure

Further study on the chemical reasons of this unexpected behaviour might also be useful. Different thermal treatments are in fact likely to result in different internal structure of the resin, being the configuration of polymeric chains and the degree of cross-linking affected by the rate with which phase transformation occurs. One such characterization technique to evaluate the inner morphology of the resin, for example in terms of degree of crystallinity, may be X-ray scattering [55]. Nevertheless, there is also the possibility that such dissimilarities in the polymer network are not big enough to totally explain the observed differences in mechanical response. Residual stresses, of chemical and thermal nature, make the load measured by the machine to be non-zero at the beginning of the test, even if the material is not yet deformed. This is clearly observed from the quite high values measured by the load cell just after these specimens are mounted in the grips. Even though the initial load is manually adjusted close to zero before running the test, when the material is then elongated the stress response is higher and it appears stiffer. In other words, the modulus of these partially cured specimens may be higher than that of fully cured resin because of the summation of the internal stress field with the externally applied forces. This leads to weakening of the structure, since the failure load for the onset of plasticity or for breakage is reached applying a lower external stress.

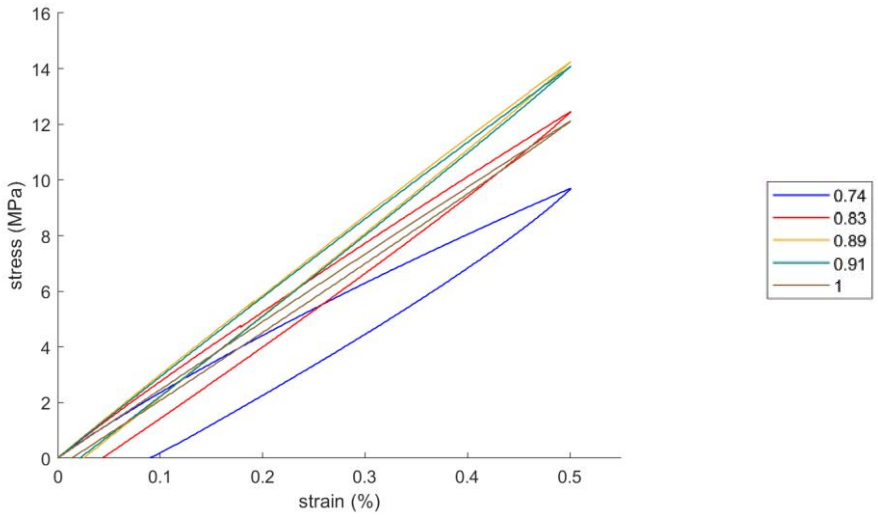

Figure 5.11 Stress-strain curves of various partially cured specimens tested at RT

Once discovered the importance of how a certain degree of cure is attained, some tests are carried out to parity of percentage of cure. Specimens having the maximum degree achievable at $50\ °C$, that is to say 0.882, are produced at three different temperatures, namely 50, 70 and $90\ °C$. The required times are those specified in Table 5.1: "infinite" time, meaning higher than about $8.4\ h$, $51\ min$ and $14\ min$. As usual, an increase in the temperature of the oven determines a great decrease in the cure time. All these specimens are tested with the loading-unloading method at RT and $50\ °C$. Higher temperatures are not possible since they would determine post-curing.

The resulting stress-strain curves are illustrated in Figure 5.12 and the measured quantities are reported in Table 5.6. Both increasing test temperature and increasing cure temperature reduce the maximum stress and the modulus whereas they enhance the residual strain and hysteresis area. Considering the trends in Figure 5.13, 5.14 and 5.15, relative to the three distinct cure cycles, it is observed that for all these quantities the difference between RT and $50\ °C$ increases with the temperature used for cure.

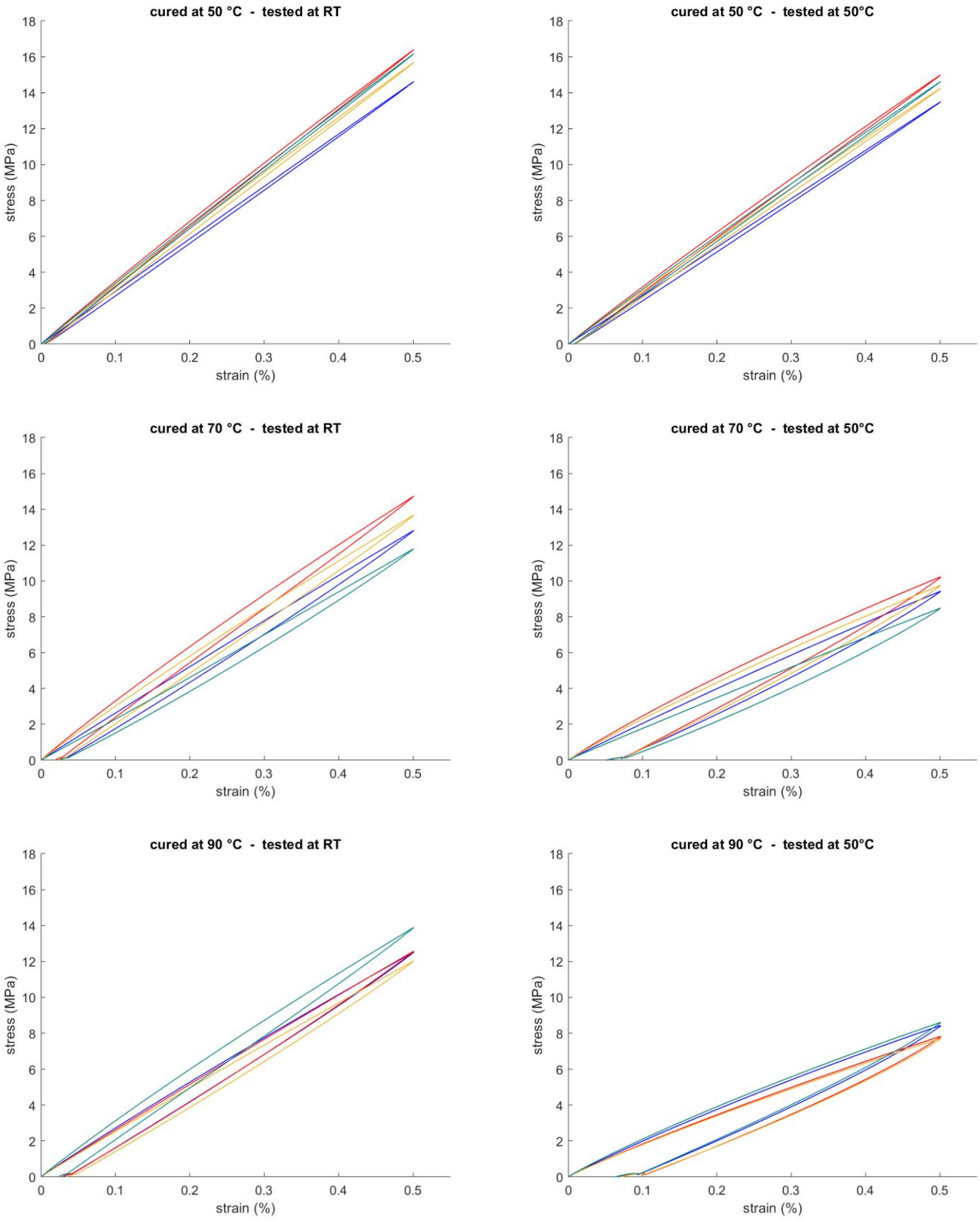

Figure 5.12 Stress-strain curves of specimens with degree of cure 0.882, cured at three different curing temperatures and tested at RT and 50 °C

Table 5.6 Quantities calculated from the loading-unloading of specimens with degree of cure 0.882, cured at various curing temperatures and tested at RT and 50 °C

curing temperature (°C)	testing temperature	maximum stress (MPa)	apparent modulus (GPa)	interpolation modulus (GPa)	residual strain (%)	area of hysteresis ($10^4\ J/m^3$)
50	RT	14.6117	2.9223	2.9202	0.0070	0.0999
		16.3909	3.2782	3.2624	0.0060	0.1122
		15.6835	3.1367	3.1267	0.0070	0.1146
		16.1708	3.2342	3.2212	0.0040	0.0888
	50 °C	13.5003	2.7001	2.6978	0.0080	0.1064
		14.9962	2.9992	2.9845	0.0090	0.1331
		14.2505	2.8501	2.8409	0.0090	0.1317
		14.6263	2.9253	2.9135	0.0070	0.1207
70	RT	12.8137	2.5627	2.5587	0.0250	0.3364
		14.7296	2.9459	2.9205	0.0200	0.3489
		13.6672	2.7334	2.7166	0.0230	0.3658
		11.7994	2.3599	2.3650	0.0250	0.3011
	50 °C	9.4288	1.8858	1.8775	0.0510	0.5240
		10.2318	2.0464	2.0113	0.0540	0.6357
		9.7503	1.9501	1.9225	0.0540	0.5913
		8.4798	1.6960	1.6913	0.0530	0.4833
90	RT	12.5167	2.5033	2.4851	0.0300	0.4127
		12.5655	2.5131	2.5073	0.0290	0.3738
		12.0245	2.4049	2.3912	0.0350	0.4093
		13.8860	2.7772	2.7518	0.0240	0.3940
	50 °C	8.4368	1.6874	1.6660	0.0650	0.6265
		7.8214	1.5643	1.5442	0.0700	0.6195
		7.7050	1.5410	1.5186	0.0700	0.6030
		8.6018	1.7204	1.6878	0.0640	0.6532

Specimens having degree of cure 74% and 83% are then also manufactured by performing cure cycles at 50 or 90 °C. Times required to attain these cure states are as usual calculated using the Kamal's equation and result equal to 110 and 155 min at 50 °C, 9 and 12 min at 90 °C. Stress-strain curves at RT are plotted in Figure 5.16, showing also specimens cured at 70 °C for comparison. It is of course observed that an increase in the degree of cure determines an increase in maximum stress and modulus and a decrease in residual strain and area of hysteresis. What is more interesting is that, by increasing the cure temperature, there is a reduction in the stiffness of the resin, especially for 0.74 cured resin. On the contrary, the effect of curing temperature on residual strain and hysteresis area is not appreciable. These quantities are not significantly affected by the discontinuity in the final part of the unloading ramp, which is due to the change in the unloading speed.

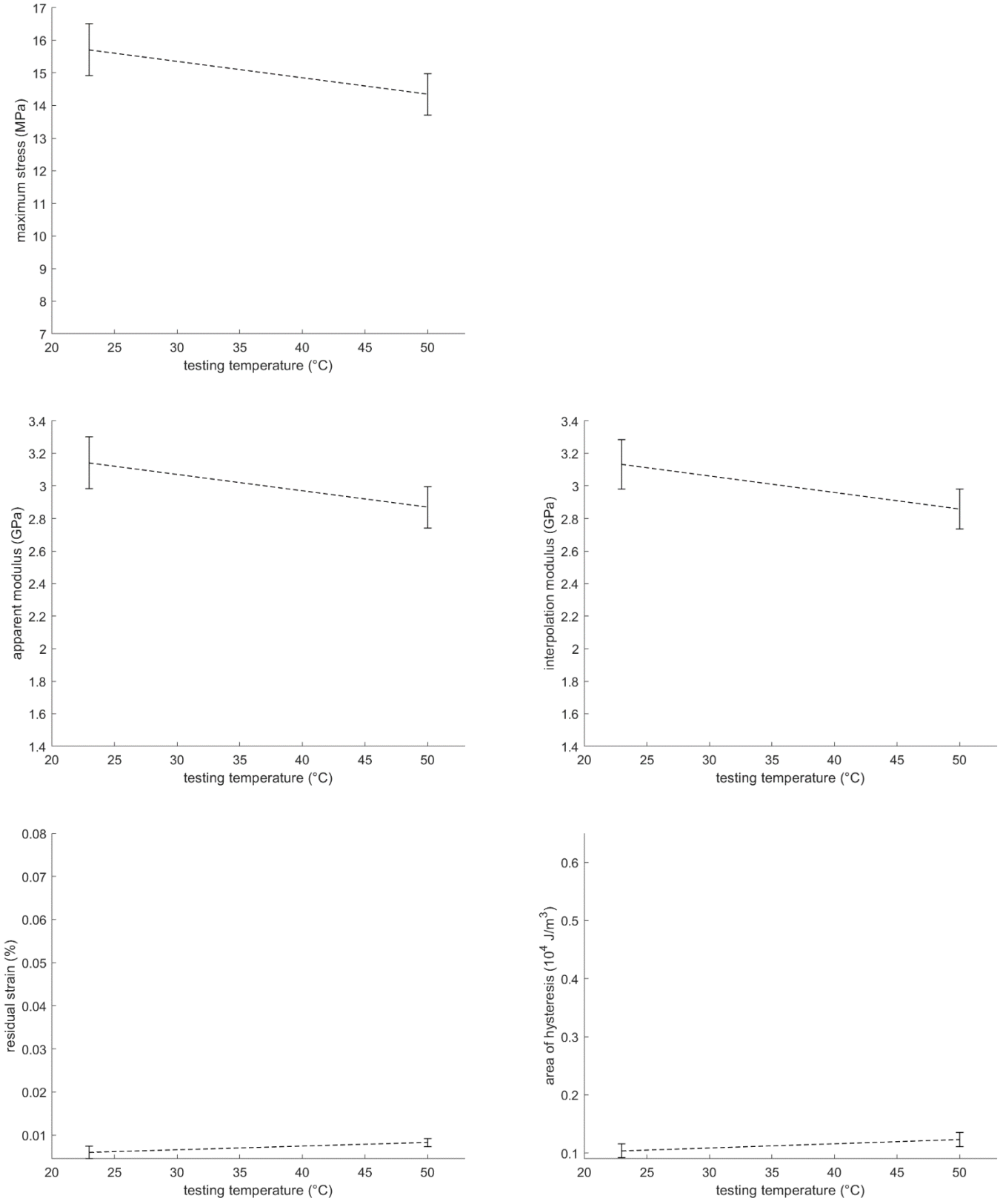

Figure 5.13 Error bars and trends for the loading-unloading of specimens with degree of cure 0.882, cured at 50 °C and tested at RT and 50 °C

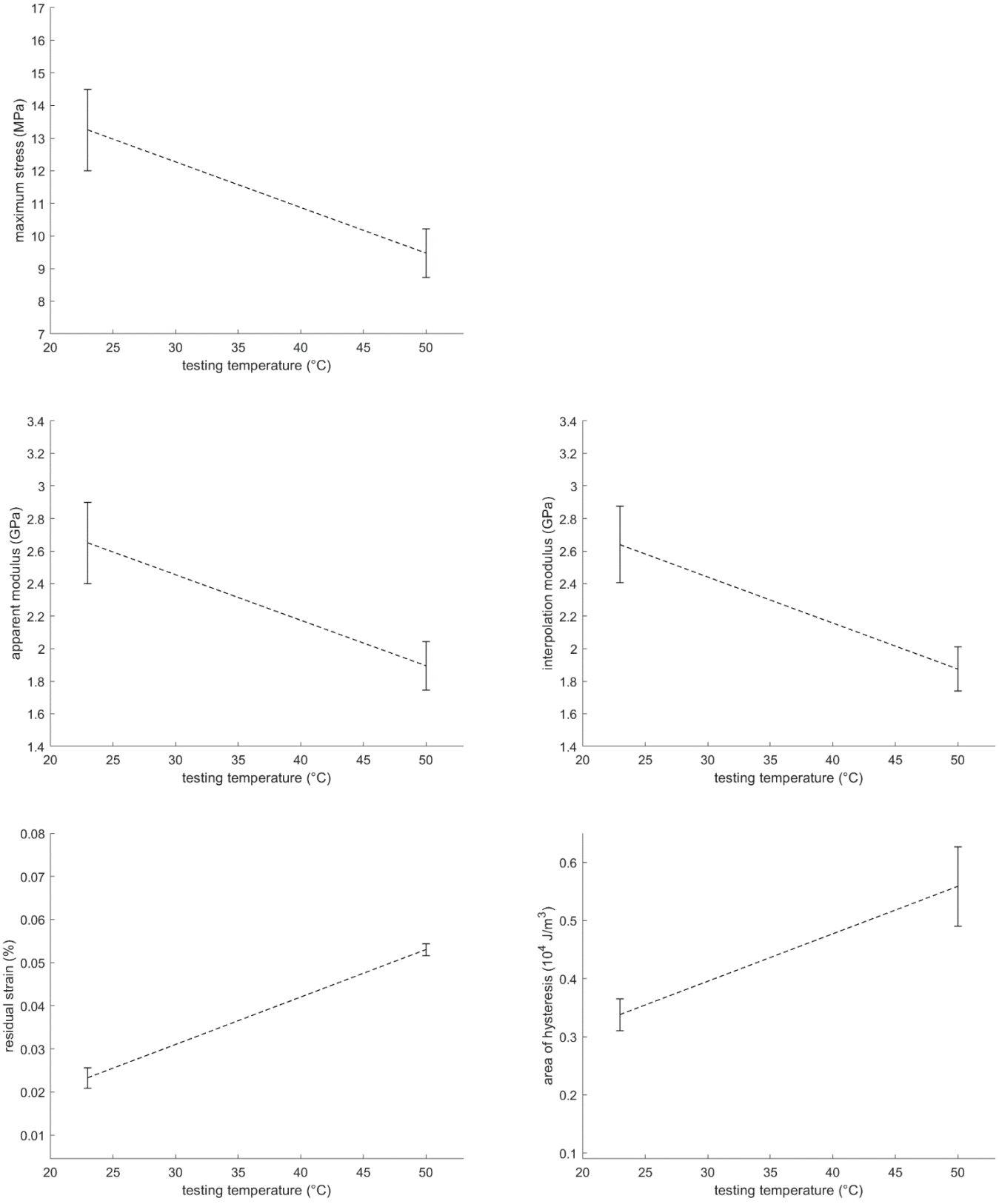

Figure 5.14 Error bars and trends for the loading-unloading of specimens with degree of cure 0.882, cured at 70 °C and tested at RT and 50 °C

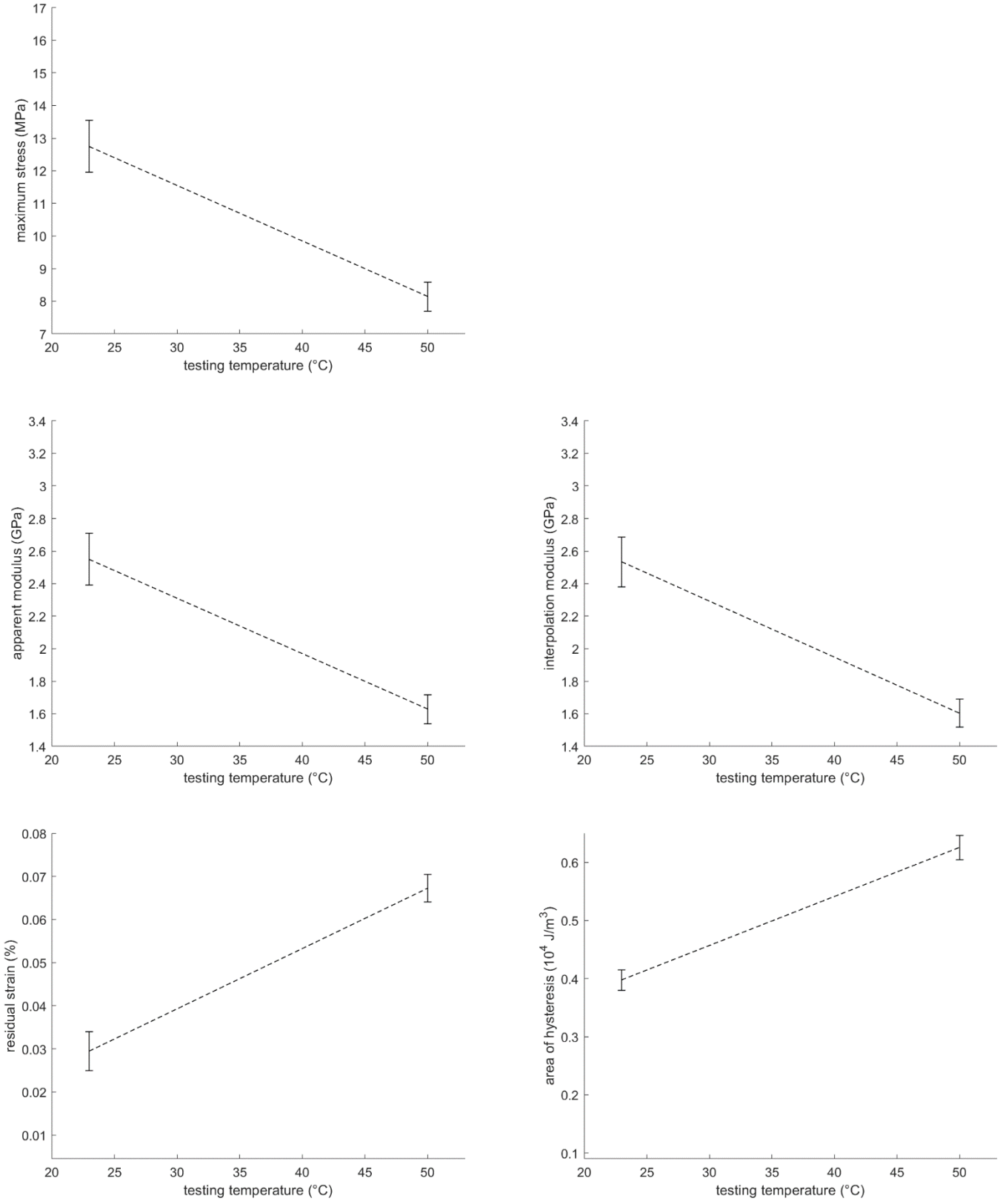

Figure 5.15 Error bars and trends for the loading-unloading of specimens with degree of cure 0.882, cured at 90 °C and tested at RT and 50 °C

The calculated quantities are detailed in Table 5.7 and their trends are displayed in Figures 5.17, 5.18 and 5.19 along with the already presented 0.882 cured specimens tested at RT. A fairly linear correlation with respect to the degree of cure is observed for specimens cured at 50 and 90 °C. This is less evident for resin cured at 70 °C, but may be due to experimental inaccuracies and specimens variability. It is recalled that 74% and 83% cured resin cannot be tested at 50 °C without increasing its degree of cure.

Table 5.7 Quantities calculated from the loading-unloading of specimens with degree of cure 0.74 and 0.83 cured at 50 and 90 °C and tested at RT

curing temperature (°C)	degree of cure	maximum stress (MPa)	apparent modulus (GPa)	interpolation modulus (GPa)	residual strain (%)	area of hysteresis $(10^4\ J/m^3)$
50	0.74	9.6430	1.9286	1.9059	0.0620	0.6828
		8.8943	1.7789	1.7660	0.0640	0.6299
	0.83	12.7394	2.5479	2.5377	0.0300	0.3991
		14.2678	2.8536	2.8426	0.0270	0.3930
70	0.74	8.8496	1.7699	1.7287	0.0770	0.7830
		9.0325	1.8065	1.7838	0.0700	0.6953
	0.83	13.3807	2.6761	2.6548	0.0270	0.4463
		12.1669	2.4334	2.4258	0.0320	0.4185
90	0.74	7.5575	1.5115	1.4843	0.0780	0.6840
		8.5784	1.7157	1.6924	0.0700	0.7045
	0.83	10.3032	2.0606	2.0526	0.0450	0.4989
		12.1252	2.4250	2.4037	0.0310	0.4664

It has been said that different cure cycles result in a different internal structure of the polymer network. Moreover, the onset of chemical and thermal internal stresses has presumably a greater extent the faster is the solidification rate, that is to say the higher is the curing temperature. In other words, residual stresses become bigger the farther is structure from the equilibrium configuration, because less time is given to molecules to arrange properly. From a theoretical point of view, it is likely that curing is a mere scaling-up in the internal network, which remains geometrically similar to itself [3,31]. As cure proceeds, cross-linking becomes more extensive and the motion of individual chains is increasingly hindered. Because of their higher interconnection, relaxation of larger clusters occurs more slowly and therefore it is not only the number of newly generated cross-links that counts.

This scale-change has usually been described in terms of degree of cure or, to parity of cure temperature, has been redefined using cure time. Nevertheless, as said several times, the main outcome of the just presented experiments is that, from a mechanical point of view, the resin cure state is not univocally identified by the degree of cure, but only by its complete curing history, that is to say by the applied temporal profile of temperature. It should be pointed out that this may represent a drawback in the characterization of the cure state. Indeed, while the degree of cure α can be determined, for example by means of DSC, the cure temperature T_c and time t_c must be known from the manufacturer.

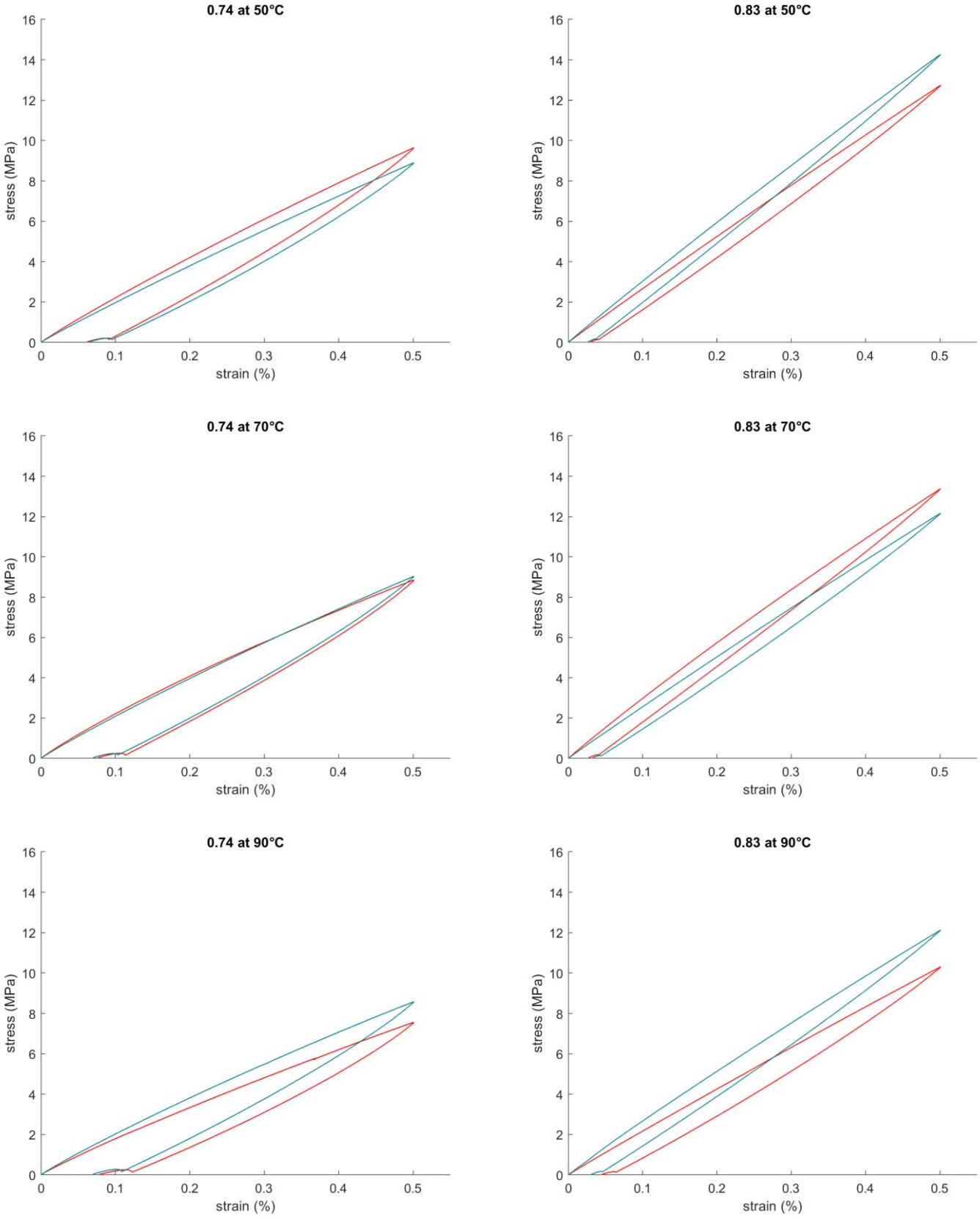

Figure 5.16 Stress-strain curves of specimens with degree of cure 0.74 and 0.83 cured at 50, 70 and 90 °C and tested at RT

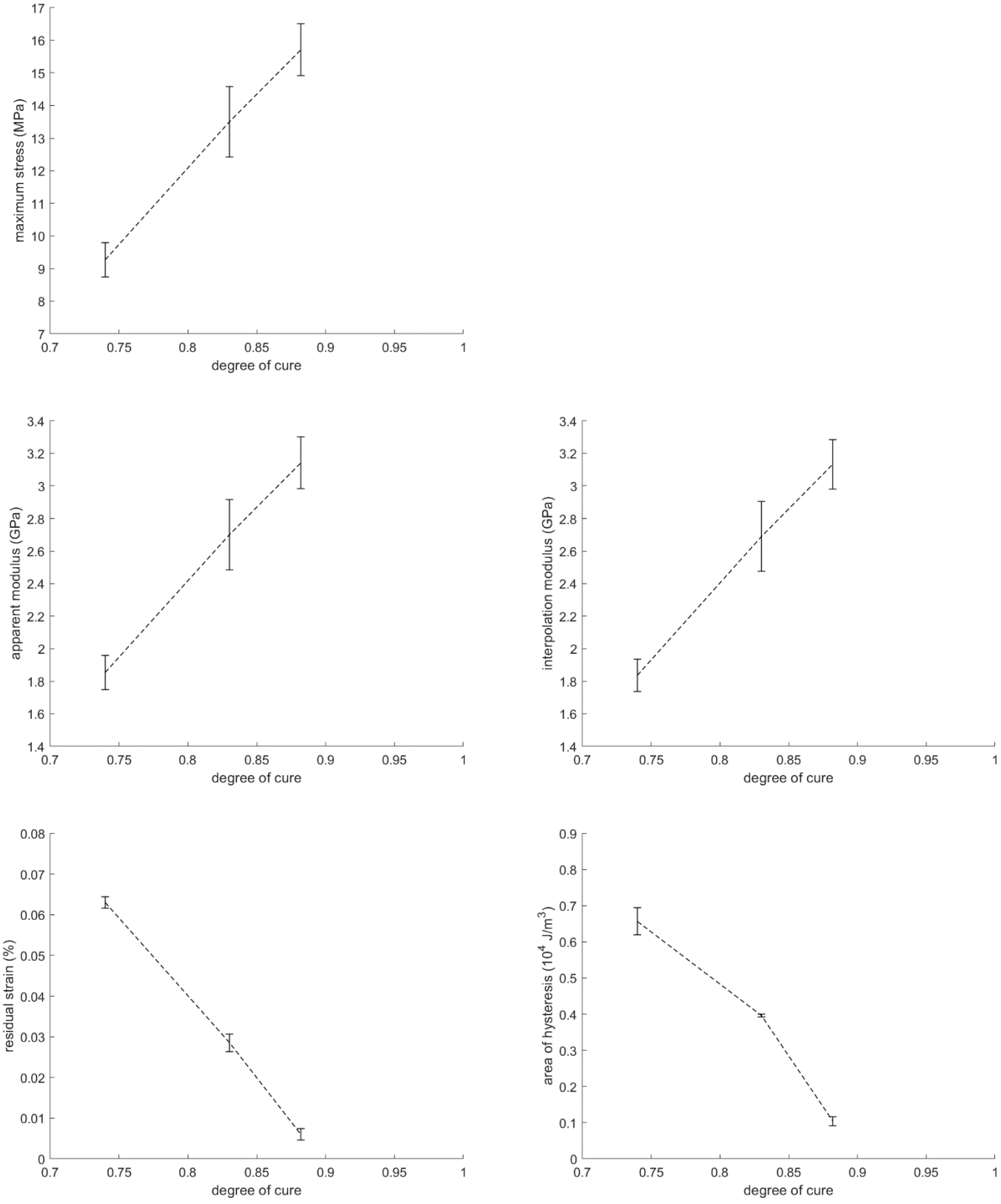

Figure 5.17 Error bars and trends for the loading-unloading of specimens with degree of cure 0.74, 0.83 and 0.882, cured at 50 °C and tested at RT

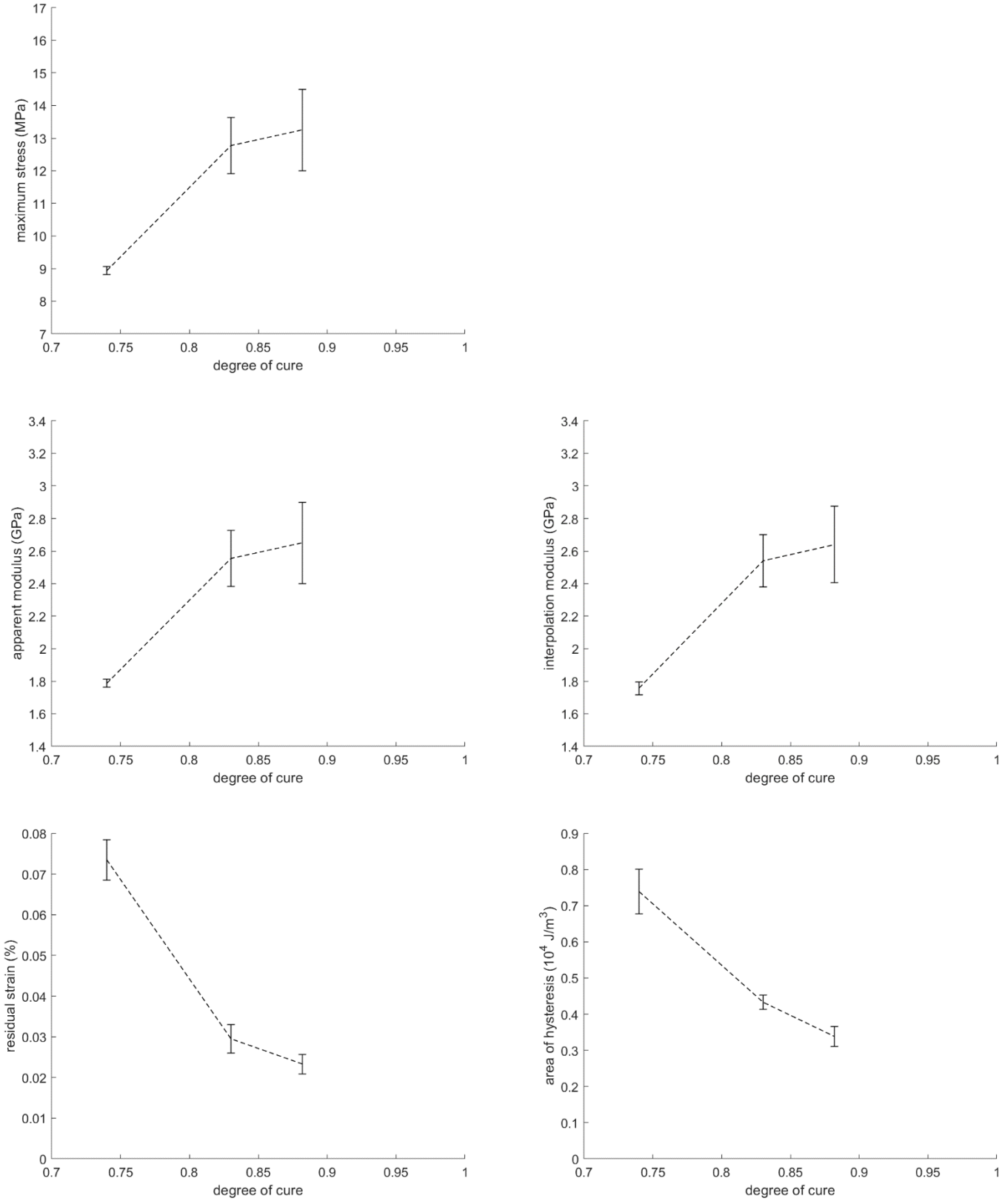

Figure 5.18 Error bars and trends for the loading-unloading of specimens with degree of cure 0.74, 0.83 and 0.882, cured at 70 °C and tested at RT

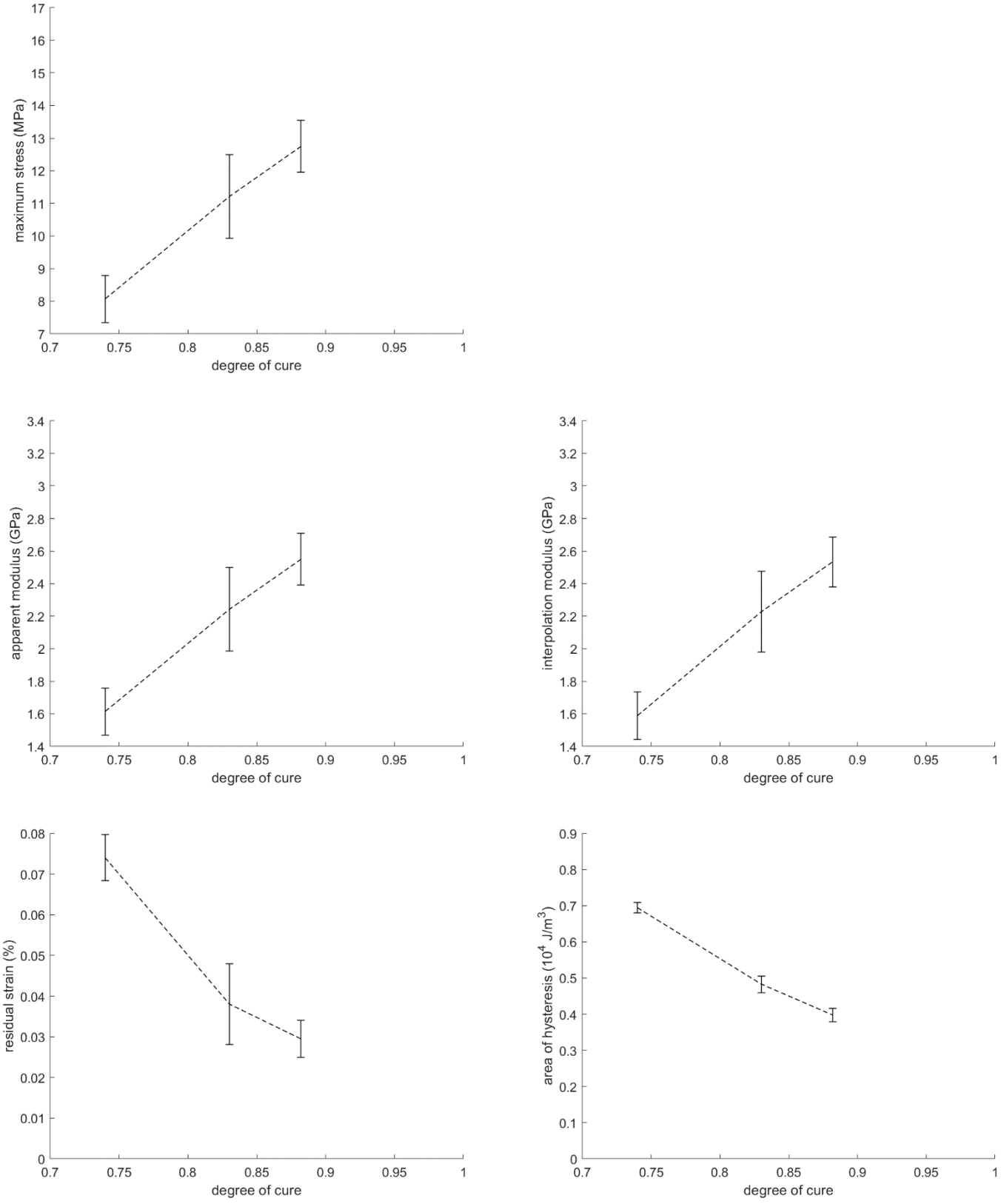

Figure 5.19 Error bars and trends for the loading-unloading of specimens with degree of cure 0.74, 0.83 and 0.882, cured at 90 °C and tested at RT

5.3.3. Comparison between fully and partially cured specimens

In the light of the results presented in the previous Sections 5.3.1 and 5.3.2 it may be useful to make a comparison between fully and partially cured specimens. Data in each loading ramp are measured at fixed test temperature and degree of cure. It is clearly observed that the effects of low degree of cure and high testing temperature make the material response more fluid-like and are therefore qualitatively equivalent on all the quantities listed in the results tables: the maximum stress and the apparent and interpolation moduli are lowered, while the residual strain and the area of hysteresis become larger. Increasing deviation from non-linearity is exhibited as testing temperature increases and the degree of cure decreases [38]. Even for the cycles closer to linearity, the unloading curve is characterised by a slightly steeper slope. This is due to hysteresis effect and is for sure not the result of increased stiffness. For consistency, the interpolation modulus has always been calculated in the loading ramp.

It is also observed that higher scatter of data, related to specimens variability, is induced by either high temperature and low degree of cure. As pointed out by the DiBenedetto Equation (2.1) the glass transition temperature is also affected by the attained degree of cure. Table 4.4 shows that T_g varies in a wide range, being considerably lower for the less cured specimens. This needs to be considered when performing temperature tests on partially cured specimens. Indeed, avoiding additional cure is not the only precaution to be taken, since the specimen may soften at relatively low temperatures.

It has been shown in Figure 5.11 that at room temperature the modulus of fully cured resin is very similar to that of specimens treated at $70\ °C$ to 83% cure and is considerably lower than those of specimens cured at the same temperature to 89% and 91%. Moreover, specimens having the same degree of cure, equal to 0.74, 0.83 or 0.882, but attained at different cure temperatures, namely 50, 70 or $90\ °C$, have shown non-negligible differences in their viscoelastic response. This may be explained by the different curing histories used to produce them.

The main difference between fully and partially cured specimens is that in the former case liquid resin is kept one day at RT whereas in the latter case it is poured in the preheated mold. Hence, the rate of solidification is significantly slower for fully cured epoxy. Its mechanical properties are then enhanced by means of post-cure. Conversely, in the manufacturing of partially cured specimens, the resin is exposed to high temperature from the very beginning and therefore undergoes a fast transformation from liquid to solid. The rate of solidification and curing increases with the cure temperature. It is thought that the resulting network of polymeric chains differs according to the cure cycle. Indeed, it is very likely that the slower is solidification, the better molecules are enabled to arrange. By increasing the cure temperature, on the contrary, the chains have less time to reach their equilibrium configuration and are very soon frozen in their initial position or close to it.

The fact that in some tests an higher modulus has been exhibited by resin with lower degree of cure may be explained by the fact that reciprocal sliding between chains is hindered by this non-equilibrium network. Another possible interpretation concerns the summation of chemically- and thermally-induced residual stresses and the external load applied by the testing apparatus. It should be specified that these two phenomena are not necessarily mutually exclusive but may be concurrent, eventually with a predominance of one of them. Whatever it is the reason for the observed unexpected behaviour, to be further investigated by means of structural characterization techniques, the considerable influence of curing history on the viscoelastic behaviour is herein experimentally proven.

5.3.4. The effect of loading rate

In order to evaluate the effect of loading rate at various service temperatures, specimens are subjected to a sequence of ramps, without interrupting the test method [59, 61]. Three increasing loading rates are used, namely 2, 25 and 50 mm/min, at three different temperatures, i.e. RT, 50 and 70 °C. The uploading and unloading ramps are as usual in displacement-controlled mode and have the same rate. Strain recovery is allowed by keeping 2 N for 2 min in-between each loading-unloading cycle, whereas uniform heating of the specimen is as usual abundantly achieved in 20 min at the same almost-zero stress condition. At the highest loading rates, the control over strain is less precise and in fact the maximum strain is seen to slightly exceed 0.5%. Higher control would be possible by using an electromechanical instrument instead of the hydraulically actuated Instron 3366.

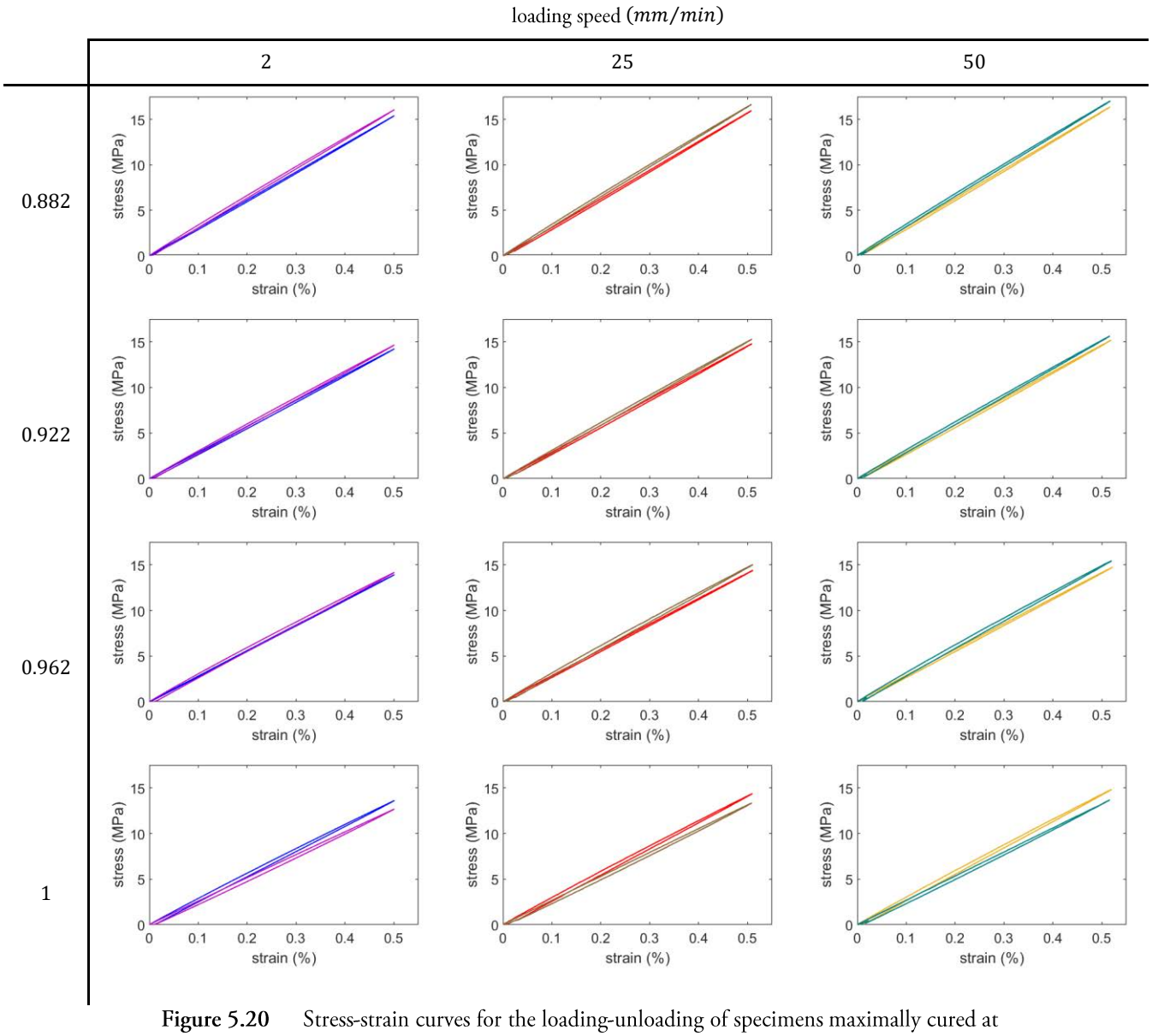

Figure 5.20 Stress-strain curves for the loading-unloading of specimens maximally cured at various temperatures and tested at RT with increasing loading rate

Table 5.8 Quantities calculated from the loading-unloading of specimens with various degree of cure and tested at RT with various loading rates

degree of cure	loading rate (mm/min)	maximum stress (MPa)	apparent modulus (GPa)	interpolation modulus (GPa)	residual strain (%)	area of hysteresis $(10^4\ J/m^3)$
0.882	2	15.3979	3.0796	3.0830	0.0030	0.0739
		16.0594	3.2119	3.1972	0.0070	0.1221
	25	15.9751	3.1950	3.1568	0.0020	0.0959
		16.6573	3.3315	3.2665	0.0010	0.1164
	50	16.3694	3.2739	3.1899	0.0010	0.1009
		17.0266	3.4053	3.3070	0	0.1198
0.922	2	14.2343	2.8469	2.8427	0.0050	0.1019
		14.6483	2.9297	2.9207	0.0070	0.1205
	25	14.8078	2.9616	2.9155	0.0020	0.1097
		15.2875	3.0575	3.0041	0.0030	0.1252
	50	15.1785	3.0357	2.9467	0.0020	0.1162
		15.6417	3.1283	3.0428	0.0020	0.1283
0.962	2	13.9255	2.7851	2.7844	0.0020	0.0454
		14.1750	2.8350	2.8146	0.0110	0.1715
	25	14.4076	2.8815	2.8236	0.0010	0.0834
		15.0391	3.0078	2.9356	0.0030	0.1587
	50	14.7632	2.9526	2.8483	0	0.1025
		15.4675	3.0935	2.9962	0.0010	0.1645
1	2	13.6129	2.7226	2.7096	0.0100	0.1539
		12.6736	2.5347	2.5306	0.0100	0.1617
	25	14.3881	2.8776	2.8143	0.0050	0.1615
		13.3491	2.6698	2.6249	0.0020	0.1532
	50	14.8393	2.9679	2.8831	0.0020	0.1647
		13.6965	2.7393	2.6633	0.0020	0.1466

The test method is performed on specimens maximally cured at various temperatures. Fully cured specimens are as usual manufactured by means of 24 h cure at RT and 4 h post-cure at 105 °C. On the other hand, partially cured specimens with degree of cure 0.882, 0.922 and 0.962 are obtained by curing for "infinite" time at 50, 70 and 90 °C respectively. In order to avoid additional curing, 0.882 cured resin is not tested at 70 °C.

The results are presented showing the three distinct loading rates at each test temperature. Stress-strain curves are plotted in Figures 5.20, 5.22 and 5.24, the usual calculated quantities are listed in Tables 5.8, 5.9 and 5.10 and their trends are displayed in Figures 5.21, 5.23 and 5.25.

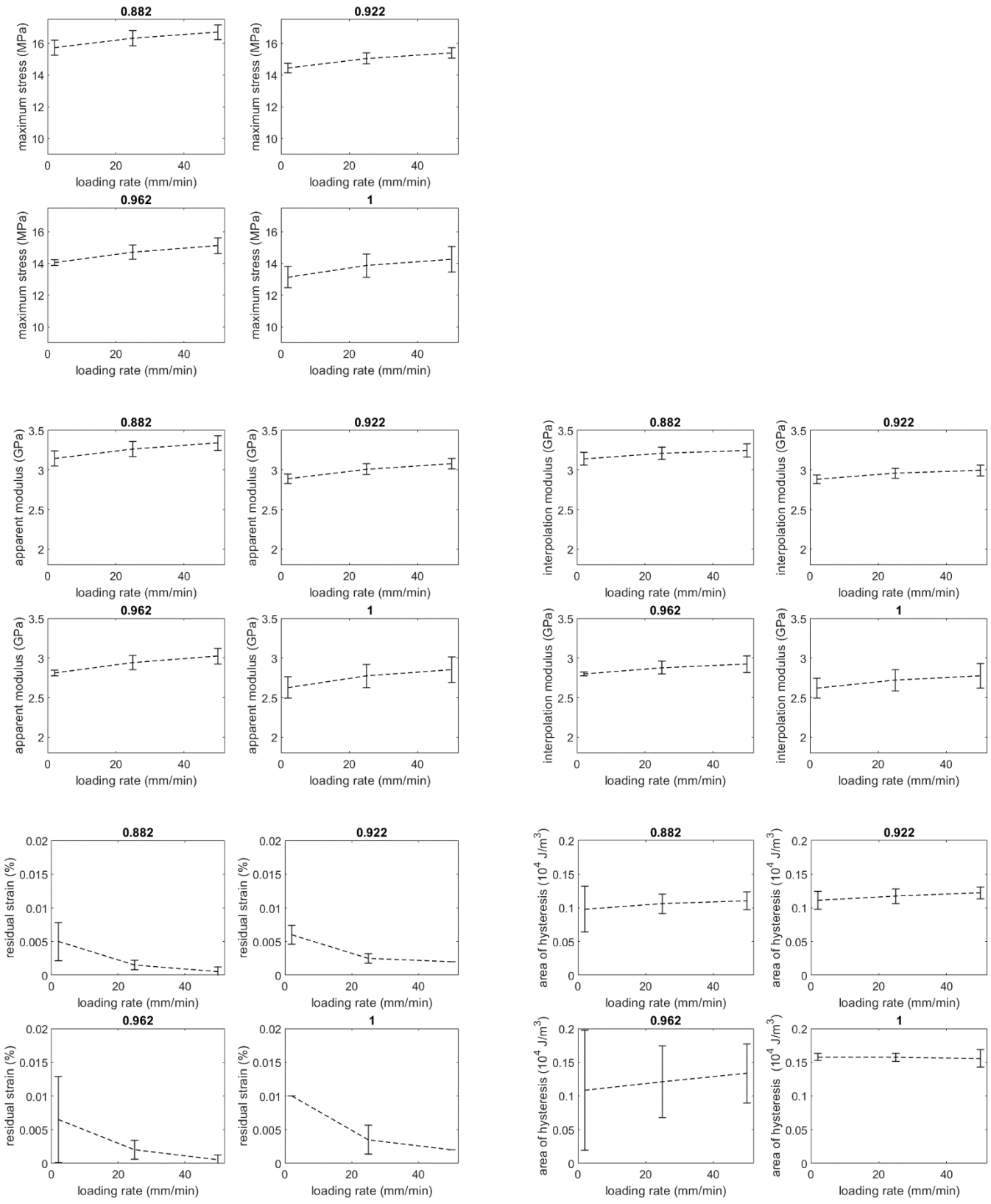

Figure 5.21 Error bars and trends for the loading-unloading of specimens with different degree of cure, tested at RT with various loading rates

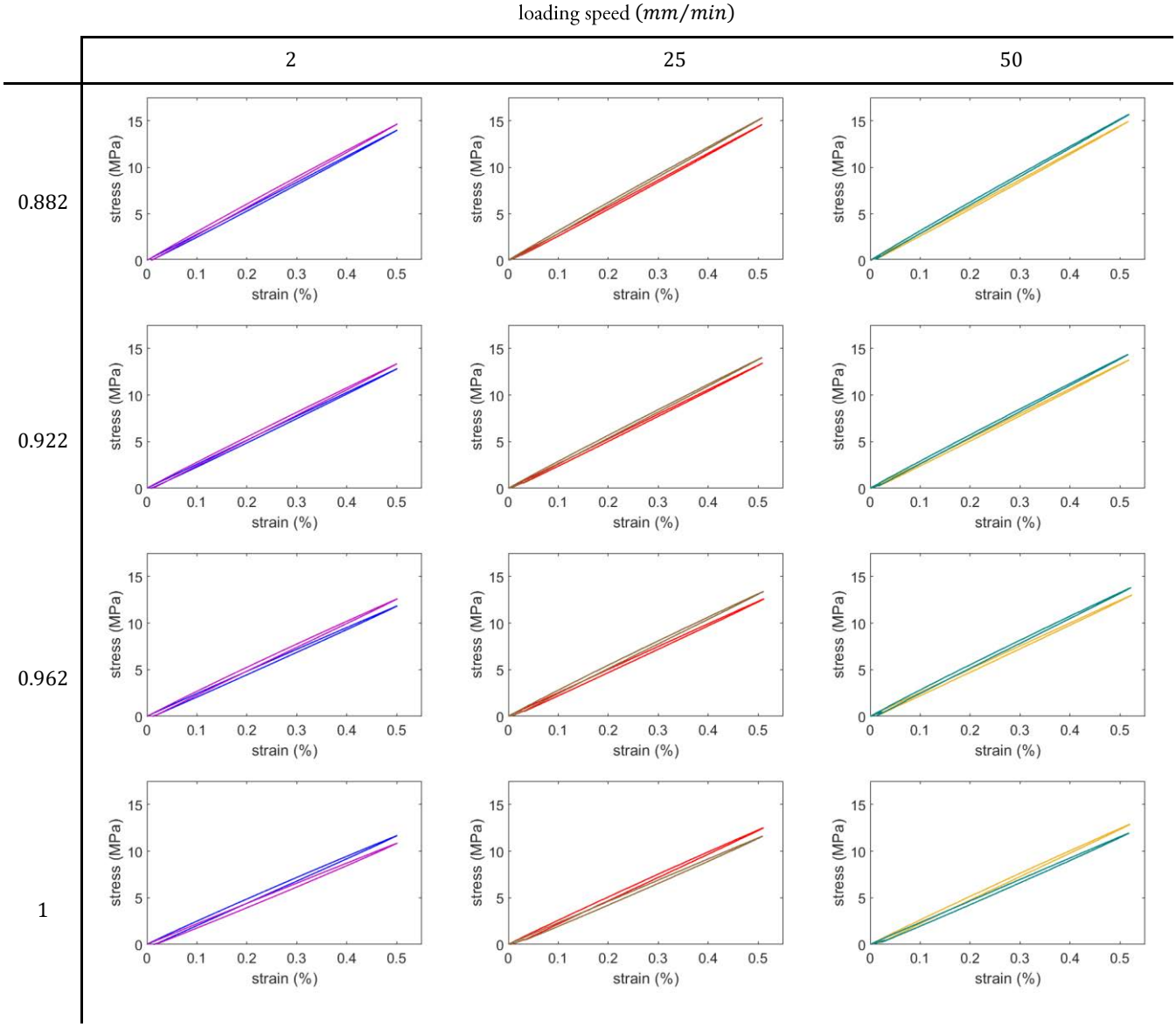

Figure 5.22 Stress-strain curves for the loading-unloading of specimens maximally cured at various temperatures and tested at 50 °C with increasing loading rate

It is seen already from the stress-strain curves that, at all testing temperatures and for all degrees of cure, the stiffness of the resin increases with the loading rate. As shown more clearly in the error bar plots, this effect is not very marked but still non-negligible. Residual strain remaining after the unloading ramp is sharply reduced by increasing the loading speed from 2 to 25 mm/min whereas its further reduction at 50 mm/min is much lower. On the other hand, the area of hysteresis does not vary to a great extent with the loading rate, usually showing a minimum at 25 mm/min.

Table 5.9 Quantities calculated from the loading-unloading test of specimens with various degree of cure and tested at $50\ °C$ with various loading rates

degree of cure	loading rate (mm/min)	maximum stress (MPa)	apparent modulus (GPa)	interpolation modulus (GPa)	residual strain (%)	area of hysteresis $(10^4\ J/m^3)$
0.882	2	14.0015	2.8003	2.8043	0.0080	0.1172
		14.6766	2.9353	2.9226	0.0090	0.1438
	25	14.6134	2.9227	2.8852	0.0020	0.1009
		15.3501	3.0700	3.0083	0.0020	0.1195
	50	14.9352	2.9870	2.9092	0.0020	0.1026
		15.7160	3.1432	3.0507	0.0010	0.1213
0.922	2	12.8265	2.5653	2.5658	0.0070	0.1158
		13.3581	2.6716	2.6644	0.0100	0.1482
	25	13.4362	2.6872	2.6453	0.0020	0.1051
		14.0290	2.8058	2.7557	0.0020	0.1205
	50	13.7739	2.7548	2.6735	0.0020	0.1097
		14.3638	2.8728	2.7895	0.0010	0.1244
0.962	2	11.8472	2.3694	2.3618	0.0110	0.1496
		12.6218	2.5244	2.5086	0.0120	0.1643
	25	12.6093	2.5219	2.4597	0.0030	0.1364
		13.3961	2.6792	2.6134	0.0030	0.1473
	50	13.0203	2.6041	2.5117	0.0010	0.1439
		13.8033	2.7607	2.6728	0.0020	0.1543
1	2	11.6777	2.3355	2.3243	0.0130	0.1831
		10.8665	2.1733	2.1704	0.0140	0.1810
	25	12.5111	2.5022	2.4461	0.0040	0.1608
		11.6255	2.3251	2.2855	0.0030	0.1549
	50	12.8966	2.5793	2.4981	0.0040	0.1646
		11.9506	2.3901	2.3265	0.0030	0.1601

Again considering the three loading rates at the same testing temperature, an unexpected result is observed: the maximum stress and modulus decrease with increasing degree of cure, whereas the residual strain and hysteresis are increased. The lower stiffness of fully cured resin with respect to some less cured specimens has already been observed in Section 5.3.2. From these results, it clearly appears that, by increasing the cure temperature, there is a decrease in stiffness and an increase in hysteresis, even though the degree of cure is higher. This is in partial disagreement with the comments made in Section 5.3.2.

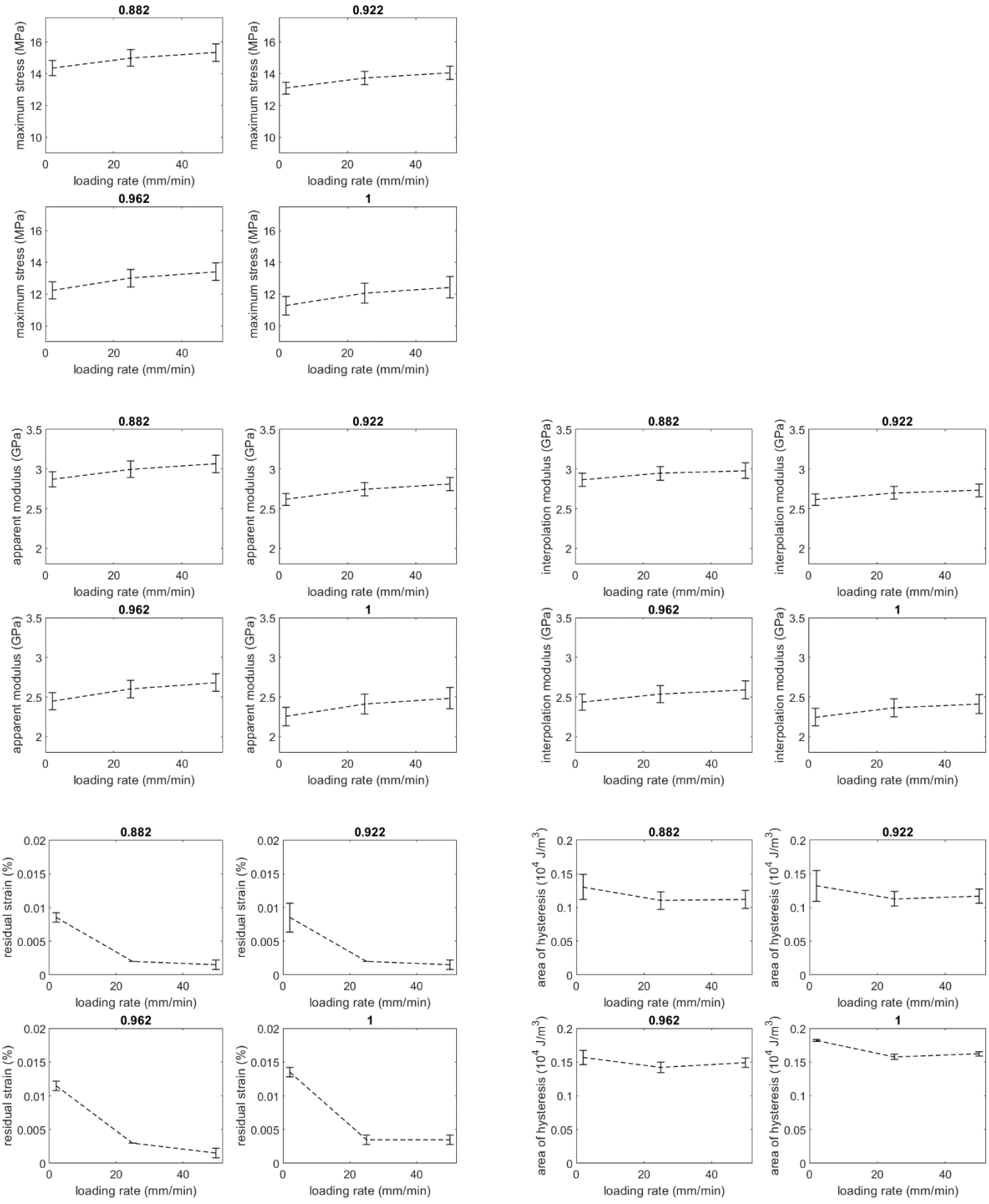

Figure 5.23 Error bars and trends for the loading-unloading of specimens with different degree of cure, tested at 50 °C with various loading rates

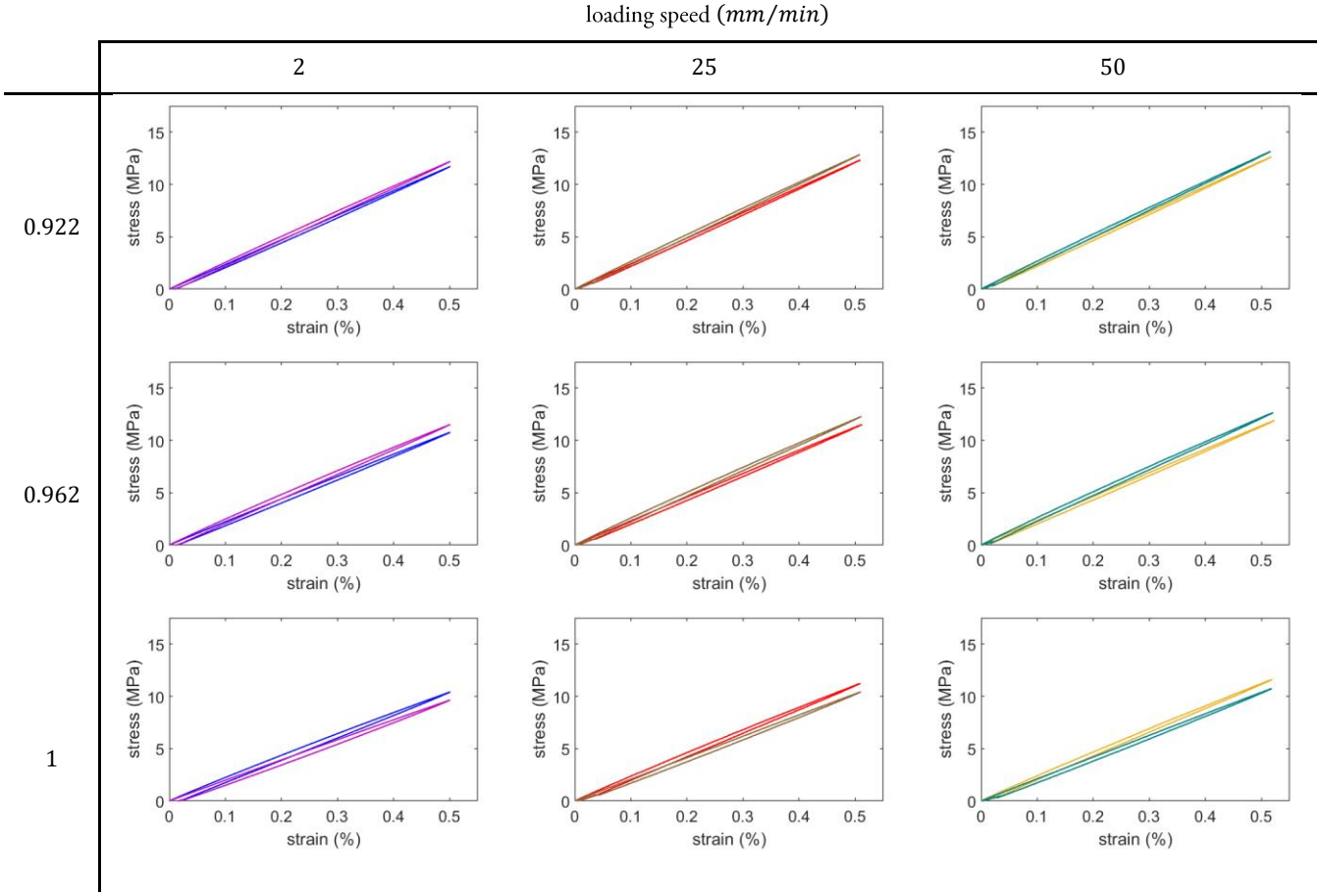

Figure 5.24 Stress-strain curves for the loading-unloading of specimens maximally cured at various temperatures and tested at 70 °C with increasing loading rate

Hence, curing at 50 °C seems to be the most beneficial, both from the point of view of modulus and residual strain. At higher cure temperatures, the solidification rate becomes much faster and polymeric chains are stuck in a non-equilibrium configuration. Eventual mutual influence between the resulting cross-linked network and the development of chemical and thermal internal stresses should be further investigated. It is however to be stressed that the glass transition temperature of specimens maximally cured at 50 °C is about 95 °C, thus significantly limiting the application at high temperature conditions, with respect to fully cured epoxy. The effect of operating temperature is instead in conformity with what was theoretically expected, that is to say a decrease in maximum stress and modulus and an increase in residual strain and hysteresis area. Quite high scatter of data is observed in these last two quantities for 0.962 specimens tested at RT.

Table 5.10 Quantities calculated from the loading-unloading of specimens with various degree of cure and tested at $70\ °C$ with various loading rates

degree of cure	loading rate (mm/min)	maximum stress (MPa)	apparent modulus (GPa)	interpolation modulus (GPa)	residual strain (%)	area of hysteresis $(10^4\ J/m^3)$
0.922	2	11.7297	2.3459	2.3466	0.0090	0.1196
		12.2024	2.4405	2.4316	0.0100	0.1430
	25	12.3439	2.4688	2.4323	0.0020	0.1063
		12.8611	2.5722	2.5270	0.0030	0.1200
	50	12.6617	2.5323	2.4633	0.0020	0.1100
		13.1632	2.6326	2.5567	0.0020	0.1215
0.962	2	10.7842	2.1568	2.1516	0.0120	0.1532
		11.5204	2.3041	2.2900	0.0120	0.1643
	25	11.5241	2.3048	2.2531	0.0030	0.1317
		12.2788	2.4558	2.3958	0.0030	0.1431
	50	11.9014	2.3803	2.2935	0.0020	0.1364
		12.6535	2.5307	2.4396	0.0020	0.1474
1	2	10.4208	2.0842	2.0714	0.0160	0.1904
		9.6436	1.9287	1.9287	0.0170	0.1889
	25	11.2462	2.2492	2.1990	0.0040	0.1552
		10.4226	2.0845	2.0489	0.0040	0.1535
	50	11.6179	2.3236	2.2500	0.0020	0.1567
		10.7453	2.1491	2.0937	0.0030	0.1542

Even though only two specimens have been tested at each experimental condition, resulting trends are quite clearly identified. In addition to more testing, possibly also at higher loading rates, ongoing research should focus on explaining the causes of the counterintuitive mechanical response of differently cured epoxy. The applied methodology has used only one specimen for the nine consecutive loading-unloading cycles, thus reducing the experimental scatter that would be observed if a different specimen was tested at each ramp.

All the performed loading-unloading tests have allowed to assess the viscoelastic response of epoxy in the short term. When included in the method, the very small residual strain has shown to recover in a relatively short time interval, less than $20\ min$. Longer term viscoelastic behaviour will be hereinafter analysed in Sections 5.4 and 5.5, regarding creep, strain recovery and stress relaxation.

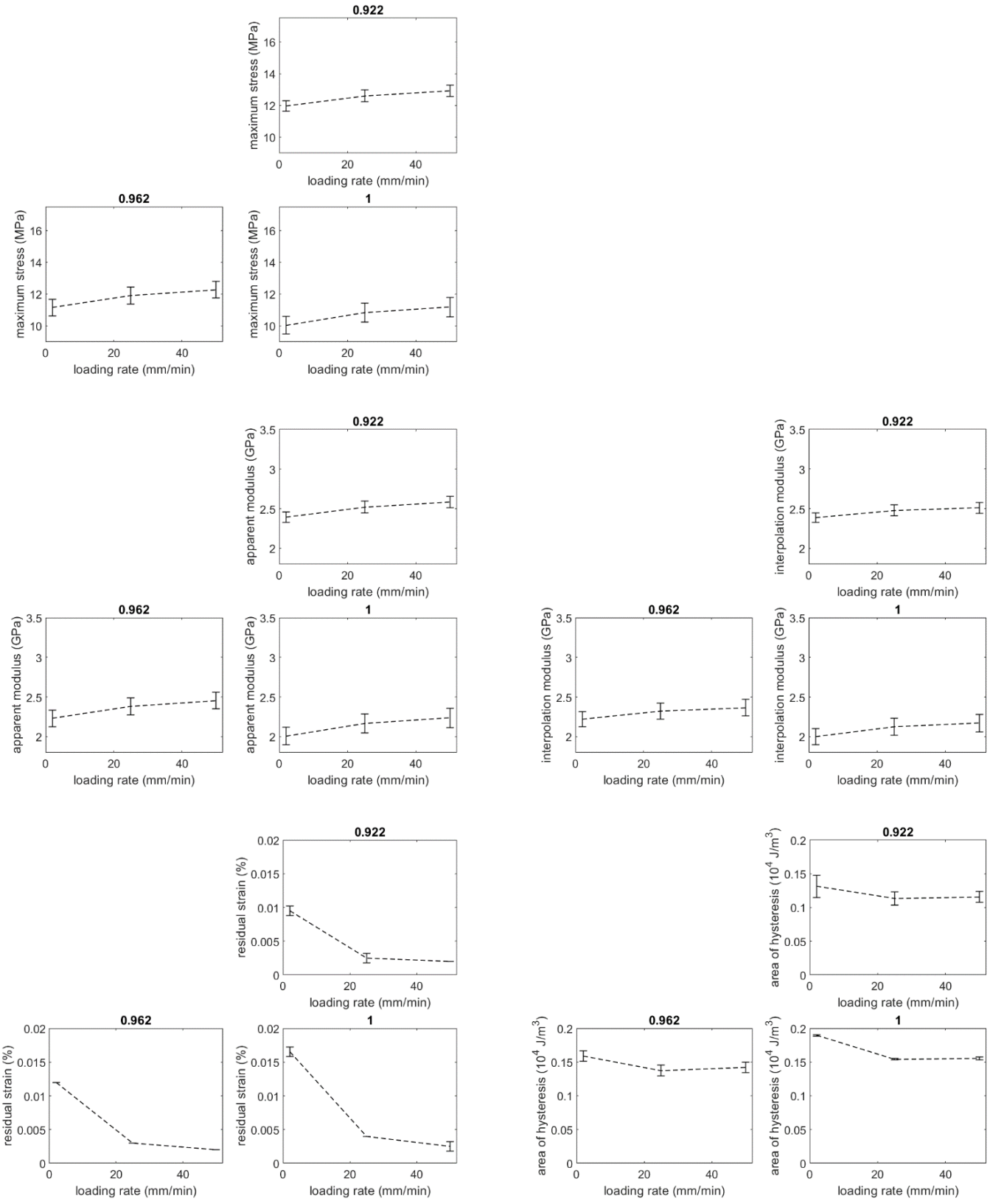

Figure 5.25 Error bars and trends for the loading-unloading of specimens with different degree of cure, tested at 70 °C with various loading rates

5.4. Creep and strain recovery

Creep and strain recovery test is first of all performed on fully cured specimens at 110 °C. The constant load, corresponding to a stress of 6 MPa, is maintained for 10 min. Then, after unloading to almost-zero stress, strain is allowed to recovery for 12 h. Figure 5.26 presents the time-profiles of strain during the two stages of the test, here carried out on four specimens.

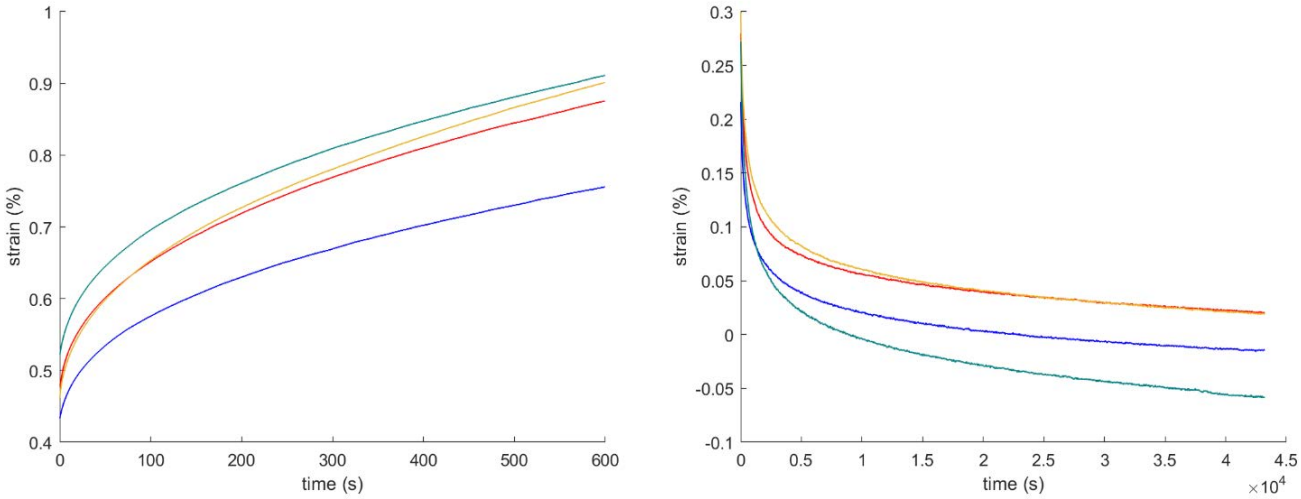

Figure 5.26 Creep and strain recovery at 110 °C of fully cured specimens

In both the creep and strain recovery plots, strain and stress are expressed by subtracting their values at the end of the heating stage, that is to say just before loading to the constant creep stress. Some quantities are calculated to make useful comparisons between different specimens and listed in Table 5.11: increase of strain due to creep, decrease of strain during recovery, residual strain at the end of recovery and an indication of the rate with which both phenomena occur. For the creep part, this is provided by the times at which strain equals 90, 95 and 99% of the total increase in creep strain. Similarly, for the recovery stage it is given by times corresponding to 90, 95 and 99% of the entire strain reduction. The calculation of the first derivative would provide similar and more comprehensive information, but is however not possible because of the extreme slowness of variation of strain.

Table 5.11 Calculated quantities for the creep and strain recovery at 110 °C of fully cured specimens

creep				strain recovery				
	time (s) to reach % of final strain					time (s) to reach % of strain decrease		
strain increase (%)	90	95	99	strain decrease (%)	residual strain (%)	90	95	99
0.3230	474.0	533.5	587.2	0.2300	-0.0140	16781	25996	39549
0.3970	468.1	532.6	582.3	0.2600	0.0200	15825	27702	40877
0.4390	475.0	534.5	586.1	0.2790	0.0200	16148	26666	38805
0.3890	470.6	534.0	583.6	0.3300	-0.0580	18624	28840	40134

The four specimens are observed to have similar trends both during creep and recovery, meaning that strain development and strain reduction occur with quite defined time-evolving rate. Saseendran et al. have reported that the recovery time should be at least 8 times longer than the creep loading [50]. However, some preliminary tests performed herein have shown that a longer time is required, after load removal, to have significant strain recovery. It results in fact that 90, 95 and 99% strain reduction take in average about 4.68, 7.58 and 11.07 h respectively. On the other hand, mean times to reach 90, 95 and 99% of total increase in creep strain are much shorter, namely 7.87, 8.89 and 9.75 min. Average strain increase during creep and its successive recovery are equal to 0.387% and 0.275% respectively. From the curves, strain at the end of the recovery period seems to be still decreasing, even though with quite limited speed, and not to have reached a proper plateau. Nevertheless, 99% decrease is achieved almost 1 h before the end of the test, and therefore the final value of strain could arguably be considered viscoplastic. After the selected 12 h, the residual strain is however extremely small, and sometimes even slightly negative, which means that the measured value is lower than the reference baseline.

110 °C is arguably retained a very high temperature to perform the creep and recovery analysis. The same testing method is therefore carried out at 70 °C, which is a significantly less severe operating condition, this time keeping the constant load for 30 min. Fully cured specimens are tested, as well as those maximally cured at 70 or 90 °C, hence having degree of cure 0.922 and 0.962 respectively. For them all, additional curing during the long-term test can be ruled out. This allows to assess the influence of cure state on the viscoelastic behaviour at extended time-scale and on the eventual development of viscoplasticity. Strain as a function of time for the fixed 6 MPa stress level and during the following recovery is displayed in Figure 5.27. Only one specimen cured at 90 °C is tested instead of two. It is clearly observed that in both stages, strain varies much less quickly and to a much smaller extent at 70 °C than at 110 °C. This slow temporal change in the measured strain with respect to acquisition time is responsible for the observed step-wise trends.

It appears that the increase in strain due to creep is significantly higher for fully cured specimens, suggesting that a faster solidification rate leads to a network in which viscous sliding of molecules is more hindered. Also the initial strain seems to slightly increase with the degree of cure, maybe indicating a progressively larger thermal expansion. The extent of strain recovery is proportional to the creep strain and is probably explained by the same structural considerations. These observations are confirmed by comparing the quantities listed in Table 5.12 and plotted in Figure 5.28.

Table 5.12 Calculated quantities for the creep and strain recovery at 70 °C of specimens fully cured and maximally cured at various temperatures

degree of cure	creep				strain recovery				
		time (s) to reach % of final strain					time (s) to reach % of strain decrease		
	strain increase (%)	90	95	99	strain decrease (%)	residual strain (%)	90	95	99
0.922	0.0280	1041.2	1452.4	1690.8	0.0360	-0.0110	30588	37968	43200
	0.0290	927.7	1290.4	1521.8	0.0370	-0.0110	24339	34432	43200
0.962	0.0300	1177.0	1539.3	1734.3	0.0290	-0.0030	22686	38841	43200
1	0.0690	1107.9	1433.7	1626.0	0.0740	-0.0130	23126	31597	42876
	0.0660	1052.4	1394.7	1614.6	0.0800	-0.0200	22896	32136	40430

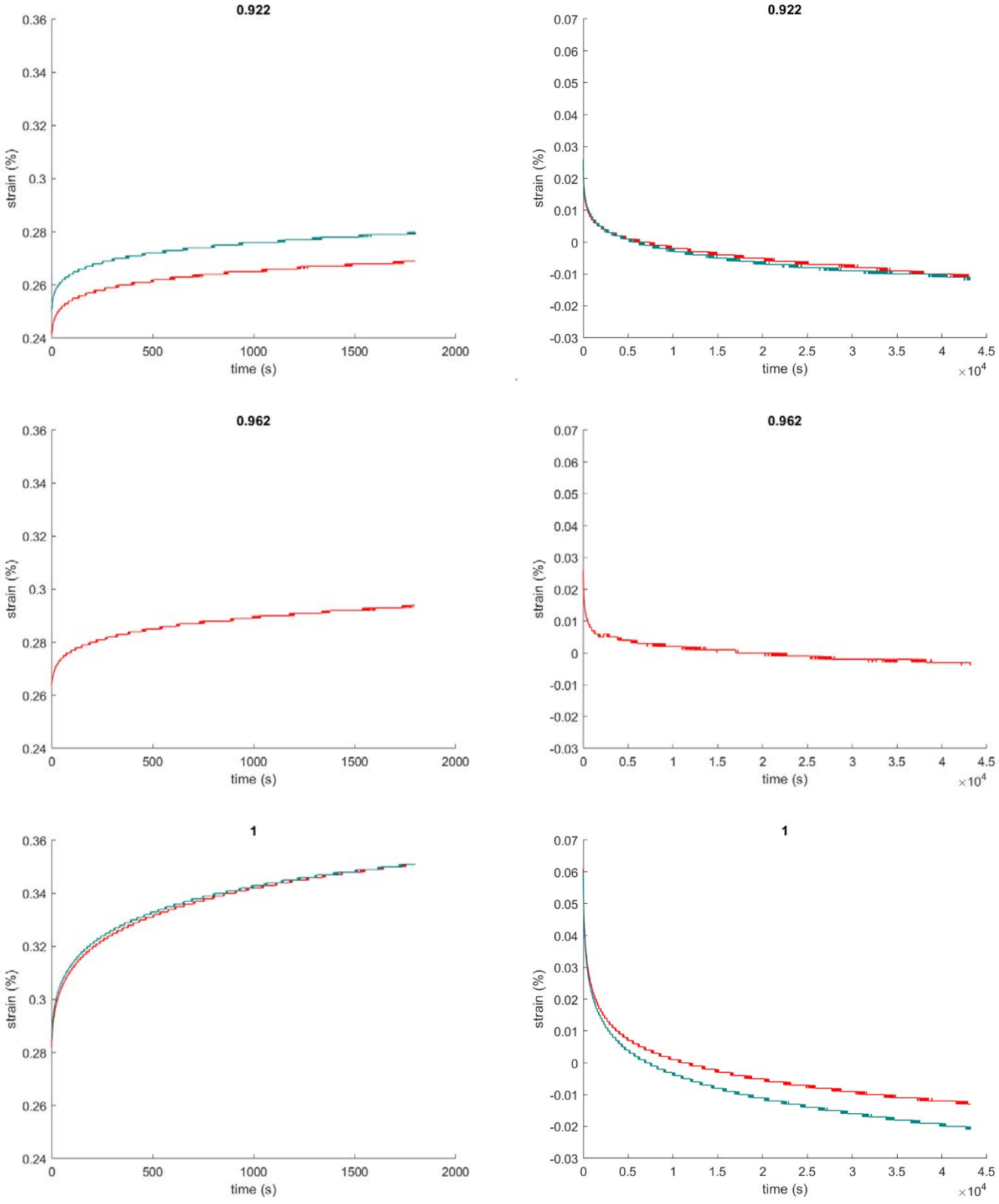

Figure 5.27 Creep and strain recovery at 70 °C of specimens fully cured and maximally cured at various temperatures

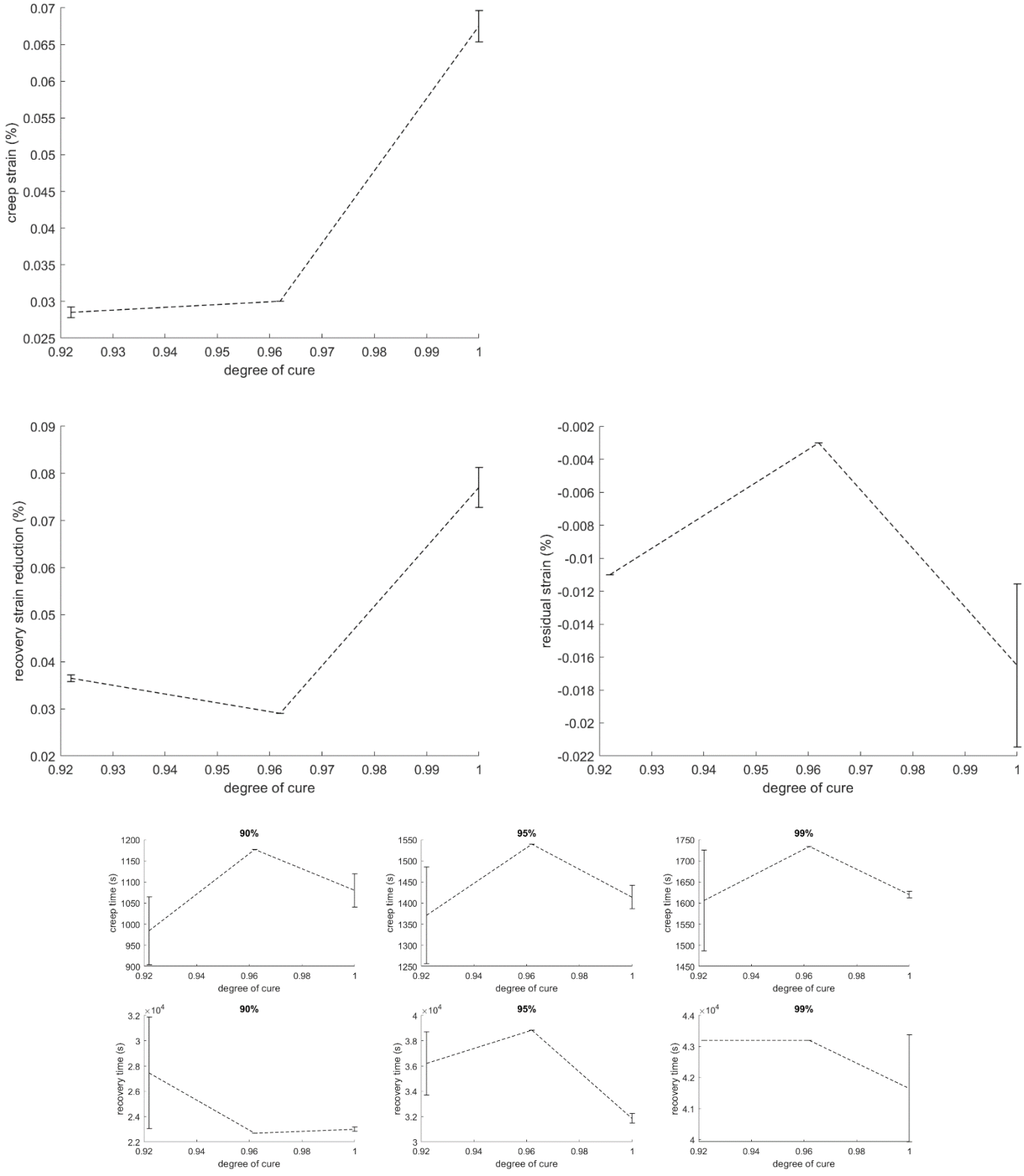

Figure 5.28 Error bars and trends for the creep and strain recovery at 70 °C of specimens fully cured and maximally cured at various temperatures

It is seen more evidently that strain increase during creep and its decrease in recovery are quite similar for specimens maximally cured at 70 and 90 °C whereas they are significantly lower compared to fully cured resin. Residual strain is instead maximum for 0.962 cured epoxy. These results might be considered counter-intuitive since lower degrees of cure are expected to develop higher creep, and eventual viscoplasticity, at shorter times. As already mentioned, such experimental evidence may be explained by the easiness with which polymeric chains are allowed to slide past each other. If molecules are early "frozen" in their non-equilibrium configuration, they appear to be more tightly entrapped in the cross-linked network. Considering the recovery plots, 0.922 and 0.962 specimens show a more evident plateau. The final strain is negative in all the performed tests, being the value measured by the machine below that due to thermal expansion. Times corresponding to 90, 95 and 99% of creep and recovery strains do not show notable trends.

It has to be borne in mind that, being the plot asymptotic, the viscoelastic recovery time is ideally infinite. Therefore, if the remaining strain is assumed as viscoplastic, it is always slightly over-estimated, even if the curve has considerably flattened. As stated in Section 2, the viscoplastic strain evolution can be accurately modelled by means of Zapas-Crissman integral Equation (2.11) [66]. However, in all the performed tests, either at 70 or 110 °C, development of viscoplasticity seems to be very limited and therefore negligible. Hence, even though in general creep causes concurrent viscoelastic and viscoplastic effects, the analysis is herein focused on viscoelasticity and the response is considered almost pure viscoelastic. As known, creep rupture occurs at much lower stress than in simple static loading [56]. The stress level that has been fixed herein, equal to 6 MPa, is nevertheless low enough to avoid the breakage of specimens. Eventual micro-damaging is not assessed since it goes beyond the purposes of this Thesis. The constant creep load is considered to be applied and removed instantaneously with respect to the duration of the overall test.

5.5. Stress relaxation

In the stress relaxation test, 0.5% strain level is maintained for 12 h and longitudinal stress is allowed to relax for 12 h. Time required to reach the 0.5% level in strain-controlled mode is negligible in comparison to the duration of relaxation. The test is initially performed at 110 °C on four fully cured specimens, resulting in the stress versus time curves displayed in Figure 5.29. In order to make comparisons, the stress reduction and the residual stress at the end of each test are calculated, as well as times to have a decrease in stress equal to 90, 95 and 99% of the total. These quantities are detailed in Table 5.13.

Table 5.13 Calculated quantities for the stress relaxation at 110 °C of fully cured specimens

		time (s) to reach % of stress decrease		
stress decrease (MPa)	residual stress (MPa)	90	95	99
3.1429	1.1084	13275	22950	38249
3.7423	1.2486	15013	24880	39118
3.6614	1.2203	14314	24442	39082
3.3883	1.0602	14958	25687	42228

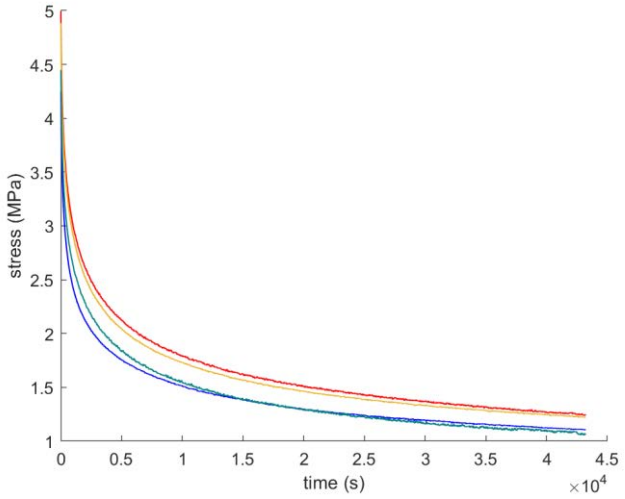

Figure 5.29 Stress relaxation at 110 °C of fully cured specimens

The mean stress reduction is 3.4837 MPa, resulting in a 1.1594 MPa stress remaining at the end of relaxation. Times required for 90, 95 and 99% stress decrease are in average equal to 4, 6.8 and 11.02 h. Similarly to strain recovery, the rate with which stress relaxation occurs becomes progressively lower along time. Although visibly the curves are still decreasing after 12 h, 99% stress relaxation is achieved almost 1h earlier. The final stress is nevertheless still quite high. The effect of viscoplasticity, if present, is to further reduce the measured stress.

As stated in the previous Section 5.4, 110 °C represents for epoxy a quite severe temperature. For this reason, the test is performed also at 70 °C, this time both with fully cured resin and with specimens maximally cured at 70 and 90 °C. Stress-time plots are shown in Figure 5.30 and the calculated quantities are reported in Table 5.14 and Figure 5.31. Only one specimen with degree of cure 0.962 is tested instead of two.

Table 5.14 Calculated quantities for the stress relaxation at 70 °C of specimens fully cured and maximally cured at various temperatures

degree of cure	stress decrease (MPa)	residual stress (MPa)	time (s) to reach % of stress decrease		
			90	95	99
0.922	2.9309	9.8180	31323	37062	41897
	2.7240	9.3137	32231	37310	42185
0.962	2.1795	8.8743	24433	33407	41360
1	2.1944	7.1960	15058	26120	38332
	2.2115	7.6256	11944	20441	40092

It is seen that the initial maximum stress decreases with increasing degree of cure, meaning that resin stiffness becomes progressively lower. This is in agreement with what has been observed in Section 5.3.2. The same trend is exhibited by the stress measured at the end of relaxation. All these residual stresses are

not very below the initial stress, and therefore relaxation does not occur to a significant extent, even in the long time interval considered. Also in this case, 99% stress relaxation is achieved by far before the end of the test. The total reduction is higher for resin cured at 70 °C whereas it is similar for 0.962 and fully cured specimens. The rate of decay clearly decreases along time, and the final plateau becomes progressively more evident with increasing degree of cure. Percentages of the total stress reduction are in fact reached at shorter and shorter times.

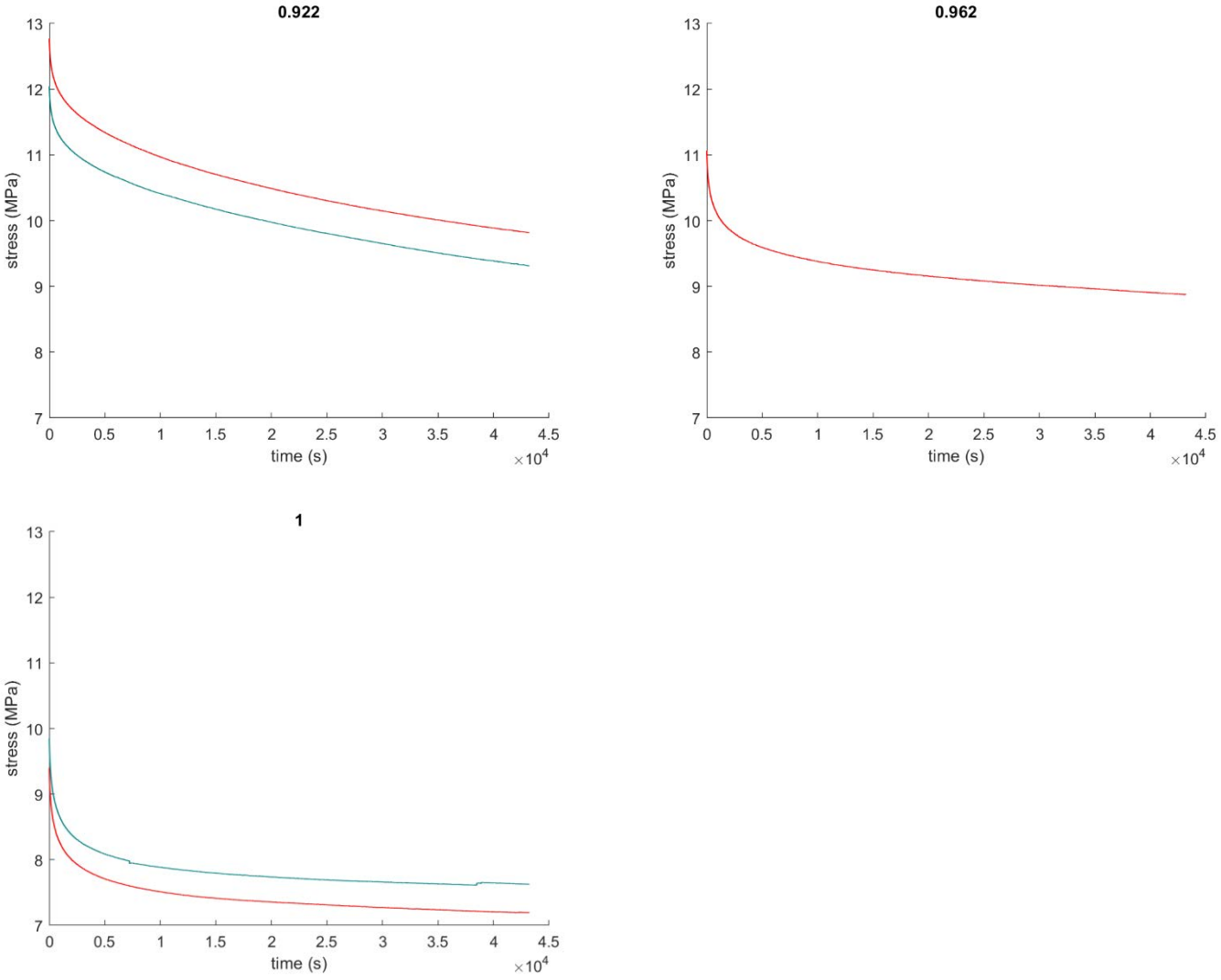

Figure 5.30 Stress relaxation at 70 °C of specimens fully cured and maximally cured at various temperatures

Loading to 0.5% strain is considered instant in comparison to the duration of the overall test. Just like strain recovery, the time required for complete stress relaxation is ideally infinite. By performing longer tests, it would be observed a decay to the stress level that corresponds to the rubbery modulus at 0.5% strain. Even though the effect of degree of cure has not been tested at 110 °C, from the obtained results it is likely that both temperature and cure state parameters have a quite large influence on stress relaxation

behaviour. As mentioned in Section 2, retardation times are often given by Prony series, which will be used in the next Section 5.6 in order perform exemplifying simulation with the VisCoR model [44].

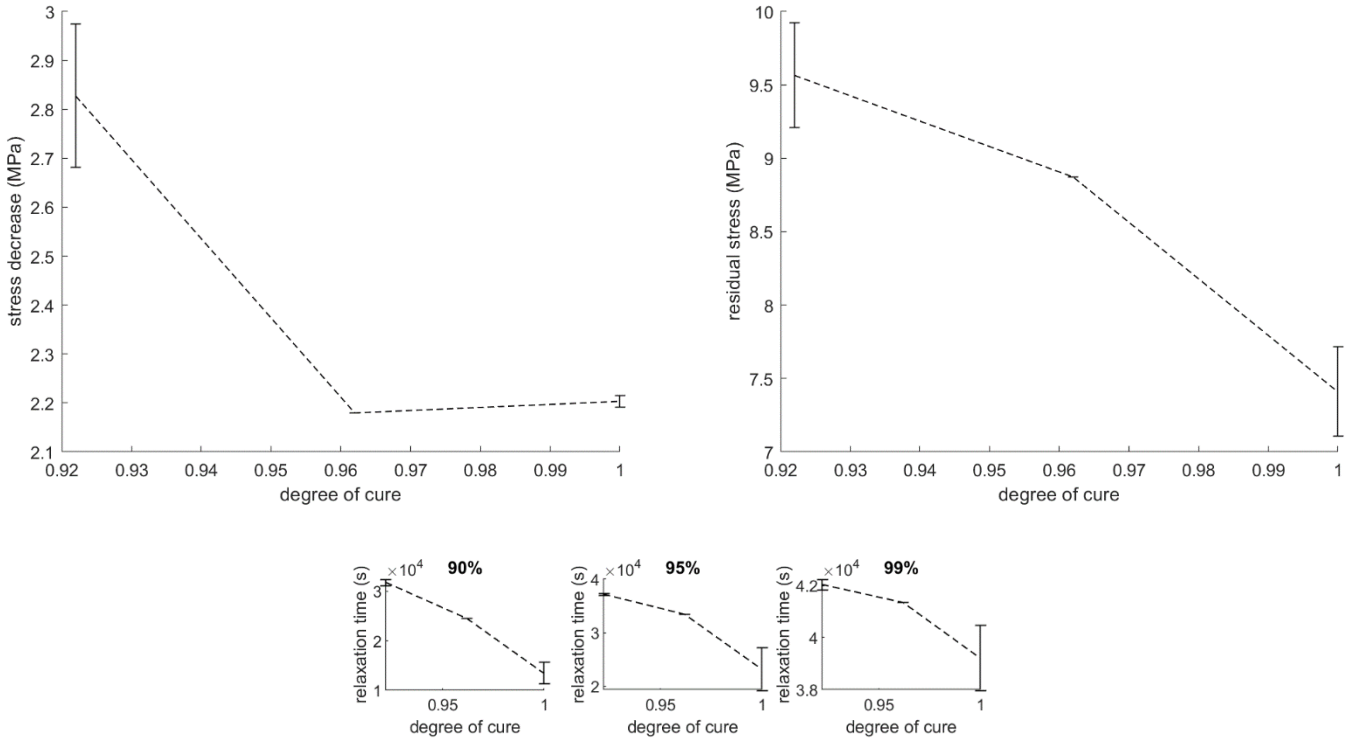

Figure 5.31 Error bars and trends for the creep and strain recovery at 70 °C of specimens fully cured and maximally cured at various temperatures

Now that both short- and long-term mechanical behaviour of epoxy has been tested, VisCoR model is used to reproduce some of the employed experimental conditions, in order to assess the predictive accuracy of computer simulation. As already explained in Section 3, this would considerably reduce the time required for experimental characterization, and therefore the manufacturing costs.

5.6. Examples of numerical validation of VisCoR model

The VisCoR model has been illustrated in its incremental strain formulation in Section 3.2 [60]. One of the aims of this Thesis is its validation, by comparing its numerical predictions with the results obtained on epoxy specimens in various experimental conditions. The importance of the development of effective modelling tools has been thoroughly explained in Section 3. Epoxy LY5052, as well as the majority of resins used in composite manufacturing, can be considered a low-weight system and therefore a thermo-rheologically simple material [13]. The focus of this work is therefore on the special case of the VisCoR model where state variables are assumed to affect only the reduced time ψ. Consequently, h_1 and h_2 are both assumed as unit and the rubbery modulus E_r, relative to the fully relaxed material, is considered

constant and equal to the value extracted from the rubbery region of the super-master curve, i.e. $28\ MPa$. By applying the TTCS principle, it follows that the total shift factor merge multiple temperature- and cure-dependent curves into a unique super-master curve.

The established total shift function a in the reduced time is expressed as the product of two shift factors, namely related to temperature and cure. The WLF fit in Equation (2.2), accounting for the testing temperature T, is referenced at room temperature, i.e. $T_{ref} = 23\ °C$. Constants c_1 and c_2 have been determined in DMTA from frequency scans performed at various temperatures on fully cured specimens, resulting equal to 131.4 and 614.9 K respectively [45]. If $T = T_{ref}$ the temperature shift factor a_T is 1, while it is smaller or larger if the operating temperature is respectively higher or lower. On the other hand, cure shifting is evaluated using Equation (2.3), containing the parameters of the applied cure cycle, i.e. the cure temperature T_c and time t_c. By substituting values typical of epoxy, it results in Equation (3.22). The reference time $t_{c,ref}$ is associated to the reference cure state and is arbitrarily selected as 100 min [45]. Instead, if the resin is fully cured, Equation (3.23) is used and the cure shift factor a_c is equal to 1. Similarly to the temperature shift, also a_c is in the range $0 \div 1$ and becomes lower moving away from the reference state.

Figure 5.32 displays the trends of the temperature and cure shift factors, respectively versus test temperature and cure time at the considered 70 $°C$ cure temperature. Because of the very high variation in the order of magnitude of the shift factors, their trends are more clearly visualized in the semilogarithmic charts, where linear correlations are observed. The same testing temperatures selected in Section 5.3.1, namely RT, 50, 70, 90 and 110 $°C$ are marked with circles, as well as times to attain the percentages of cure in Figure 5.9, i.e. 30, 40, 55 and 70 min respectively for 0.74, 0.83, 0.89 and 0.91. It is seen that a_T becomes very small already slightly above room temperature and that likewise a_c is significantly higher if the resin is cured for more than 55 min. Even if the degree of cure may be the preferred characterization of the cure state, a_c is considered against t_c for simplicity, because only in this case the linear relationship is observed. The values marked in the semilogarithmic plots are detailed in Tables 5.15 and 5.16.

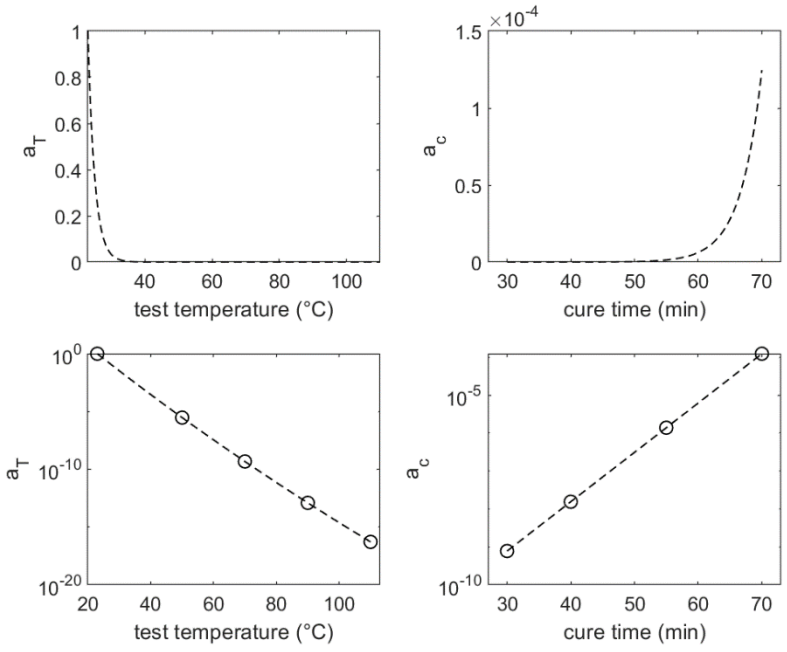

Figure 5.32 Trends of cure and temperature shift factors in linear and semilogarithmic scales

If the two shift functions are complementary, then the applied TTC shifting procedure, first in temperature or cure state, should be irrelevant, leading to the same super-master curve [48]. As already said in Section 2, it is presumably the similarity between the shift factors used for the Poisson's ratio and the storage modulus that points to the rheological simplicity of the material [47]. If this is verified, only one set of temperature- and cure-related shift factors is used for all viscoelastic properties. Even though rheological simplicity of the studied epoxy is herein an a priori assumption, it is supported by quite abundant evidence in literature.

Table 5.15 Temperature shift factors at the selected test temperatures

$T\ (°C)$	23	50	70	90	100
a_T	1	$2.9715 \cdot 10^{-6}$	$4.6729 \cdot 10^{-10}$	$1.2283 \cdot 10^{-13}$	$5.1649 \cdot 10^{-17}$

Table 5.16 Cure shift factors at the selected cure times

$t_c\ (min)$	30	40	55	70
a_c	$7.7535 \cdot 10^{-10}$	$1.5524 \cdot 10^{-8}$	$1.3908 \cdot 10^{-6}$	$1.2459 \cdot 10^{-4}$

The VisCoR model has been implemented in its strain incremental formulation because it is in this way possible to introduce strain as an input variable in order to simulate displacement-controlled tests. To check its accuracy, results numerically determined in MATLAB are compared with some of the previously presented experimental data. Loading-unloading is simulated in order to reproduce some of the operating conditions used in Sections 5.3.1 and 5.3.2. The loading cycle is created from 0 to 0.5% strain with a loading and unloading speed of $2\ mm/min$, and therefore lasts almost $30\ s$. The time interval between numerical data points is chosen equal to the experimental acquisition time, i.e. $10\ ms$. Prony series parameters for the considered epoxy are assumed as given in Table 5.17 [47].

Table 5.17 Parameters in the Prony series for the loading-unloading

$\tau_i\ (min)$	$C_i\ (MPa)$
$2.922 \cdot 10^{1}$	152.091
$2.921 \cdot 10^{3}$	170.074
$1.824 \cdot 10^{5}$	212.677
$1.103 \cdot 10^{7}$	288.871
$2.830 \cdot 10^{8}$	393.693
$7.943 \cdot 10^{9}$	673.423
$1.955 \cdot 10^{11}$	472.114
$3.315 \cdot 10^{12}$	152.240
$4.917 \cdot 10^{14}$	64.880

Considering fully cured resin, $a_c = 1$ and therefore the total shift factor equals the temperature shift. The stress-strain curves predicted using the model are displayed in Figure 5.33. As expected, increasing temperature determines an enhanced development of non-linearity, consisting in a reduction of

maximum stress and stiffness and an increase in hysteresis and residual strain. However, the comparison with Figure 5.7 shows that the model is in fairly good agreement with experimental data only at RT and $50\ °C$. The simulated effect of higher temperatures is considerably more detrimental than what is empirically observed. For the two lowest temperatures, the same quantities calculated in Section 5.3 are determined from the numerical curves and detailed in Table 5.18, along with the experimental mean values. It is noted that, while the simulated and real moduli are similar, residual strain and hysteresis are underestimated at RT, resulting equal to zero, and overestimated at $50\ °C$.

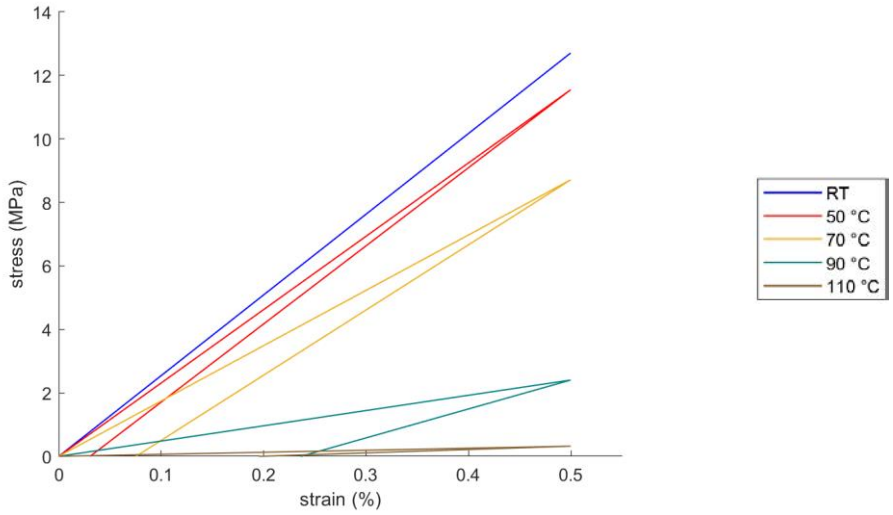

Figure 5.33 Simulated stress-strain curves of fully cured specimens at various testing temperatures

Table 5.18 Quantities calculated from the experimental and numerical loading-unloading of fully cured specimens at RT and $50\ °C$

testing temperature (°C)		maximum stress (MPa)	apparent modulus (GPa)	residual strain (%)	area of hysteresis $(10^4\ J/m^3)$
RT	VisCoR	12.7040	2.5408	0	0
	experimental	12.2165	2.4433	0.0120	0.1404
$50\ °C$	VisCoR	11.5461	2.3092	0.0307	0.1768
	experimental	11.0590	2.2118	0.0160	0.1687

The mechanical response of epoxy partially cured at $70\ °C$ and tested with the loading-unloading mode at RT is visualized in Figure 5.34, showing also fully cured resin. Being $a_T = 1$, the total shift factor is equal to the cure shift. The effect of increasing degree of cure is an increase in a_c, resulting in higher maximum stress and modulus and a lower hysteresis and residual strain. By comparing with Figure 5.11, it is seen that the model does not show the interchange that has been experimentally observed between fully and partially cured specimens. This has been partly explained by considerations related to the cross-linked network and to the residual stress distribution.

Discrepancies between the simulated curve and those coming from testing are most probably attributed to experimental inaccuracies or to the use of not very representative input parameters. Further model

adjustment could be done, as well as more in-depth investigation of the reasons of this unexpected experimental response. The simulation of tests such as stress relaxation is herein not presented because the divergence between model and reality is amplified in the long-term, especially because the Prony series parameters available in literature are on purpose selected to force the material to have a short relaxation time [45]. This allows to more easily study the relaxation behaviour but is not in perfect agreement with the small stress decays measured in the previous Section 5.5.

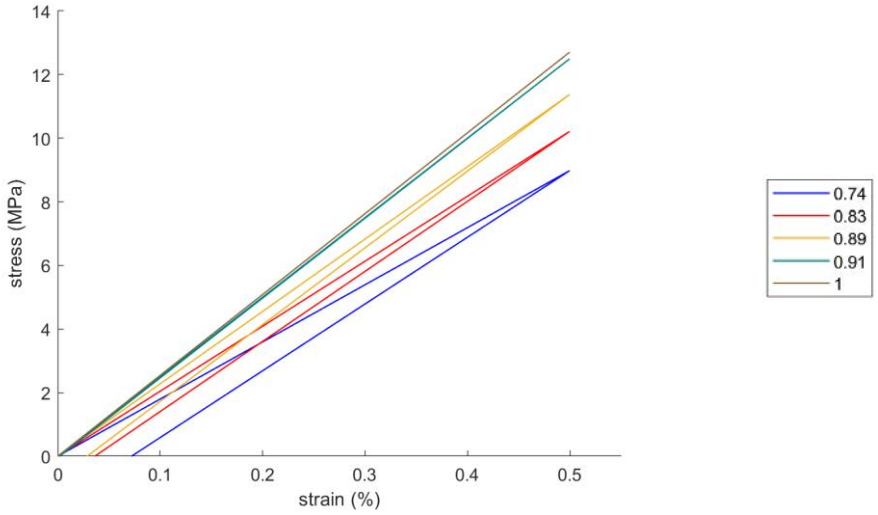

Figure 5.34 Simulated stress-strain curves of various partially cured specimens tested at RT

Although only few simulation examples have been herein implemented and discussed, VisCoR has shown its potential in easily and quickly predicting the sensitivity of the mechanical response on both temperature and cure [45]. Once its input parameters are further adjusted and its applicability is more comprehensively verified, the model will most probably help in saving costs deriving from the trial-and-error approach. In particular, the Prony series should be determined specifically for the considered epoxy and coefficients in Equation (3.22) should be identified for other cure temperatures.

The model might also be useful for providing information on the material behaviour at situations that are difficult to achieve in standard experiments, such as in the rubbery region. The insufficient amount of reliable data would however limit the possibility of validation. Of course, special attention has to be paid on verifying the accuracy of extrapolations outside the available data region. Moreover, the implementation of the model in a finite element code would allow to analyse more complex loading cases and structures [69].

6. Conclusions

In order to facilitate the development of polymeric composite products, new modelling and experimental techniques are required. The aim is to reduce design and manufacturing costs, at once improving the quality of components. One of the main areas of interest is the prediction of process-induced imperfections, such as residual stresses and shape distortions. Indeed, their development during manufacturing has a direct influence on product quality, in terms of strength and dimensional accuracy. The mechanical behaviour of the epoxy matrix, especially at high temperature conditions and during cure, is accurately described only by models based on viscoelasticity. Simple elasticity would in fact lead to rough errors, as in the case of CHILE and path-dependent models. The fundamental challenge is therefore to replicate in numerical simulations the complex phenomena taking place during manufacturing and at high service temperatures, but resorting to a mathematical formulation as simple as possible. Indeed, a combination of many factors, the most important of which are thermal and chemical in nature, contribute to shape distortions within the part and the weakening of the structure itself. Procedures for the release of residual stresses can be set up, as well as compensation techniques to accommodate shape distortions in the mold geometry.

This Thesis seeks to establish a simple and reliable experimental methodology to efficiently characterize the viscoelastic behaviour of commercial LY5052 epoxy and to provide data to be used for the validation of VisCoR model. The results of the performed experiments could support the adjustment of the model parameters, in order to improve its accuracy in predicting the mechanical response in various loading modes. The focus has been on thermo-rheologically simple materials, considering the dependence of the material behaviour on two state variables, namely operating temperature and the degree of cure. One of the main advantages of VisCoR is that it is quite accurate but significantly less computationally expensive than other models available in literature, often requiring long calculation time and large memory. Also preliminary material characterization, aimed at finding input parameters, is not particularly time-consuming. As the majority of viscoelastic models, VisCoR is based on the superposition of time, temperature and cure.

The applicability of the TTC superposition to all viscoelastic properties of epoxy has been investigated by several authors, and in particular stated in the studies by Adolf et al. and Saseedran et al. This corroborates the hypothesis of rheological simplicity of the studied material, making it correct to assume as universal the shift functions calculated from DMTA. The complementarity of the temperature and cure shift factors implies that the total shift function is the product of the two shifts. This allows to generate unique super-master curves that include the effect of all state variables, with the ultimate goal of comprehensively describing the viscoelastic response of epoxy matrix.

Thermal expansion has been characterized in Section 5.2, confirming that $20\,min$ is a more than sufficiently long time to ensure uniform temperature distribution within the specimen, when performing tests at high temperatures. Cure kinetics has been studied in Section 5.1 by simulating the cure profiles

through Kamal's model when the resin is subjected to various exemplified temperature ramps. Different sets of cure times and temperatures have been determined in order to attain specific degrees of cure. In the light of the experimental evidence provided in Sections 5.3-5.5, it results that there is not a one-to-one relationship between the degree of cure α and the mechanical properties of the material at a given temperature. This is univocally defined by the previous curing history, that is to say by the combination of cure temperature T_c and time t_c. Therefore in Equation (2.4), the independent variables on whom the shift factors depend are better specified as

$$a(T, T_c, t_c) = a_T(T) \cdot a_c(T_c, t_c) \tag{6.1}$$

The downside of this clarification is that T_c and t_c must be know a priori from the manufacturer, whereas α can be measured, for example by means of DSC, even though with an experimental accuracy to be better evaluated.

In all the tests performed in the thermal chamber, including the long-term creep and relaxation tests, experimental conditions were selected so that it was correct to assume that the degree of cure has not changed during testing, or its increase was negligible. It should be emphasised that, in the case of additional curing, the characterization methodology is much more complicated because the time-dependent response of the resin is continuously changing. Tensile stress-strain curves have been traced at different temperature levels on both fully and partially cured specimens, in each test quantifying slope and hysteresis. It was expected that both low degree of cure and high test temperature cause enhanced viscoelastic effects, that is to say lower stiffness and larger viscous dissipation. The viscoelastic modulus is the property that is more directly dependent on test temperature and cure state and that is more easily representative of the material behaviour. Creep and strain recovery tests, as well as stress relaxation, are on the other hand useful in characterizing the viscoelastic behaviour over extended time scales. Indeed, during the relatively short loading-unloading tests, viscoelastic phenomena do not have enough time to develop significantly. Limited analysis of viscoplasticity and irreversible strains has also been performed. Future work may include analysis of transverse viscoelastic properties, and of other loading modes.

Quite high scatter is visible in the results of many experiments. Trends are sometimes not obvious, for example if disparities in the behaviour of specimens with slightly differing degree of cure are to be detected. Therefore, reliable testing methodologies and raw data reduction procedures are of scientific and practical importance, in order to reduce as much as possible the required number of specimens. The execution of multiple tests sequentially on the same specimen is less time-consuming and it is also arguably considered a better way to characterize viscoelasticity, since it beneficially reduces the experimental scatter introduced by small and undefined differences between batches produced under the same conditions. The preferred methodology was therefore to subject a single specimen to a combination of the three primary test methods described in Section 4.2, in various operating conditions. Specimens were not taken out of the experimental setup and the test method was not interrupted in-between its consecutive parts. This is possible only if there is no development of viscoplastic strains before the final part of the overall test. The presence of viscoplasticity would in fact complicate viscoelastic parameters identification. Actually, besides the recovery stages included in the method, eventual irreversible strain accumulation has been implicitly considered for all the presented results, by assuming as a baseline the strain and stress values at the very beginning of the considered test part. In the light of these considerations, creep and stress relaxation, in which there may be development of viscoplasticity to a larger extent, were never followed by other tests.

A strong dependence of the modulus on both test temperature and cure state has been detected. In general, moisture is along with temperature an environmental factor greatly affecting the mechanical response of polymers. Nevertheless, air humidity has been herein not considered, since it could be assumed constant with good approximation and especially because epoxy is very little sensitive on it. While the observed effect of testing temperature was in line with expectations and theoretical background, some surprising results have been found in the investigation of the influence of the degree of cure. Indeed, specimens differently cured to the same degree have shown different thermo-mechanical behaviour, and the stiffness of some partially cured specimens has appeared higher than that of fully cured resin. It is reasonable to infer that this is the consequence of a combination of their slightly differing internal structure and of residual stresses, both deriving from the applied cure cycle. To comparable number of cross-links, it is likely that the arrangement of polymer chains is the farther from equilibrium the faster is the solidification of the resin, that is to say the higher is the cure temperature, and this influences the easiness with which molecules are able to slide past each other. Currently, such considerations are only qualitative and need additional examination to be concretely demonstrated.

This may be arguably considered the main outcome of research enclosed within this Thesis. Even if some of these results are still not totally understood, the possibility to perform cure at lower temperatures and for shorter times is promising, since it would allow cost saving in the production of components. The toxicity of partially cured epoxy, given by the presence of unreacted monomers, has however to be taken into consideration. The main reason why the dependence of viscoelastic response on cure state is much less understood with respect to the temperature-dependence is that it is significantly more difficult to carry out reliable experiments on partially cured specimens. Theoretical assertations are still not extensively supported by empirical results and the characterization of the cure state itself needs to be more precisely defined. Experiments carried out herein, along with model simulations, will help in leading to a deeper understanding of stress and strain distributions across composite parts, and of their eventual shape distortions. The main final purpose, useful from an industrial point view, is to find procedures for the compensation of shape distortions and for the release of frozen-in stresses.

The model derived by Schapery and written in incremental form by Varna et al. concurrently covers the dependence of the overall viscoelastic response on time, test temperature and cure state parameters. Its main advantages over other material models are that it is thermodynamically consistent and that it takes into account the inherently non-linear behaviour of thermosets. By systematically introducing the simplifying assumptions leading to a thermo-rheologically simple material, loading-unloading of fully and partially cured resin have been simulated. Discrepancies with respect to the results presented in Sections 5.3-5.5 may be ascribed to experimental errors or to eventual not perfect representativeness of the assumed input parameters, such as in the Prony series or in the expression of shift factors. Current and future work should therefore include more advanced and differentiated tests and data analysis schemes, in order to provide further model adjustment and its more comprehensive validation. Its implementation in commercial predictive tools requires in fact more abundant experimental proof of its adequacy to the real behaviour.

In conclusion, the presented experimental and numerical approach has proven to be effective in characterizing the viscoelastic behaviour of LY5052 epoxy resin and may be suggested for similar material systems used in the composite industry. In addition to the effect of temperature, a more detailed understanding of the evolution of properties with cure has also been provided. If the applicability of VisCoR model is verified, it could be used to simulate the outcomes of processes occurring during cure and at high temperatures. An easy and accurate prediction of residual stresses and shape distortions could

in fact reduce characterization and manufacturing costs, at the same time improving the quality of the final product.

References

[1] Adolf D.B., Martin J.E., *Time-cure superposition during crosslinking*, Macromolecules, July 1990, 23, 15, 3700-3704

[2] Adolf D.B., Martin J.E., Chambers R.S., Burchett S.N., Guess T.R., *Stresses during thermoset cure*, Journal of Materials Research, Volume 13, Issue 3, March 1998, pp. 530-550

[3] Adolf D.B., Martin J.E., Wilcoxon J.P., *Evolution of structure and viscoelasticity in an epoxy near the sol-gel transition*, Macromolecules, January 1990, 23, 2, 527-531

[4] Advani S.G., Sozer E.M., *Process Modeling in Composites Manufacturing*, 2nd Edition, CRC Press

[5] Benavente M., Marcin L., Courtois A., Lévesque M., Ruiz E., *Numerical analysis of viscoelastic process-induced residual distortions during manufacturing and post-curing*, Composites Part A 107 (2018) 205–216

[6] Bogetti T.A., Gillespie J.W., *Process-Induced Stress and Deformation in Thick-Section Thermoset Composite Laminates*, Journal of Composite Materials, March 1992, Volume 26, Issue 5

[7] Brauner C., Soprano P., Herrmann A.S., Meiners D., *Cure-dependent thermo-chemical modelling and analysis of the manufacturing process of an aircraft composite frame*, Journal of Composite Materials, Volume 49, Issue 8, 2015

[8] Brockman R.A., Lee C.W., Storage T.M., Volk B.L., *OMC Processing Simulation using an Elastic-Viscoplastic Material Model*, SAMPE Conference at Baltimore, May 2015

[9] DiBenedetto A.T., *Prediction of the glass transition temperature of polymers: A model based on the principle of corresponding states*, Journal of Polymer Science Part B: Polymer Physics, Volume 25, Issue 9, September 1987

[10] Ding A., Li S., Wang J., Ni A., Zu L., *A new path-dependent constitutive model predicting cure-induced distortions in composite structures*, Composites Part A: Applied Science and Manufacturing, Volume 95, April 2017, pp. 183-196

[11] Ding A., Li S., Wang J., Zu L., *A three-dimensional thermo-viscoelastic analysis of process-induced residual stress in composite laminates*, Composite Structures 129 (2015) 60–69

[12] Eom Y., Boogh L., Michaud V., Sunderland P., Månson J.A., *Time-cure-temperature superposition for the prediction of instantaneous viscoelastic properties during cure*, Polymer Engineering and Science, Wiley, Volume 40, Issue 6, April 2004

[13] Emri I., *Rheology of Solid Polymers*, Rheology Reviews 2005, pp. 49 – 100

[14] Ernst L.J., Zhang G.Q., Jansen K.M.B., Bressers H.J.L., *Time- and Temperature-Dependent Thermo-Mechanical Modeling of a Packaging Molding Compound and its Effect on Packaging Process Stresses*, Journal of Electronic Packaging, Volume 125, Issue 4, December 2003

[15] Fan M., Fu F., *Advanced High Strength Natural Fibre Composites in Construction*, Woodhead Publishing Series in Composites Science and Engineering: Number 74, 1st edition, 2011

[16] Frank G.J., Brockman R., *A viscoelastic–viscoplastic constitutive model for glassy polymers*, July 2001, International Journal of Solids and Structures, 38(30-31):5149-5164

[17] Giannadakis K., Varna J., *Analysis of non-linear shear stress-strain response of unidirectional GF/EP composite*, Composites. Part A, Applied science and manufacturing, 2014, Volume 62, pp. 67-76

[18] Guedes R.M., Marques A.T., Cardon A., *Analytical and Experimental Evaluation of Nonlinear Viscoelastic-Viscoplastic Composite Laminates under Creep, Creep-Recovery, Relaxation and Ramp Loading*, Mechanics of Time-Dependent Materials, June 1998, Volume 2, Issue 2, pp. 113–128

[19] Hossain M., Possart G., Steinmann P., *A small-strain model to simulate the curing of thermosets*, Computational Mechanics, May 2009, Volume 43, Issue 6, pp. 769-779

[20] Hossain M., Steinmann P., *Degree of cure-dependent modelling for polymer curing processes at small-strain. Part I: consistent reformulation*, Computational Mechanics, April 2014, 53(4)

[21] Hull D., Clyne T.W., *An Introduction to Composite Materials*, 2nd Edition, Cambridge University Press, 1996

[22] Johnston A., Vaziri R., Poursartip A., *A Plane Strain Model for Process-Induced Deformation of Laminated Composite Structures*, Journal of Composite Materials, Volume 35, Issue 16, August 2001

[23] Kamal M.R., Sourour S., *Kinetics and thermal characterization of thermoset cure*, Polymer Engineering and Science, Wiley, Volume 13, Issue 1, January 1973, pp. 59-64

[24] Kappel E., Stefaniak D., Hühne C., *Semi-analytical spring-in analysis to counteract CFRP manufacturing deformations by tool compensation*, 28th International Congress of the Aeronautical Sciences (ICAS) 2012

[25] Karkanas P.I., Partridge I.K., Attwood D., *Modelling the cure of a commercial epoxy resin for applications in resin transfer moulding*, Polymer International, Volume 41, Issue 2, October 1996, pp. 183-191

[26] Kiasat M.S., *Curing Shrinkage and Residual Stresses in Viscoelastic Thermosetting Resins and Composites*, PhD Thesis, May 2000, Delft University of Technology, Netherlands

[27] Kim Y.K., White S.R., *Stress relaxation behavior of 3501-6 epoxy resin during cure*, Polymer Engineering and Science, Wiley, Volume 36, Issue 23, December 1996, pp. 2852-2862

[28] Lee W.I., Loos A.C., Springer G.S., *Heat of Reaction, Degree of Cure, and Viscosity of Hercules 3501-6 Resin*, Journal of Composite Materials, Volume 16, November 1982, pp. 510-520

[29] Lienhard J.H. IV, Lienhard J.H. V, *A Heat Transfer Handbook*, Phlogiston Press, July 2018

[30] Lou Y.C., Schapery R.A., *Viscoelastic Characterization of a Nonlinear Fiber-Reinforced Plastic*, Journal of Composite Materials, Volume 5, Issue 2, 1971

[31] Mours M., Winter H.H., *Relaxation Patterns of Nearly Critical Gels*, Macromolecules, 1996, 29(22), 7221-7229

[32] Msallem Y.A., Jacquemin F., Boyard N., Poitou A., Delaunay D., Châtel S., *Material characterization and residual stresses simulation during the manufacturing process of epoxy matrix composites*, Composites Part A: Applied Science and Manufacturing, 41(1):108-115, January 2010

[33] Nawab Y., Shahid S., Boyard N., Jacquemin F., *Chemical shrinkage characterization techniques for thermoset resins and associated composites*, Journal of Materials Science, Springer Verlag, 2013, 48 (16), pp. 5387-5409

[34] O'Brien D.J., Mather P.T., White S.R., *Viscoelastic Properties of an Epoxy Resin during Cure*, Journal of Composite Materials, Volume 35, No. 10/2001

[35] Peng X., Gillham J.K., *Time–temperature–transformation (TTT) cure diagrams: Relationship between T_g and the temperature and time of cure for epoxy systems*, Journal of Applied Polymer Science, December 1985

[36] Prasatya P., McKenna G.B., Simon S.L., *A Viscoelastic Model for Predicting Isotropic Residual Stresses in Thermosetting Materials: Effects of Processing Parameters*, Journal of Composite Materials, May 2001, Volume 35, Issue 10

[37] Pupure L., *Non-linear Model Applied on Composites Exhibiting Inelastic Behavior: Development and Validation*, Doctoral Dissertation, Luleå University of Technology, Luleå, Sweden, April 2015

[38] Pupure L., Saseendran S., Varna J., *Effect of Degree of Cure on Non-linear Behaviour of Polymeric Materials*, Presentation at CompTest 2019, May 2019, Luleå, Sweden

[39] Pupure L., Varna J., Joffe R., *Natural fiber composites: challenges simulating inelastic response in strain controlled tensile tests*, Journal of Composite Materials, 2015

[40] Pupure L., Varna J., Joffe R., *On viscoplasticity characterization of natural fibers with high variability*, Advanced Composite Letters, 2015

[41] Rozite L., Varna J., Joffe R., Pupurs A., *An analysis of nonlinear behaviour of lignin based flax composites, Mechanics of Composite Materials*, 2013, 49 (2): 139-153

[42] Sadeghinia M., Jansen K.M.B., Ernst L.J., Pape H., *Thermo-Mechanical Properties Of An Epoxy Molding Compound In Pressure Cooker Environment*, 15th European Conference on Composite Materials (ECCM15), Venice, Italy, June 2012

[43] Saeb M.R., Bakhshandeh E., Khonakdar H.A., Mäder E., Scheffler C.,Heinrich G., *Cure Kinetics of Epoxy Nanocomposites Affected by MWCNTs Functionalization: A Review*, The Scientific World Journal 2013:703708, November 2013

[44] Saseendran S., *Effect of Degree of Cure on Viscoelastic Behavior of Polymers and their Composites*, Doctoral Dissertation, Luleå University of Technology, Luleå, Sweden, August 2017

[45] Saseendran S., Berglund D., Varna J., *Stress relaxation and strain recovery phenomena during curing and thermo-mechanical loading: thermo-rheologically simple viscoelastic analysis*, Journal of Composite Materials, draft manuscript

[46] Saseendran S., Wysocki M., Varna J., *Characterisation of Viscoelastic Material Properties During Curing Processes*, Challenges in Mechanics of Time Dependent Materials, Volume 2, January 2016

[47] Saseendran S., Wysocki M., Varna J., *Cure-state dependent viscoelastic Poisson's ratio of LY5052 epoxy resin,* Advanced Manufacturing: Polymer & Composites Science, July 2017

[48] Saseendran S., Wysocki M., Varna J., *Evolution of viscoelastic behavior of a curing LY5052 epoxy resin in the glassy state*, Advanced Manufacturing: Polymer & Composites Science, October 2016

[49] Saseendran S., Wysocki M., Varna J., *Evolution of viscoelastic behavior of a curing LY5052 epoxy resin in the rubbery state*, Advanced Composite Materials, April 2017

[50] Saseendran S., Varna J., Pupure L., *Effect of Polymer Cure State on Composites*, August 2017

[51] Schapery R.A., *Further development of a thermodynamic constitutive theory: stress formulation*, Lafayette: Purdue Research Foundation, 1969

[52] Schapery R.A., *Nonlinear Viscoelastic and Viscoplastic Constitutive Equations Based on Thermodynamics*, Mechanics of Time-Dependent Materials, June 1997, Volume 1, Issue 2, pp. 209–240

[53] Schapery R.A., *On the characterization of nonlinear viscoelastic materials*, Polymer Engineering and Science, Wiley, Volume 9, Issue 4, July 1969, pp. 295-310

[54] Simon S.L., McKenna G.B., Sindt O., *Modeling the evolution of the dynamic mechanical properties of a commercial epoxy during cure after gelation*, Journal of Applied Polymer Science, Volume 76, Issue 4, pp. 495-508, April 2000

[55] Solimando X., Babin J., Arnal-Herault C., Wang M., Barth D., Roizard D., Doillon-Halmenschlager J.R., Ponçot M., Royaud I., Alcouffe P., David L., Jonquières A., *Highly selective multi-block poly(ether-urea-imide)s for CO 2 /N 2 separation: Structure-morphology-properties relationships*, Polymer 131, 2017, pp. 56-67

[56] Sperling L.H., *Introduction to Physical Polymer Science*, Fourth Edition, John Wiley & Sons

[57] Svanberg M., *Predictions of Manufacturing Induced Shape Distortions*, Doctoral Thesis, Luleå University of Technology, Piteå, Sweden, October 2002

[58] Svanberg M., Holmberg A., *Prediction of shape distortions Part I. FE-implementation of a path dependent constitutive model*, Composites Part A Applied Science and Manufacturing 35(6):711-721, June 2004

[59] Thiruppukuzhi S.V., Sun C.T., *Models for the strain-rate-dependent behavior of polymer composites*, Composites Science and Technology, January 2001, 61(1):1-12

[60] Varna J., Pupure L., Joffe R., *Incremental forms of Schapery's model: convergence and inversion to simulate strain controlled ramps*, Mechanics of Time-Dependent Materials, 2016

[61] Weeks C.A., Sun C.T., *Modeling non-linear rate-dependent behavior in fiber-reinforced composites*, Composites Science and Technology, Volume 58, Issues 3-4, March-April 1998, pp. 603-611

[62] White S.R., Hahn H.T., *Process Modeling of Composite Materials: Residual Stress Development during Cure. Part I. Model Formulation*, Journal of Composite Materials, 1992, Volume 26, Issue 16

[63] Williams M.L., Landel R.F., Ferry J.D., *The Temperature Dependence of Relaxation Mechanisms in Amorphous Polymers and Other Glass-forming Liquids*, Journal of the American Chemical Society, July 1955, 77, 14, 3701-3707

[64] Winter H.H., Mours M., *Rheology of Polymers Near Liquid-Solid Transitions*, Neutron Spin Echo Spectroscopy Viscoelasticity Rheology, Advances in Polymer Science, Volume 134, 1997, Springer, Berlin, Heidelberg

[65] Wisnom M.R., Gigliotti M., Ersoy N., Campbell M., Potter K., *Mechanisms generating residual stresses and distortion during manufacture of polymer–matrix composite structures*, April 2006, Composites Part A, Applied Science and Manufacturing, 37(4):522-529

[66] Zapas L.J., Crissman J.M., *Creep and recovery behaviour of ultra-high molecular weight polyethylene in the region of small uniaxial deformation*, Polymer, Volume 25, Issue 1, January 1984, pp. 57-62

[67] Zarrelli M., Skordos A., Partridge I.K., *Toward a constitutive model for cure-dependent modulus of a high temperature epoxy during the cure*, European Polymer Journal 46(8):1705-1712, September 201

[68] Zhang J.T., Zhang M., Li S., Pavier M.J., Smith D.J., *Residual stresses created during curing of a polymer matrix composite using a viscoelastic model*, Composites Science and Technology 130, May 2016

[69] Zocher M.A., Groves S.E., Allen D.H., *A three-dimensional finite element formulation for thermoviscoelastic orthotropic media*, International Journal for Numerical Methods in Engineering, Volume 40, Issue 12, June 1997, pp. 2267-2288

[70] Data sheet: Araldite LY 5052 / Aradur 5052, Huntsman